Carbohydrate-carbohydrate interaction provides adhesion force and specificity for cellular recognition and adhesion.

Inauguraldissertation

zur

Erlangung der Würde eines Doktors der Philosophie

vorglegt der

Philosophisch-Naturwissenschaftlichen Fakultät

der Universität Basel

von

Iwona Bucior

aus Gdynia, Polen

Basel, 2003

Canon Schweiz AG

Genehmigt von der Philosophisch-Naturwissenschaftlichen Fakultät

auf Antrag von

Herrn Prof. Dr. Max M. Burger

und Frau Privatdozentin Dr. Ruth Chiquet-Ehrismann

Basel, den 8 Juli 2003   Prof. Dr. Marcel Tanner

                                                          (Dekan)

TABLE OF CONTENTS

I. LIST OF ABBREVIATIONS

AFM   atomic force microscopy

BSA   bovine serum albumin

BSW   bicarbonate-buffered seawater

Cer   ceramide

CMFBSW   calcium- and magnesium-free bicarbonate-buffered seawater

CMFTSW   calcium- and magnesium-free Tris-buffered seawater; artificial seawater

CS   chondroitin sulfate

CsCl   cesium chloride

DS   dermatan sulfate

EDTA   ethylenediamidetetraacetic acid

Fuc   fucose

Gal   galactose

GalN   N-acetylgalactosamine

GlcN   N-acetylglucosamine

GlcA   glucuronic acid

g-6   6 kDa glycan obtained from *Microciona prolifera* proteoglycan

g-200   200 kDa glycan obtained from *Microciona prolifera* proteoglycan

GAG   glycosaminoglycan

Gb4   globoside (GalNAcβ1$\rightarrow$4Galβ1$\rightarrow$4Glcβ1$\rightarrow$1Cer)

Gg$_3$ gangliotriaosylceramide (GalNAcβ1$\rightarrow$4Galβ1$\rightarrow$4Glcβ1$\rightarrow$1Cer)

G$_{M3}$ sialosyllactosylceramide (NeuAcα2$\rightarrow$3Galβ1$\rightarrow$4Glcβ1$\rightarrow$1Cer)

GSL   glycosphingolipid

HA   hyaluronic acid

HRP	horseradish peroxidase
HS	heparan sulfate
KS	keratan sulfate
Le^x	Lewis^x determinant (Galβ1→4[Fucα1→3]GlcNAcβ1→3Galβ1→4Glcβ)
MAFp3	*Microciona prolifera* protein found in the ring of the proteoglycan
MAFp4	*Microciona prolifera* protein found in the arms of the proteoglycan
Man	mannose
nLc$_4$	lactoneotetraosylceramide (Galβ1→4GlcNAcβ1→3Galβ1→4Glcβ1→1Cer)
PAGE	polyacrylamide gel-electrophoresis
PBS	phosphate buffered saline
SDS	sodiumdodecylsulfate
SSEA	stage specific embryonic antigen
TBE	Tris-borate-EDTA buffer
Tris	Tris(hydroxymethyl)aminomethane

II. INTRODUCTION

II.1. CARBOHYDRATE-CARBOHYDRATE INTERACTIONS IN CELLULAR RECOGNITION AND ADHESION

One of the fundamental features of a living cell is a prompt and adequate behavior during formation, maintenance, and pathogenesis of tissues. Thus, during development of the nervous system reversible cell extensions and connections are formed[1]. During embryogenesis adhesive forces between cells are repeatedly being built up and destroyed[2]. Lymphoid cells find their homing centers through intermediate adhesions to the vessel wall[3]. Cell surface receptors can be misused by microbial pathogens[4,5,6] or tumor cells[7]. These short-term adhesion and recognition events require reversible but still specific molecular surface interactions, rather than tight and stable adhesions between stationary cells. Carbohydrates, the most prominently exposed structures on the surface of living cells, with flexible chains and many binding sites are ideal to serve as the major players in these events. In contrast to the rapid progress in studies of cell recognition and adhesion through protein-protein[8] or protein-carbohydrate[9] interactions, the number and progress of studies on the possible role of carbohydrate-carbohydrate interactions in these events is still very small. There are mainly two model systems for studying the occurrence of carbohydrate-carbohydrate interactions. In vertebrates, glycosphingolipid self-interactions have been studied in early embryos and embryonic cell lines on one hand, and in tumor cell lines on the other hand. In invertebrates, marine sponge's cell-cell interactions mediated by carbohydrate-rich cell surface proteoglycan molecules have been studied.

II.1.1. CARBOHYDRATE INTERACTIONS IN VERTEBRATES – GLYCOSPHINGOLIPIDS

Eukaryotic cell membranes are characterized by a specific composition and enrichment of sphingolipids and glycosphingolipids (GSLs)[10]. GSLs are multifunctional molecules and dramatic and continuous changes in their surface expression and composition have been associated with differentiation, development and oncogenesis. The functional role of GSLs in these processes is still fragmentary, but they have been clearly identified as tumor-associate antigens[11,12], as receptors for microorganisms and their toxins[13], initiators of signal transduction[14], and finally as cell-type-specific antigens in cellular recognition and regulation of cell growth[15] (Fig.1).

GSLs can be classified as neutral, acidic (anionic), or basic (cationic). GSLs are also classified into three main series, i.e. ganglio-series, globo-series, type 1 lacto-series, and type 2 lacto-series, according to their core carbohydrate structure which may include one of two hundred different oligosaccharides. The main constituent of the plasma membrane is represented by acidic GSLs: gangliosides containing sialic acid. Other acidic GSLs contain a sulfate group. Gangliosides occur not only as well known ganglio-series but also as globo-series or lacto-series gangliosides. Each ganglioside series shows distinctive cell type or tissue type specificity, and they may play different functional roles in cell adhesion[10].

GSLs are present at the surface of the plasma membrane in the form of large clusters independent from the clusters of transmembrane glycoproteins[16] (Fig. 2). These GSL microdomains are variously referred to as glycosphingolipid-enriched domains, lipid rafts, or caveolae membranes[17,18]. Along with GSLs, also present in lipid rafts are sphingomyelin, cholesterol, glycosylphosphatidylinositol (GPI)-anchored proteins, and a variety of signaling molecules. Although the need for cholesterol in promoting assembly of gangliosides has been questioned[19], removal of cholesterol from plasma

membranes profoundly perturbs the physical state of microdomains[20] and compromises their function[21].

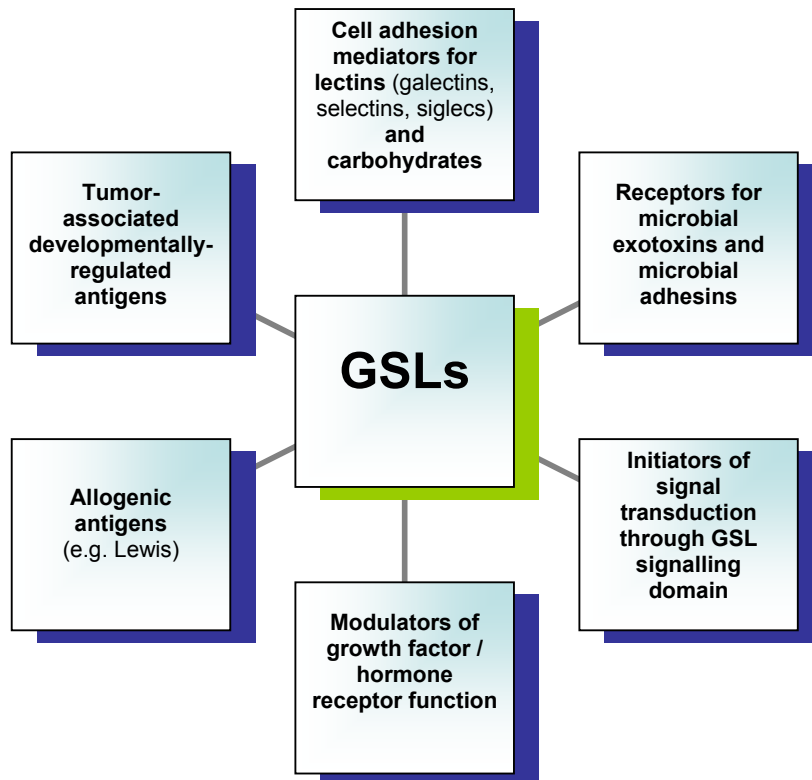**Fig. 1. Glycosphingolipids (GSLs) functions.** Six functions are shown schematically:
- Cell adhesion mediators (major topic of the introduction): [2, 10, 15, 28, 30, 34]
- Tumor-associated antigens: [7, 10, 11, 12, 38]
- Allogenic antigens: [10, 30, 105]
- Modulators of growth factor receptor function: [10]
- Initiators of signal transduction: [2, 14, 15, 19, 33, 35]
- Receptors: [4, 10, 13]

According to minimum energy conformation model[22], a common hydrophobic backbone of GSLs, i.e. ceramide, is inserted into the lipid bilayer of the plasma membrane (Fig. 3). The axis of the carbohydrate chain in GSLs is oriented perpendicular to the axis of ceramide. Ceramide consists of a fatty acid chain linked to the sphingosine base. It holds GSL carbohydrates in defined orientation through insertion in plasma membrane, and forms GSL microdomains separately from glycoprotein microdomains[23]. In the model, the outer surface of the carbohydrate chain, exposed at the cell surface, constitutes a hydrophobic domain surrounded by a hydrophilic area. Various ligands with a complementary structure can bind to this exposed hydrophobic domain, and two mechanisms of GSL-mediated cell adhesion have been observed: 1) Mediated by carbohydrate-binding proteins (lectins) that recognize specific GSL structures[24,25], and by siglecs, receptors with Ig homology whose N-terminal domain displays lectin activity to recognize various sialyl epitopes[26]; 2) Mediated by complementary carbohydrate moieties of GSLs through carbohydrate-to-carbohydrate interaction. In either model, cell adhesion based on the carbohydrate-carbohydrate interaction is the earliest event in cell recognition, followed by the involvement of adhesive proteins and of integrin receptors (Fig. 4).

Hakomori's group was first to show GSLs self-interactions as a possible basis for cellular recognition at the morula stage of mouse embryogenesis, in embryonal carcinoma cells, in specific aggregation of human embryonal carcinoma cells, and in recognition between lymphoma and melanoma cells.
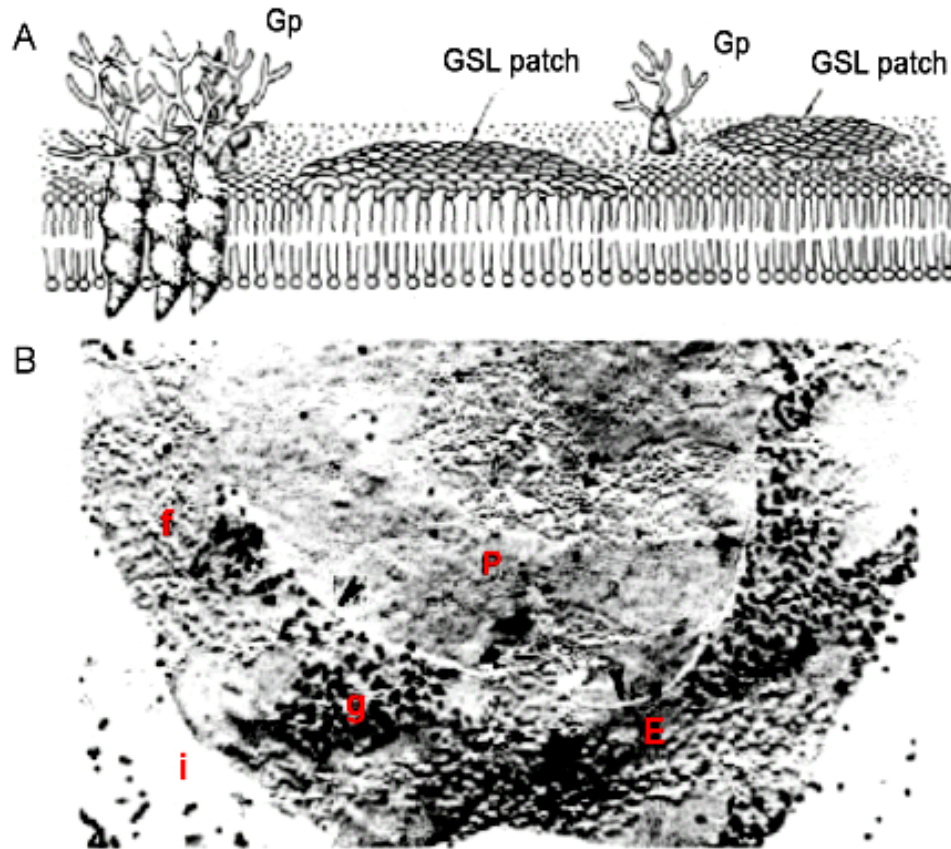
Fig. 2. Organization and distribution pattern of glycosphingolipids (GSL) and glycoproteins (Gp) at the cell-surface membrane. *A*, Proposed clustering of GSLs and Gp. *B*, Freeze-etch electron micrograph of a human erythrocyte membrane double-labeled with ferritin-wheat germ lectin and rabbit anti-globoside staphylococcal protein A colloidal gold. Ferritin-labeled areas (*f*) are well separated from the gold-labeled area (large black dots; *g*) at the external surface (*E*), indicating that these two major glycoconjugates form separate clusters.
i, surrounding ice; *P*, intramembranous particle surface, i.e. P face. The arrowhead indicates the fracture line.
Hakomori. S. 1993 (2).

Binding specificity to ligands (GSLs, lectins, antibodies)

Organization of GSLs in membranes
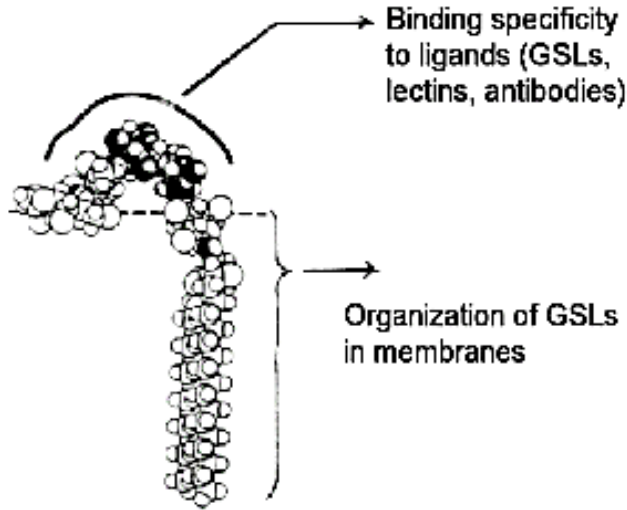
Fig. 3. Minimum-energy conformational model of globoside (Gb4Cer). The carbohydrate chain is oriented perpendicular to the axis of the ceramide. The outer surface of the carbohydrate chain, exposed at the cell surface, consists of a hydrophobic domain surrounded by hydrophilic groups, and a specific binding site for complementary GSLs, lectins, and antibodies.
Hakomori, S. 1993 (2).
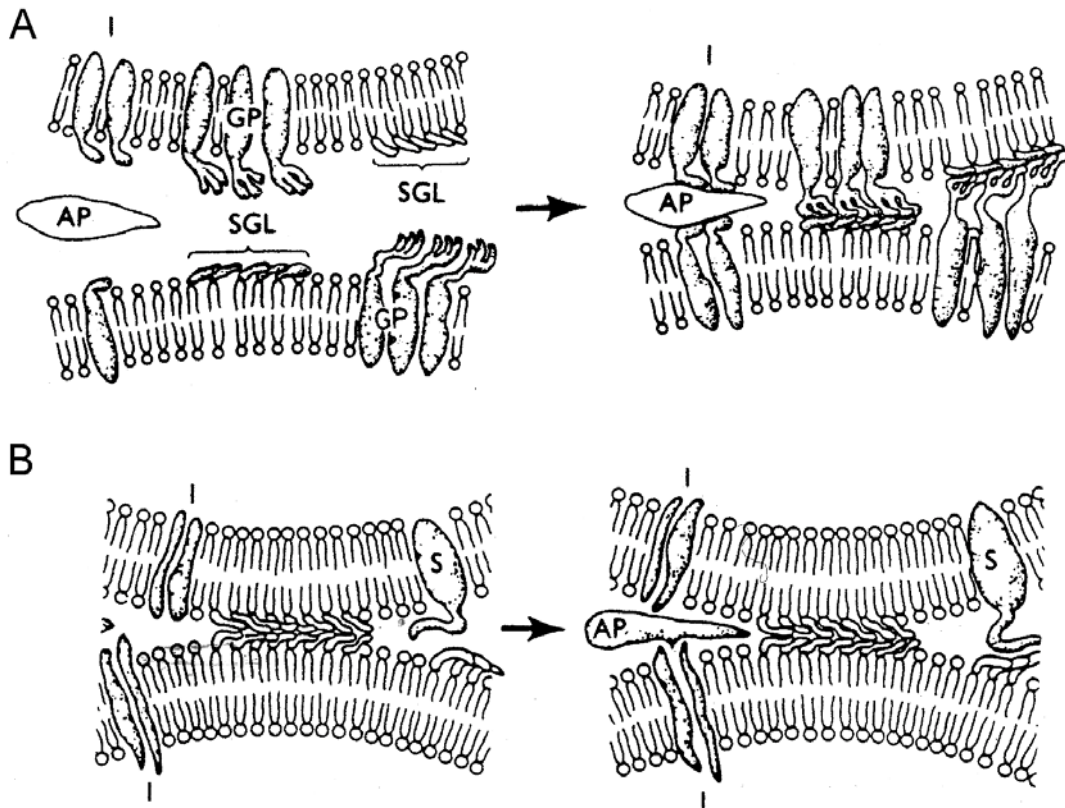
Fig. 4. The model of GSL-dependent cell adhesion based on the membranous organization of GSLs and glycoproteins (Gp). Compare with Fig. 2. **A**, The GSL cluster interacts with the Gp cluster; simultaneously, adhesive protein (AP) interacts with the integrin receptor (I). **B**, Interaction between GSL clusters on neighboring cells, subsequently reinforced by adhesive protein-integrin receptor interaction. *S*, selectin; *I*, integrin receptor; *AP*, adhesive protein.
Hakomori, S., et al. 2000 (15).

11

II.1.1.1. *Glycosphingolipids in embryonal development and in embryonal cell adhesion*

Patterns of GSL expression change greatly during development and differentiation. Early mouse embryos at the early 8- to 32-cell stage specifically express the Lewis[x] (Le[x]) determinant (also referred to as stage specific embryonic antigen-1 or SSEA-1) related to the Lewis blood group determinants. Le[x] shows maximal expression at the 16- to 32-cell stage and declines rapidly after compaction[27], i.e., tight aggregation of embryonal cells, beginning approximately after the third division of the fertilized egg. This pattern indicated a role of Le[x] in mediating compaction of the mouse embryo at the morula stage. Experimental evidence for a functional role for surface Le[x] was provided by the finding that a multivalent derivative of the oligosaccharide lacto-N-fucopentaose III (LNF III), which contains Le[x] determinant in its structure, caused decompaction of fully compacted mouse embryos[28]. Compaction is a Ca^{2+}-dependent cell adhesion event, the first of many specific cell-cell interactions occurring during mammalian embryogenesis. Without this adhesion subsequent development of the embryo may not occur.

A remarkable similarity has been demonstrated between the processes of morula compaction in early embryogenesis and aggregation of undifferentiated F9 mouse embryonal cells. F9 cells mimic the morula-stage preimplantation embryo and show Ca^{2+}-dependent cell aggregation. They also express high levels of cell surface Le[x] at the undifferentiated stage, which declines upon differentiation[29]. It has been found that Le[x] at the cell surface is recognized *per se* by another Le[x], and that this Le[x]-Le[x] interaction mediates aggregation of F9 cells in the presence of a bivalent cation[30]. Both results, with mouse embryos and mouse embryonal cells, clearly indicated that Le[x], a specific carbohydrate structure, is capable of self-interacting, and suggest that this carbohydrate-carbohydrate interaction may account for cellular recognition.

Many human embryonal carcinoma cells, particularly at the undifferentiated stage, show high expression of globo-series GSLs structures including SSEA-3 and -4,

which are down-regulated upon differentiation in parallel with a decrease in cell adhesion[31,32]. Undifferentiated human embryonal carcinoma 2102 cells express high amounts of the Le^x precursor lactoneotetraosylceramide (nLc$_4$) and SSEA-3 (with the major epitope GalGb4), and moderate level of globoside (Gb4)[33]. Expression of these GSLs declines in association with a decline of homotypic adhesion during the differentiation process. 2102 cells adhere strongly to Gb4 and gangliotriaosylceramide (Gg3) coated on plates, while they do not adhere to other GSL epitopes[33]. Adhesion of 2102 cells to Gb4, which stimulates cell aggregation, is based on carbohydrate-carbohydrate interaction between nLc$_4$ or GalGb4 (expressed on cells) and Gb4 (coated on plates). Furthermore, binding to Gb4 induces signal transduction in terms of activation of transcription factors AP1 and CREB. Binding to Gg3 does not result in any cell activation indicating that there is also some qualitative difference in binding to different GSL layers. These findings prove that Gb4 and globo-series GSLs are involved in cell adhesion, analogous to the involvement of Le^x in compaction of mouse embryo and aggregation of F9 cells.

II.1.1.2. Glycosphingolipids in specific recognition between lymphoma and melanoma cells

Further support for the role of carbohydrate-carbohydrate interactions in cellular recognition was provided by the demonstration of the specific aggregation of mouse lymphoma L5178 cells with mouse melanoma B16 cells based on the interaction between two gangliosides: Gg$_3$ and G$_{M3}$[34]. Gg$_3$ is highly expressed at the surface of mouse lymphoma cells and G$_{M3}$ (sialosyllactosylceramide) is expressed at the cell surface of mouse melanoma cells. The interaction between cells was inhibited by monoclonal anti-Gg$_3$ and anti-G$_{M3}$ antibodies. Since these antibodies are highly specific for the gangliosides and do not cross-react with carbohydrates on glycoproteins, it has been assumed that the specific cellular recognition between the lymphoma and melanoma cells is indeed based on molecular carbohydrate-carbohydrate interactions between Gg$_3$ and G$_{M3}$. Adhesion of B16 melanoma cells to

Gg3-coated surfaces enhanced tyrosine phosphorylation of FAK[35]. Direct binding between G_{M3} on the cell surface to Gg3 on the coated plates has been suggested as the activating mechanism since antibodies against G_{M3} could activate FAK.

The adhesion and spreading of B16 melanoma cells on coated culture dishes was mostly obvious at early stages of cell plating, which indicates that GSL-mediated interaction are very early phenomena in cellular interactions to be overtaken in later stages by protein- mediated binding[36]. Furthermore, melanoma cells could adhere and spread faster on glycolipids coated on plates than to extracellular matrix proteins: laminin or fibronectin coated on plates[37]. Different clones of the B16 line with different expression levels of the predominant GSL were tested for their binding behavior to non-activated endothelial cells. Binding of melanoma cells to endothelial cells was faster but weaker than binding to laminin or fibronectin, and was dependent on G_{M3} expression level. Under shear forces, binding strength of the mutant B16 cells was still correlated to the expression level of G_{M3}, but it was stronger than the binding via extracellular proteins. Upon these findings, it has been suggested that matastatic tumor cells make use of the high expression rates of certain glycolipids to attach to the unstimulated endothelium, before next steps in cell activation and transmigration are mediated by protein-protein interactions[38].

GSL-dependent cell adhesion can modulate signal transduction. G_{M3}-dependent adhesion of melanoma cells enhanced tyrosine phosphorylation of cSrc and FAK, and enhanced GTP binding to Rho A and Ras[15]. Enhanced motility of melanoma cells caused by G_{M3}-dependent adhesion to endothelial cells was regarded as the initial step of melanoma cell metastasis[38].

II.1.2. CARBOHYDRATE INTERACTIONS IN INVERTEBRATES – PROTEOGLYCANS

Virtually all animal cells produce proteoglycans, which vary greatly in structure, expression and functions[39,40]. They are found in all connective tissues, extracellular matrix, and on the surfaces of many cell types. Proteoglycans participate in and regulate cellular events and (patho)physiological processes via either their carbohydrate chains (glycosaminoglycans, GAGs) or their core proteins (Fig. 5). The GAG chains have the ability to fill the space, bind and organize water molecules and repel negatively charged molecules. Because of high viscosity and low compressibility they are ideal for a lubricating fluid in the joints. On the other hand their rigidity provides structural integrity to the cells and allows the cell migration due to providing the passageways between cells. For example the large quantities of chondroitin sulfate (CS) and keratan sulfate (KS) found on aggrecan play an important role in the hydration of cartilage. They give the cartilage its gel-like properties and resistance to deformation. Proteoglycans have the ability to regulate proteolytic enzymes and protease inhibitors. Functions of proteoglycans in cell and tissue development and physiology are mediated by specific binding of GAGs or core proteins to other macromolecules. They bind to signalling molecules, which can lead to the stimulation or prevention of the activity of growth factors. Cell surface proteoglycans act as co-receptors, e.g. syndecans serve as a receptor with integrin for fibronectin and other matrix proteins. Despite their structural and functional diversity, proteoglycans do have a general propensity to be extracellular matrix components and to mediate specific matrix interactions and biological activities related to different aspects of cell adhesion[41,42], but many of their roles in these cellular processes are still poorly understood.
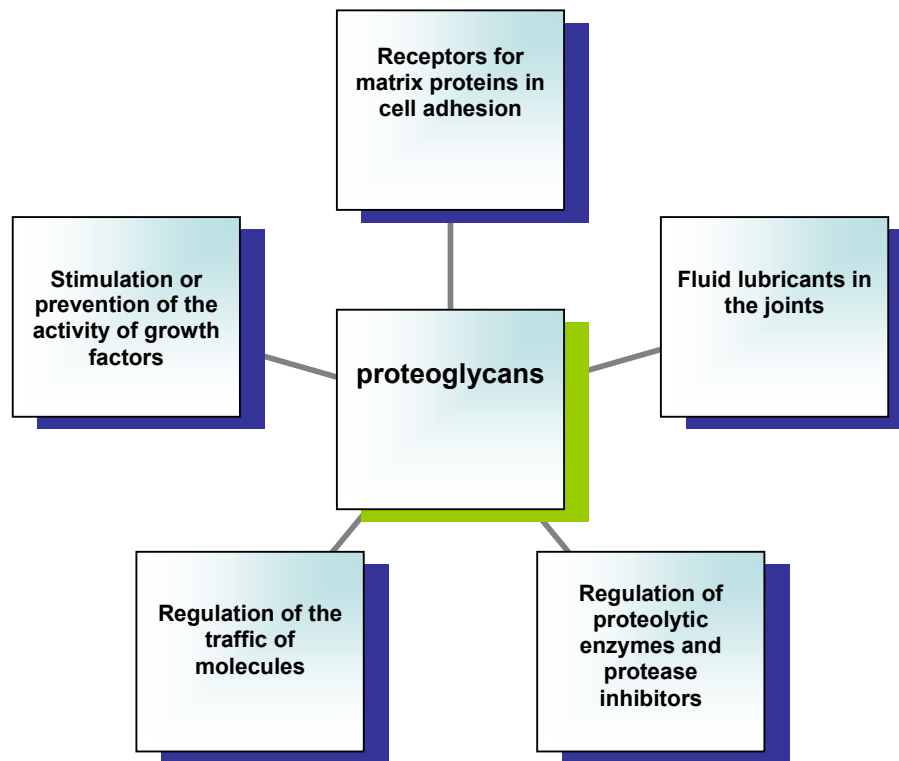
Fig. 5. Proteoglycans functions. Five different functions are shown schematically and they are reviewed in 39-42, and in 48.

A sulfated carbohydrate component of proteoglycan molecules, glycosaminoglycan (GAG), is covalently linked to the core protein (Fig. 6). Core proteins vary in size from 11'000 to about 220'000 Da. The number of GAG chains attached to the core protein varies from one to about 100. There are four main types of GAGs: 1) heparin / heparan sulfate (HS)[43], 2) chondroitin sulfate (CS)[44] / dermatan sulfate (DS)[45], 3) keratan sulfate (KS)[46], and 4) hyaluronic acid (HA)[47]. Each GAG is a polymer of a disaccharide, which in heparin, HS, and HA consists of N-acetyloglucosamine and uronic acid, in CS and DS of N-acetylogalactosamine and uronic acid, and in KS of N-acetyloglucosamine and galactose. The sugars in GAGs are sulfated to varying degrees. An exception is HA, which is not sulfated and is the only GAG present

under its free form and possessing the ability to aggregate with the class of proteoglycans termed hyalectans[48]. There is a potential for an enormous number of proteoglycans due to the variations in the molecular weight of the core protein, in the types and number of GAG chains attached to the protein core, and in sulfation degree[39].
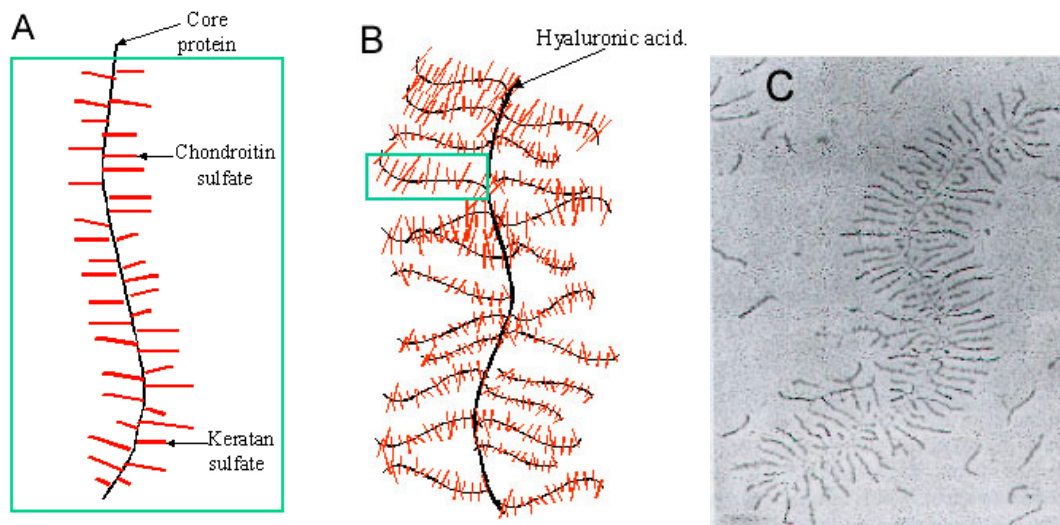
Fig. 6. Schematic representation of a proteoglycan structure. *A*, A single proteoglycan consists of a core protein molecule to which a large number of glycosaminoglycan chains (GAGs, shown in red) are covalently attached. ***B*,** In the cartilage matrix, individual proteoglycans (in box from fig. *A*) are linked to a non-sulfated GAG, called hyaluronic acid (HA), to form a giant complex with a molecular mass of about 3'000'000. ***C*,** Electron micrograph of a proteoglycan complex isolated from cartilage complex.

The very first experimental demonstration of cellular recognition and adhesion phenomena in the animal kingdom was assigned to the cell surface proteoglycan[49] and came from invertebrates, i.e. from marine sponge model system[50,51]. Sponges evolved from their unicellular ancestors about 1 billion years ago by developing cellular recognition and adhesion mechanisms to discriminate against "non-self".

They are the simplest and earliest multicellular organisms. They do not have any defined organs or tissues, and only a limited number of cells remain motile within the animal. Remarkably, dissociated sponge cells from two different species have the capacity to reaggregate through surface proteoglycans by sorting out according to their species of origin, in the same way as mixtures of dissociated embryonic cells from two vertebrate tissues sort out according to their tissue of origin.

The purification of proteoglycans is often complicated, but sponge proteoglycans are very easy to extract in large quantities by removal of extracellular calcium, and they are abundant in the sponge extracellular matrix. It makes sponges one of the best potential models to study proteoglycan structure and function. Consequently, this simple and highly specific cellular recognition phenomenon of cell-cell aggregation in sponges has been used for almost a century as a model system to study specific cellular recognition and adhesion occurring during tissue and organ formation in multicellular organisms.

II.1.2.1. Structure and function of sponge proteoglycan

The extracellular matrix of the sponge is similarly composed to that of higher Metazoans, containing proteoglycan molecules, collagens and other glycoproteins. Sponge surface proteoglycans[52], otherwise known as aggregation factors (AFs), are large molecules with an approximate molecular weight raging from 2 x 10^4 kDa[53,54] to 1.4 x10^6 kDa[55]. Based on their composition and on their electron[56] and atomic force microscope (AFM) images[57], sponge cell surface proteoglycan molecules show either a linear or a sunburst-like core structure with 20-25 radiating arms (Fig. 7). AFM visualization of sponge proteoglycans allowed a better estimation of their molecular dimensions and showed remarkable similarities between molecules from different species (Table 1).   Prolonged (4-weeks) EDTA-treatment of the

proteoglycan disrupts the arms from the core structure, indicating that the cation is important for the structural integrity of the complex[57].

Specific cellular recognition of marine sponges is mediated by cell surface proteoglycan molecules in a Ca^{2+}-rich environment (~ 10 mM, as in seawater). The model of proteoglycan-mediated cell-cell adhesion currently used assumes that the proteoglycan molecule is immobilized via its arms onto the cell surface and the core structure interacts with the core structure immobilized on another cell (Fig. 8). The molecular basis of the selective cell-cell adhesion in most multicellular animals is mediated by two distinct classes of molecules: a Ca^{2+}-idependent activity like that typical of the glycoproteins from the Ig superfamily[58], and a Ca^{2+}-dependent cell-cell adhesion, whose best example is the cadherins[59]. Interestingly, sponge proteoglycans reunite both functions in the same molecule and mediate species-specific cell-cell recognition via two functionally distinct domains: 1) a calcium-independent cell-binding domain and 2) a calcium-dependent self-association domain which is providing the intercellular adhesion force.

Receptors for sponge proteoglycans are called baseplates. *Microciona prolifera* cellular receptors include membrane-associated glycoproteins of 210 kDa and 68 kDa[60] with low carbohydrate content, and with a high affinity to both the cells and the proteoglycan molecules[61,62]. *Geodia cydonium* receptors are of low molecular weight (M_r = approximately 20'000) and consist chemically of glycoproteins with high carbohydrate content[63].

The binding of surface proteoglycans to sponge cells triggers a wide variety of cellular responses. The addition of purified proteoglycans to primary cell aggregates of *Geodia cydonium* resulted in increased DNA, RNA, and protein synthesis, and in higher mitotic activity[64,65]. Moreover, binding of the surface proteoglycan to *Geodia* cells triggered protein phosphorylation[66] and *ras* gene expression[67]. Finally, involvement of main proteins of *Microciona prolifera* surface proteoglycan in sponge histocompatibility has been suggested[68].

Microciona prolifera proteoglycan

Halichondria panicea proteoglycan

Suberites fuscus proteoglycan
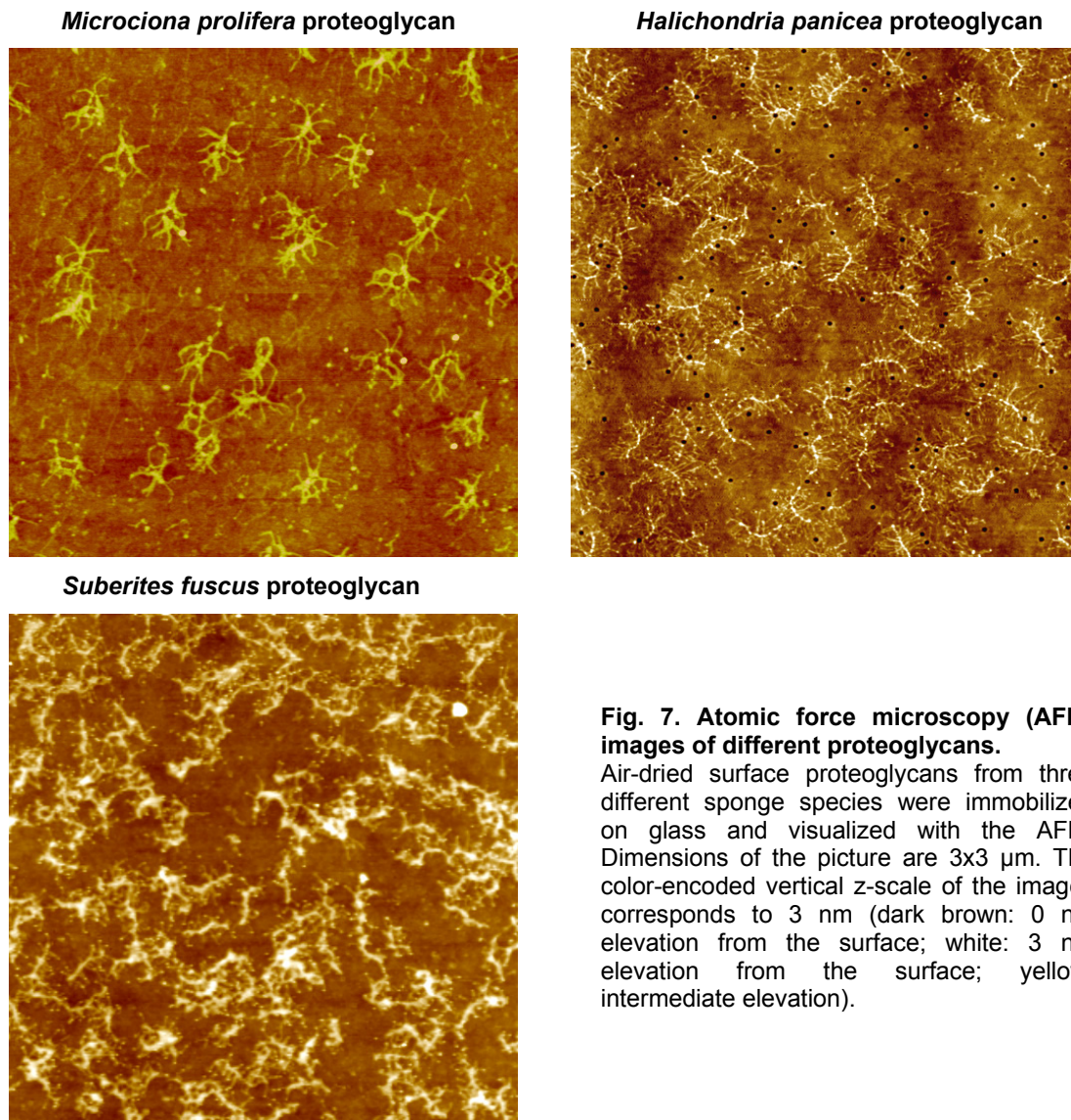
Fig. 7. Atomic force microscopy (AFM) images of different proteoglycans.
Air-dried surface proteoglycans from three different sponge species were immobilized on glass and visualized with the AFM. Dimensions of the picture are 3x3 µm. The color-encoded vertical z-scale of the images corresponds to 3 nm (dark brown: 0 nm elevation from the surface; white: 3 nm elevation from the surface; yellow: intermediate elevation).

Table 1. Molecular dimensions of proteoglycans from three different sponge species as estimated from AFM images.

proteoglycan	backbone shape	backbone length (nm)	arm length (nm)	number of arms
M. prolifera	Ring	285	143	ca. 20
H. panicea	Rod	280	140	ca. 20
S. fuscus	Rod	220	80	ca. 20

Jarchow, J., et al. 2000 (57).
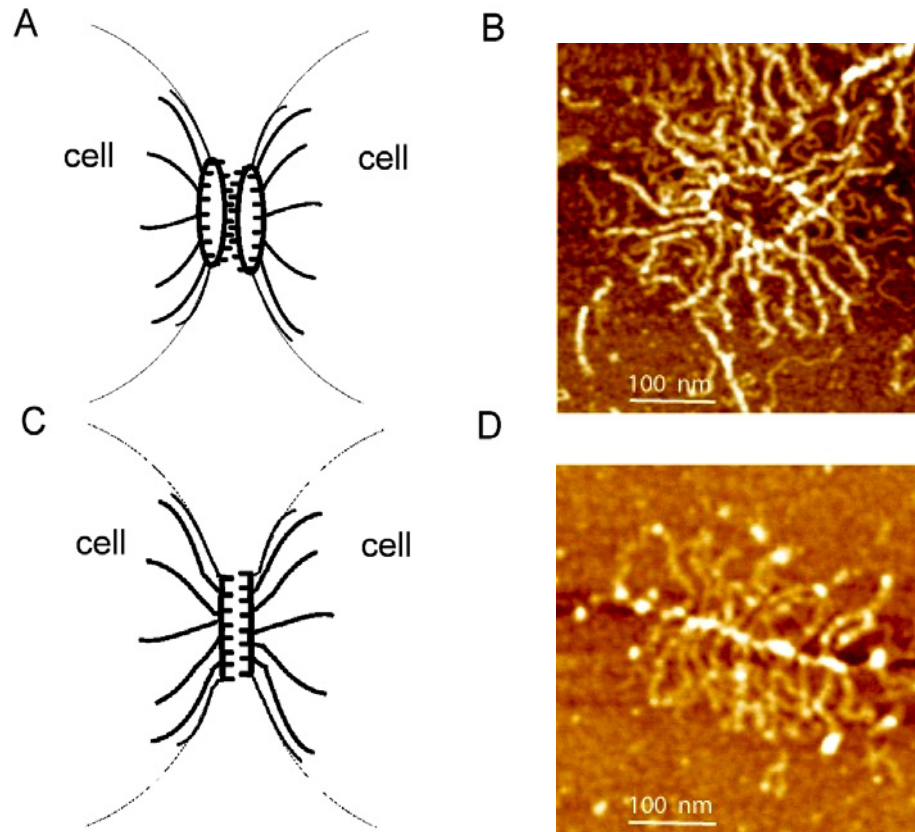
Fig. 8. The model of proteoglycan-mediated cell-cell adhesion.
A, Proteoglycan molecule with a ring core structure is immobilized via its arms to the cell surface and mediates cell-cell interaction via its ring structure. *B*, Atomic force microscopy (AFM) image of a circular-structure proteoglycan. *C*, Proteoglycan molecule with a backbone core structure is immobilized via its arms to the cell surface and mediates cell-cell interaction via its backbone structure. *D*, AFM image of a backbone-structure proteoglycan.

The protein and carbohydrate content in purified proteoglycans varies among different sponges. Proteoglycans can consist of as high as ~75% protein and just ~25% carbohydrates, as in indicated for *Geodia cydonium*[69] and *Suberites domuncula*[70]. In contrast, *Microciona prolifera* proteoglycans consist of about 60% carbohydrates and 40% proteins[49].

At present, the surface proteoglycan from the read beard sponge, *Microciona prolifera*, is best characterized. There are two main proteins in *Microciona* circular proteoglycan, termed MAFp3 (ranging from 30 to 50 kDa) and MAFp4 (~400 kDa)[57]. Both molecules are extremely polymorphic[71]. MAFp3 is found exclusively in the ring structure, while MAFp4 is found exclusively in the arms[57]. As in most large proteoglycans, the MAFp4 core protein has a modular structure made of tandem repeats[68]. However, MAFp4 does not have significant sequence homologies with any known proteoglycans. The closest matches, i.e. 30% identity with MAFp4 repeats, were found in two apparently unrelated proteins: the intracellular loop of Na^+-Ca^+ exchangers[72] and a similar domain-structured endoglucanase from the symbiotic bacterium *Azorhizobium caulinodans*[68]. Two different carbohydrates with molecular masses of ~6 and ~200 kDa are found in the core structure and the arms of adhesion proteoglycans.

II.1.2.2. Carbohydrate moiety of sponge proteoglycan

Microciona prolifera surface proteoglycans carry two N-linked glycan molecules: one with a mass of 6.3 kDa[73] (termed g-6), believed to bind to a cell surface receptor independently of Ca^{2+} ions, and one with a mass of ~200 kDa[74] (termed g-200) that self associates in a Ca^{2+}-dependent manner[75] (Fig. 9). G-6 is the main glycan present on MAFp4 protein in the arms of proteoglycan molecule, and each arm contains about 50 g-6 units[57]. G-200 is the main glycan present on MAFp3 protein in the ring structure of the proteoglycan. One *Microciona* proteoglycan molecule has ~26 copies of g-200 glycan. In AFM images, 20 globular structures forming the ring of the molecule can be seen (Fig. 10). If each of this structure represents a MAFp3 protein, one or two g-200 units should be present on the protein. Indeed, one or two short linear structures protruding from each of the 20 globular structures can be seen on AFM images (Fig. 10), suggesting that they are g-200 glycan molecules. In agreement with this hypothesis, their height: 0.55 ± 0.1 nm is almost identical to the

AFM thickness measurements of glycosaminoglycan chains like hyaluronan[76]. These observations consent to the model of proteoglycan-mediated cell-cell interactions (Fig. 8), which assumes that the proteoglycan-surface receptor binding is mediated through the arms (where g-6 glycan is found), whereas proteoglycan-proteoglycan binding is mediated through the core (ring or backbone) structure (where g-200 glycan is found).

Carbohydrate moiety participation in the adhesion process was anticipated after it was found that glycosidase treatment[77] and periodate oxidation[75] destroyed the aggregation activity of proteoglycan molecules. Glass aminopropyl beads, coated with protein-free200 kDa glycan, showed a Ca^{2+}-dependent aggregation equivalent to that of proteoglycan-coated beads[74]. The monoclonal antibody raised against the purified surface proteoglycan of *Microciona prolifera* (Table 2) blocked cell aggregation, for which the epitopes recognized were identified as short carbohydrate units of the 200 kDa glycan: a sulfated disaccharide[78] and a pyruvylated trisaccharide[79]. Recently, a concept of self-recognition of defined carbohydrate epitopes playing a role in cellular adhesion was confirmed[80]. To investigate this phenomenon a system has been designed, surface plasmon resonance detection, to mimic the role of carbohydrates in cellular adhesion of *Microciona*. The results showed self-recognition of the sulfated disaccharide to be a major force behind the calcium-dependent cell-cell recognition event. Nevertheless, specific interactions between 200 kDa glycan molecules from different sponge species have not yet been investigated to prove the existence of specific carbohydrate-carbohydrate recognition in proteoglycan-mediated cellular recognition and adhesion systems, as it has been done with glycosphingolipids.
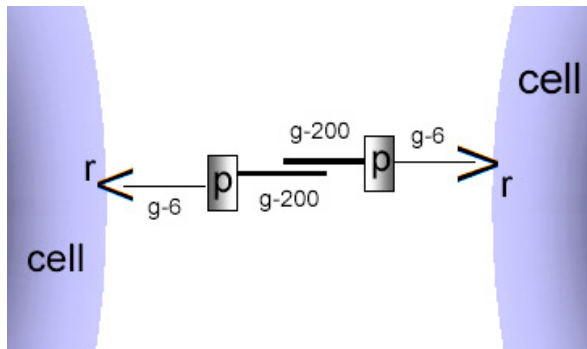
Fig. 9. The model of carbohydrate-mediated cell-cell adhesion in *Microciona prolifera* sponge.
g-6 glycan (6.3 kDa) binds to the cell surface receptor (*r*). g-200 glycan (~200 kDa) from one cell interacts with g-200 glycan from another cell mediating cell-cell adhesion. *p*, proteoglycan core protein.
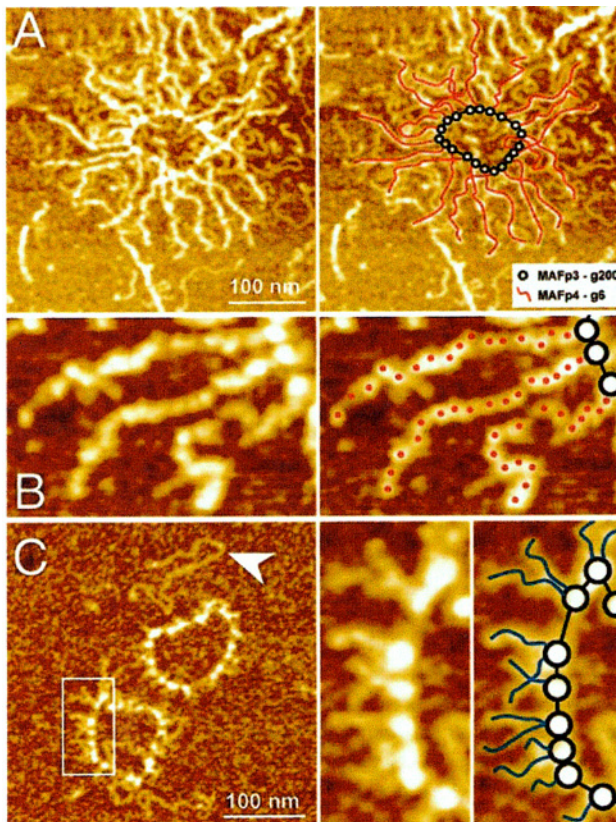
Fig. 10. The model of *Microciona prolifera* cell surface proteoglycan structure. *A*, Atomic force microscopy (AFM) image of native *Microciona* proteoglycan showing the localization of MAFp3 in the ring (*black circumferences*) and of MAFp4 in the arms (*red lines*). MAFp3 carries the g-200 glycan and MAFp4 the g-6 glycan. *B*, Detail of an AFM image of the proteoglycan molecule showing 15-16 domains (*red dots*) observed in each arm in the native structure. *C*, AFM image of the proteoglycan rings and of an isolated rod-like chain (*arrowhead*). It has been suggested that in the native proteoglycan the rod-like molecules runs along the circumference of the ring, stabilizing its interaction with the arms. The enlarged inset shows a detail of the ring structure with short chains protruding that might represent the g-200 glycan (*blue lines*).
The color-encoded vertical z-scale of all the images corresponds to 3 nm.
Jarchow, J., et al. 2000 (57).

Table 2. Antibodies against *Microciona prolifera* proteoglycan and their epitopes.

antibody	nr of binding sites / *Microciona* proteoglycan	reactivity	epitope structure[78]
block 1 (clone 12)	1'100[108] (200-300)[79]	g-6 and g200	Pyr< $^6_4$ >Galβ1-4GlcNAcβ1-3Fuc
block 2 (clone 17)	2'500[74]	g-200	GlcNAcβ1-3Fuc I 3SO₃
C-16 (clone 16)	2'000[74]	g-200	Galα1-2Galβ1-4GlcNAcβ1-3Fuc I 3SO₃

Misevic, G., et al. 1987 (108)
Misevic, G., et.al. 1993 (74)
Spillmann, D., et al. 1995 (78)
Spillamm, D., et al. 1993 (79)

The carbohydrate composition of the glycans is very different between at least two species. Carbohydrate analysis of *Microciona prolifera* and *Halichondria panicea* adhesion proteoglycans[81] has shown that both contain galactose, fucose, mannose, N-acetylglucosamine, N-acetylgalactosamine and glucuronic acid (Table 3). The composition between different individuals of the same species is very similar but large differences are seen between individuals from two different species (Fig. 11). The most striking differences are the low galactose and the high fucose, N-acetylgalactosamine and glucuronic acid content in *Microciona* as compared to *Halichondria*.

Table 3. Carbohydrate composition of proteoglycans between two different sponge species.
Carbohydrates were analyzed by high performance anion exchange chromatography with pulsed amperometric detection as described [81]. The average values in mol% were obtained from four *Halichondria* and three *Microciona* individuals. Standard deviation (SD) is given.

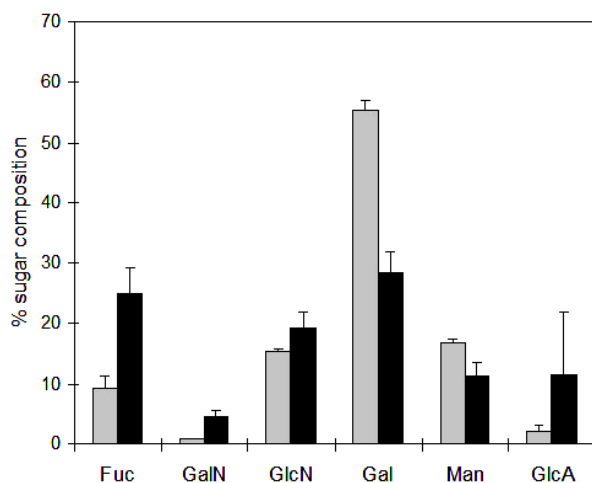| Carbohydrates (mol %)	*Halichondria panicea* ± S.D. (4 individuals)		*Microciona prolifera* ± S.D. (3 individuals)	
Fuc	9.36	± 1.87	24.89	± 4.52
GalN	0.83	± 0.13	4.54	± 0.90
GlcN	15.46	± 0.34	19.15	± 2.80
Gal	55.40	± 1.76	28.51	± 3.28
Man	16.85	± 0.55	11.38	± 2.34
GlcA	2.08	± 1.11	11.58	± 10.42

Jarchow, J., et al. 1998 (81).

Fig. 11. Comparison of the carbohydrate composition of proteoglycans between two different sponge species. *grey bar*, carbohydrate composition of *Halichondria panicea* proteoglycan. *black bar*, carbohydrate composition of *Microciona prolifera* proteoglycan.

II.2. MOLECULAR BASIS OF CARBOHYDRATE-CARBOHYDRATE INTERACTIONS

II.2.1. POLYVALENT CHARACTER OF CARBOHYDRATE-CARBOHYDRATE INTERACTIONS

Molecules involved in cell-cell or cell-matrix adhesion must have an adequate affinity or avidity, i.e. bind strongly enough to mediate specific biological recognition under natural circumstances. Molecular interactions where carbohydrates are involved are usually considered as weak interactions. The definition of "weak interaction" is rather arbitrary and based upon binding strength of carbohydrates surviving extensive washing during procedures such as direct binding to cells, affinity chromatography, or detection by blotting (described by IC_{50}[24] or K_a values[82]). Although the data is incomplete, it is generally accepted that biologically relevant recognition involves higher order structures, i.e. multimerisation of carbohydrate molecules in order to generate a sufficient affinity or/and avidity to function *in vivo*[24,83]. Such biological relevance can be achieved through polyvalence, i.e. the repetition of the binding motif to ensure sufficient binding strength. A suitable mechanism for keeping two interacting carbohydrate chains arranged in a polyvalent array together would be a zipper (Fig. 12)[83]. This model provides the simplicity by which nature may create specificity between two compositionally rather similar structures interacting with one another.
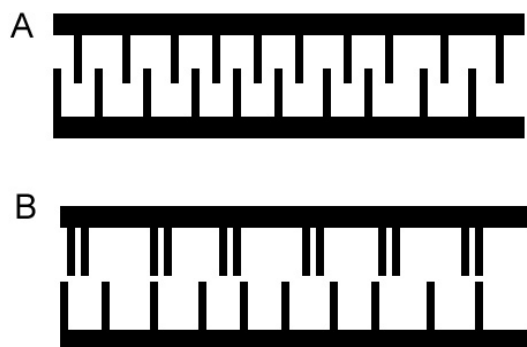
Fig. 12. Schematic representation of the polyvalent sugar zipper as a possible model of the carbohydrate-carbohydrate interaction. *A*, An optimal spacing and pattern of "zipper teeth" (interacting components) allows optimal pairing and promotes the interaction between two carbohydrate molecules. *B*, Faulty spacing and pattern of "zipper teeth" does not allow pairing and restricts the interaction between two carbohydrate molecules.

The creation of repetitive, interacting glycan sequences *in vivo* is feasible in different modes. Oligosaccharide motifs can be repeated along the primary glycan sequence as seen in plant cell wall carbohydrates. Glycans can also be arranged in a repetitive pattern along the backbone structure which is not directly participating in binding, e.g. in mucin structures on protein backbones[24], or by branching carbohydrates on a glycan scaffold, e.g. blood group antigens on poly-N-acetyllactosamine type glycan backbones[27,84]. Proteoglycans, glycoproteins or glycolipids can be presented on cell surfaces in clusters or superstructures[17,18]. It has been shown that GSLs form clusters within membranes and are not randomly distributed[85,86]. They accumulate on apical surfaces of epithelial cells[13,87], and form patches in blood cells[10]: e.g. erythrocyte membranes[88], peripheral lymphocytes[89,90], monocytes and macrophages[91], and particularly in myeloid cells and neutrophils[92,93].

Polyvalence *in vitro* allowed carbohydrate molecules to bind together and gave the chance to measure carbohydrate-carbohydrate interactions by different methods. Polyvalence could be achieved by crosslinking of the g-200 glycans isolated from *Microciona* surface proteoglycan (M_r = 200 kDa) with diepoxybutane / glutaraldehyde to form polymers containing a similar number of g-200 repeats to that in the native proteoglycan molecule. The cross-linked polymer of $M_r > 15 \times 10^6$ were

28

attached to glass aminopropyl beads, which then could aggregate mimicking specific cell-cell aggregation[74]. Similarly, binding of g-6 *Microciona* glycan to cell surface receptor through a carbohydrate-protein interaction has been reconstituted by polymerizing the glycan. G-6 glycan (M_r = 6.3 kDa) binds to its cell with a $K_a < 10^3$ M^{-1}, when molecules involved in cellular adhesion have mostly association constants above 10^5 M^{-1}. However, when the g-6 glycan was *de novo* polymerized into multivalent complexes through crosslinking of the isolated glycan chains with diepoxybutane / glutaraldehyde to approximately reconstitute the native proteoglycan size (M_r = 2 x 10^4 kDa), the binding to the cell was raised by more than six orders of magnitude (1.6 x 10^9 M^{-1})[73,94]. This essentially restituted the full biologically relevant binding strength.

Similarly, in GSL-GSL interactions, the adhesion of tumor cells to GSLs coated on the plates was strictly dependent on the concentration of GSLs on the solid phase[34,36]. Interactions between GSL liposomes varied with the respective densities of the GSL on liposomes[35]. Moreover, hydroxylation and increase in the length of the fatty acid chain of either galactosylceramide (GalCer) or cerebroside sulfate (CBS) significantly affected the extent of the interaction between the two glycolipids[95]. This suggested that developmental control or pathological changes can effect cellular interactions mediated by carbohydrate-carbohydrate interactions.

Polyvalence can be easily controlled by various means: surface density of presented structures, ionic strength to modulate attractive vs. repulsive forces, subtle changes in biosynthesis of the carbohydrate sequences, etc. These allow changing the affinity of the interactive molecules and therefore creating a highly flexible and specific model of recognition system. The model assumes gradual adhesion between two different cells or cell and matrix by allowing cells to test surrounding surfaces and first slightly complex before releasing or reinforcing adhesion[96].

II.2.2. MOLECULAR FORCES IN CARBOHYDRATE-CARBOHYDRATE INTERACTIONS

The molecular forces active between carbohydrates are not different from those acting between other biological molecules[82] (Fig. 13). Carbohydrates offer a rich source for hydrogen bonds due to hydroxyl-, amine- and carboxy-groups. Hydrogen bonds are considered to be dipole-dipole type interactions, but they are stronger than dipole-dipole and dispersion forces[97]. They are formed when an H-atom in a polar bond (e.g. H-F, H-O, or H-N) can experience an attractive force with a neighboring electronegative molecule or ion, which has an unshared pair of electrons (usually F, O, or N atom on another molecule).

Hydrogen bonding can be seen both intramolecular and intermolecular or in combination with the solvent[98,99]. Very high number of hydrogen bonds could be seen in the crystal of Le[x] with bonds between the trisaccharide and water, and between the carbohydrates themselves[100]. An indirect consequence of intramolecular hydrogen bonding has been suggested for HA. Exposure of a larger hydrophobic patch in the chain for neighboring residues in HA could favor hydrophobic interactions between different chains[101]. A different interpretation based on similar data from molecular dynamics models for short saccharide sequences would suggest the rapid exchange of different intramolecular hydrogen bonds in favor of a prolonged solubility of even high concentrations of HA[102]. Nevertheless, it is still unknown which are the driving forces *in vivo*.
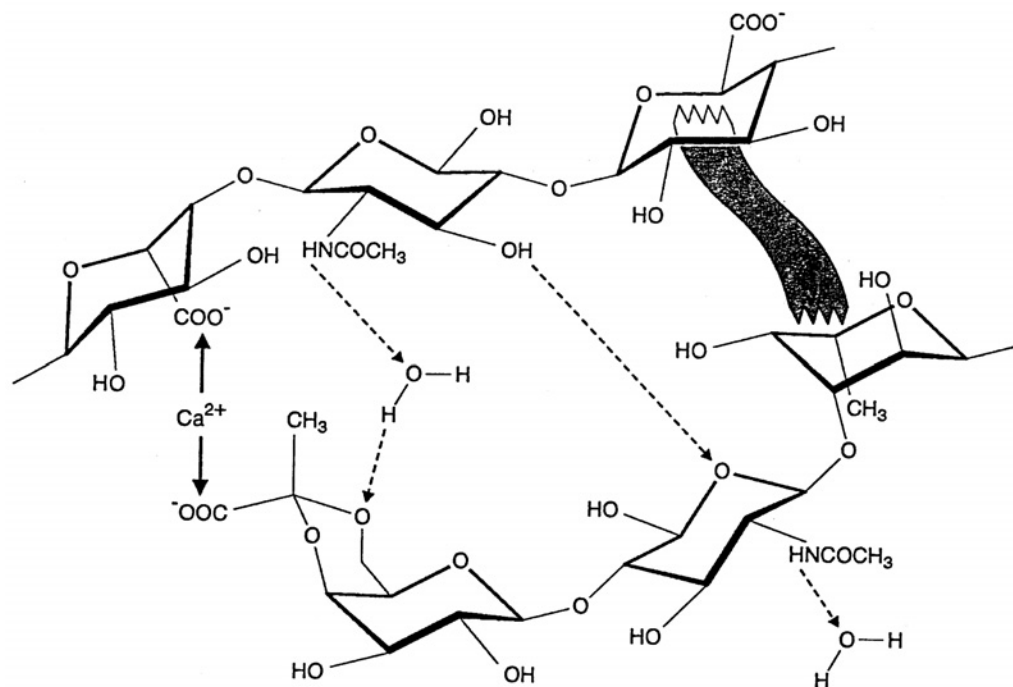
Fig. 13. Schematic representation of stabilizing forces between two carbohydrate chains in sponge glycans. Possible hydrogen bridges (*arrows with dashed lines*), hydrophobic surfaces (*shaded area*), and ionic interaction (*Ca^{2+} between arrows*) sites are sketched between two carbohydrate chains. Interactions do not have to occur between different oligosaccharide sequences of a glycan as depicted, but they can also occur between identical sequences.
Spillmann, D., et al. 1996 (82).

Carbohydrate-carbohydrate interactions are based mainly on van der Waals contacts between the corresponding polyaphilic surfaces involved in the process[103]. Van der Waals forces typically include dipole-dipole and London dispersion forces, and sometimes the hydrogen bonding forces are also included with this group[104]. The complementary nature of polyaphilic surfaces in carbohydrate-mediated interactions make the interaction highly specific and Ca^{2+}-ions seem to be crucial for this process to occur in biological and other model systems[103]. The role of calcium in carbohydrate-carbohydrate interactions is not well understood. Ca^{2+}-ions could be responsible for the approach and organization of the sugar moieties which provide the adequate surfaces for interaction. They may also enhance the adhesion force

between complementary surfaces, acting as a bridge between specific hydroxy groups.

In marine sponges, Ca^{2+}-ions are essential in carbohydrate-carbohydrate interactions. On the molecular level, they probably provide coordinating forces[80], though ionic forces cannot be excluded. Most carbohydrates are neutral or negatively charged due to carboxy- and sulfate- groups, but also positively charged glycans occur and rare ionic interactions can take place. Ca^{2+} effect is not merely a charge effect since it has been shown that not just every acidic sponge glycan is interacting in the presence of Ca^{2+}. Although single hydroxyl groups are too weak to coordinate cations, the combination of two to three well positioned hydroxyl groups on one sugar residue or over two adjacent residues can coordinate cations to the carbohydrate chain in the presence of water molecules. These Ca^{2+} interactions together with hydrogen bonds may lead to a sort of super-structure even allowing some lipophilic interactions[82].

Other carbohydrate-carbohydrate interactions occur not only in the presence of Ca^{2+}-ions but also in the presence of various other metal cations[30], including Mg^{2+}. According to molecular modeling, Ca^{2+}-ions in G_{M3}-Gg3 and Le^x-Le^x interactions lock the association of the molecules that occur via their hydrophobic sides[34,105]. However, no Ca^{2+} is present in the Le^x crystal[100]. On another hand, corneal epithelial cell-cell adhesion through the Le^x determinant is highly dependent on the presence of Ca^{2+}-ions[106]. Also self-aggregation of Le^x molecules in aqueous solution, where the molecules move freely, occurs only in the presence of Ca^{2+}-ions[107]. Further studies are required to resolve the exact role of Ca^{2+} and other divalent cations in carbohydrate-carbohydrate interactions.

III. ABSTRACT

Carbohydrates at the cell surface have been proposed as mediators in cell-cell recognition events involved in embryogenesis, metastasis, and other proliferation processes by calcium-dependent carbohydrate to carbohydrate interactions. They are the most prominently exposed structures on the surface of living cells, and with flexible chains and many binding sites are ideal to serve as the major players in initiating these cellular events. However, biological relevance of these type interactions is often questioned because of the very low affinity binding of single carbohydrate molecules and that they manifest themselves only through the contact of a large number of molecules tightly arranged in the membrane. Weak interactions are considerably more difficult to study and only a few biologically significant examples of direct carbohydrate-carbohydrate interactions have been reported, e.g. pioneering work showing glycosphingolipid self-interactions through multivalent interaction of Lewis X epitopes. However, there are no reports on the existence of specific proteoglycan self-interactions through carbohydrate-carbohydrate interactions in cellular recognition system, as it has been done with glycosphingolipids.

Here, we used sponges, organisms on which the first proteoglycan-mediated cell-cell recognition in the animal kingdom was demonstrated, as a model system to study carbohydrate-mediated cellular recognition. We show that the interaction between single oligosaccharides from surface proteoglycans is relatively strong and comparable to protein-carbohydrate interactions, highly specific, and dependent on Ca^{2+}-ions.

200 kDa glycans from the core protein of *Microciona prolifera* cell surface proteoglycans have been previously shown to mediate homotypic *Microciona*

proteoglycan-proteoglycan interactions. Here, 200 kDa glycans from four different sponge species: *Microciona prolifera*, *Halichondria panicea*, *Suberites fuscus* and *Cliona celata* were purified and investigated for species-specific interactions.

Selective recognition of glycans by live cells was studied to confirm the existence of glycan-glycan recognition system in biologically relevant situations. Mature sponge cells have the ability to reaggregate species-specifically and form homogenous aggregates on a shaker at the right shear forces in the presence of physiological 10 mM Ca^{2+}. Live cells were allowed to aggregate with glycan-coated beads similar in size to small sponge cells in the presence of calcium. They specifically recognized beads coated with their own glycans and did not mix but separated from beads coated with glycans isolated from different species.

The glycan-glycan recognition assay was developed to mimic species-specific cell-cell recognition in sponges. 200 kDa glycans immobilized onto beads similar in size to small sponge cells assembled species-specifically in the presence of physiological calcium, at the same shear forces as in cell-cell aggregation. Glycans coated on beads aggregated with glycans from the same species coated on beads, and separated from glycans from other species. The glycan density necessary for specific live cell-cell recognition in sponges is 828 molecules/μm^2. In our studies, the glycan density necessary for specific glycan-coated bead was very similar: ~810 molecules/μm^2.

Mature live cells demonstrated specific recognition of 200 kDa glycans during selective-binding to glycans coated on surfaces in the presence of calcium. They strongly adhered to glycans from their own surface proteoglycans coated onto a solid polystyrene phase, while the binding to glycans from different proteoglycans was 3 - 5 times lower. Moreover, homotypic adhesion to glycan-coated plates enhanced sponge cell differentiation and formation of mineral skeleton (spicules).

Larval cells, after settlement and spreading of larvae, can fuse species-specifically in nature. In our studies, live larval cells recognized and adhered specifically to glycans

purified from adhesion proteoglycans from their "mother sponge". They showed almost no interaction with glycans from other species.

As in cell-glycan adhesion assays, highly species-specific adhesion of 200 kDa glycans to glycan-coated surfaces could be observed in the presence of physiological calcium. Tested glycans bound strongly to glycans from the same species and showed up to a six fold reduction in binding to glycans from other species.

Atomic force microscopy (AFM) was performed to measure for the first time adhesion forces between single glycan molecules obtained from different surface proteoglycans. Measurements revealed equally strong adhesion forces in the range of several hundred piconewtons (pN) between glycan molecules as between proteins and glycans measured in another recognition system. Moreover, statistically significant differences (p value < 0.01) were seen between homotypic (glycans from the same species) and heterotypic (glycans from different species) interactions. Moreover, the polyvalent character of binding characterized mainly interactions between glycans from the same species. This indicates that not only the higher adhesion force per binding site as such but also the higher amount of multiple interactions between glycans from the same species versus mixture of glycans from different species guaranteed the specificity of the glycan-mediated recognition.

These findings confirm for the first time the existence of specific glycan-glycan recognition system between cell surface proteoglycans. We propose that these cell's outermost surface structures serve as important players in initiating the very first contacts between cells through highly species-specific and flexible carbohydrate-carbohydrate interactions.

IV. MATERIAL AND METHODS

IV.1. SPONGES, CELLS AND LARVAE

Four different sponge species, i.e. *Microciona prolifera*, *Halichondria panicea*, *Suberites fuscus* and *Cliona celata* (Fig. 14) were collected by the Marine Biological Laboratory Marine Resources Department in Woods Hole, MA. Only freshly colleted specimens were used for the preparation of cells, cell surface proteoglycans and glycans.

Microciona prolifera

Halichondria panicea

Suberites fuscus

Cliona celata

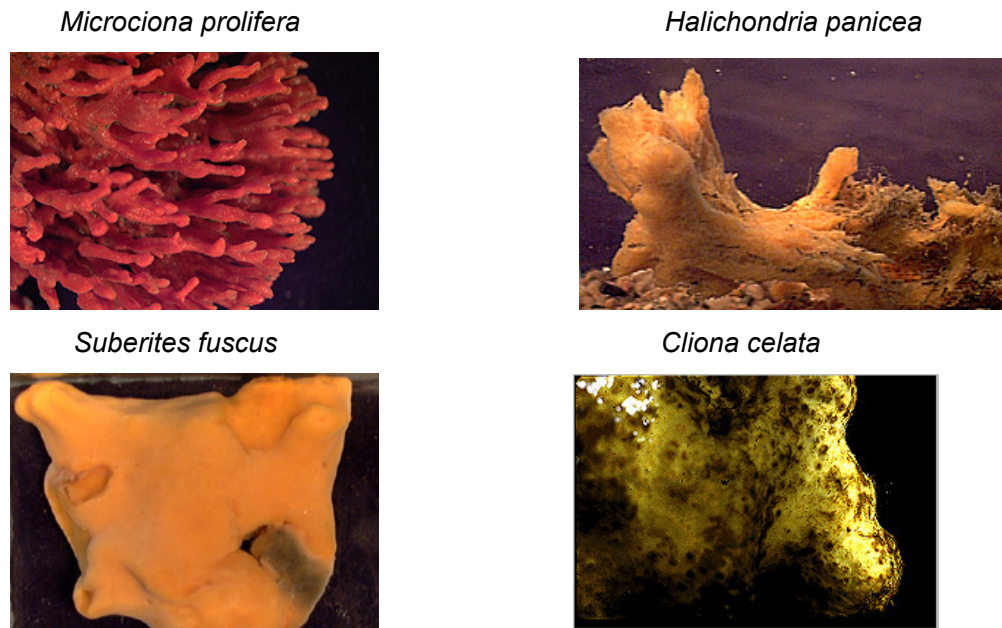**Fig.14. Pictures of four different sponge species used in these studies.**

Sponges were rinsed in BSW (0.49 M NaCl, 11 mM KCl, 10 mM $CaCl_2$, 2 mM $MgCl_2$, 7 mM $MgSO_4$, buffered with 2.1 mM $NaHCO_3$ to pH 7.4), cut into small pieces and incubated in BSW for 2 h at 4°C with gentle shaking. Afterwards, they were filtered and sponge pieces were gently squeezed through a 50 µm size nylon

mesh. The pellet of cells was obtained by centrifugation (1'000g / 5 min.). Viable cell number was determined by Trypan Blue staining and cells were counted in hemacytometer chamber.

Larvae of *Microciona prolifera* and *Halichondria panicea* were caught in a mesh and recovered in a small volume of BSW into a 15-ml tube. After brief vortexing, larvae came apart and larval cells were obtained. Total cell counts and viable cell number were determined as before.

IV.2. PURIFICATION OF CELL SURFACE PROTEOGLYCANS

Isolation and purification of sponge cell surface proteoglycans was carried out essentially as described[53,108].

Sponges were rinsed in CMFBSW (0.49 M NaCl, 11 mM KCl, 7 mM Na_2SO_4, buffered with 2.1 mM $NaHCO_3$ to pH 7.4), cut into small pieces and incubated in CMFBSW for 4 h at 4°C with gentle shaking. Afterwards, they were decanted and sponge pieces were gently squeezed through a 210 μm size nylon mesh. Cells and larger particles were removed by centrifugation (2'000g for 10 min. and 10'000g for 20 min.). Proteoglycans were precipitated by increasing the calcium concentration to 30 mM and leaving them overnight at 4°C with gentle shaking. The gel-like precipitate was spun down at 8'000g for 15 min. and homogenized in 20x of its volume CMFBSW buffered with 20 mM Tris and supplemented with 2 mM $CaCl_2$ (CMFTSW; artificial seawater). The last debris was removed by centrifugation at 12'000g for 30 min., and proteoglycans were precipitated at 35'000g for 3h at 4°C. The final purification of proteoglycans was performed by centrifugation in cesium-chloride gradient (50% CsCl in CMFTSW) at 38'000g for 48h at 4°C in quick-seal tubes (Beckmann). *Microciona* proteoglycan was collected as a final pellet and the other as discrete bands in the lower third of the gradient. All proteoglycans were

dialyzed against CMFTSW (3 x 1h) and stored in CMFTSW containing 0.05% NaN$_3$. Protein concentrations were determined using the Biorad DC assay.

IV.3. EDTA-TREATMENT OF CELL SURFACE PROTEOGLYCANS

Long term EDTA-treatment of purified proteoglycans was essentially done as described[109]. Briefly, 2 ml of 0.7 mM EDTA, pH 7.0 was added to lyophilized proteoglycans, and left at 4°C for a 4-week period. Following this treatment, separation of the core and the arms was done on A-15m BioRad column (1.5 x 90 cm), eluted with 0.5 M NaCl, 10 mM Tris, pH 7.4. Collected fractions were lyophilized.

IV.4. GLYCAN PURIFICATION

10 mg of purified and lyophilized cell surface proteoglycans were delipidated in water:chloroform:methanol with a final ratio of 3:8:4 (v/v/v) and the resulting pellet was extracted with ethanol to remove the organic solvents[110]. Glycans were obtained by extensive pronase digestion as described[108,110]. The pellet was suspended in 6 ml of 0.1 M Tris-HCl, 1 mM CaCl$_2$, pH 8.0 and incubated over a period of 72h at 60°C with three additions of prewarmed pronase (300 μl of 10 mg/ml Pronase, Calbiochem) every 24h. The glycans were separated from amino acids and small peptides by gel filtration on a Sephadex G-25 (Pharmacia) column (2 x 32 cm) eluted with 10 mM pyridine-acetate, pH 5.0. The presence of acidic glycans was checked by dotting aliquots on a Zeta-probe membrane (Biorad) and Alcian staining (3% acetic acid, 25% isopropanol, 0.5 g Alcian Blue/100 ml final volume). Destaining was done in 10% acetic acid / 40% ethanol. Zeta-probe membranes were prewetted in destaining solution before staining with Alcian to avoid high background. Fractions containing glycans were pooled and lyophilized. Pellets were suspended in 10 mM pyridine-acetate and separation of 6 kDa and 200 kDa glycans were done on

Sephadex G-75 (Pharmacia) column (1 x 50 cm) eluted with 10 mM pyridine-acetate, pH 5.0. The presence of glycans was checked as before.

IV.5. GEL ELECTROPHORESIS AND BLOTTING OF GLYCANS

Electrophoresis of glycans was done using 5-20% or 15% TBE acrylamide gels essentially as described[111], but modified for the Biorad mini-gel system. The running buffer (TBE: 0.9 M Tris, 0.9 M borate, 24 mM EDTA, pH 8.3) was precooled to 4°C, electrophoresis was carried out at 200V and gels were not prefocused. Gels were either stained with Alcian (4h incubation in Alcian staining as described above in IV.4, and several rounds of incubation in destaining solution), or with the combined Alcian-silver method[112]. Transfer of glycans from the gel onto a Zeta probe membrane was done with semidry transfer equipment using the same buffer as for electrophoresis. Blotting was done for 50 min. at 0.8 mA/cm^2 and membranes were either stained by Alcian or blocked in Tris buffered saline, pH 7.5, 3% BSA, 0.5% Tween-20, 1% Triton X-100 (Zorro) for 1h. Incubation with the first antibodies was performed at room temperature (RT) for 2h or overnight at 4°C using 2-5 μg/ml of blocking solution. After washing, the blots were incubated with secondary antibody (HRP-coupled rabbit anti mouse) at a dilution of 1:10'000 in blocking solution at RT for 1h. Development of the washed membranes was either done by incubating them in 0.017% of 4-chloro-1-naphtol, 0.006% H_2O_2 in PBS (8.1 mM Na_2HPO_4, 1.5 mM KH_2PO_4. 131 mM NaCl, 2.1 mM KCl, pH 7.4) or with the ECL system (Amersham). Molecular weight markers (chondroitin sulfate, CS, and hyaluronic acid, HA) were from Sigma.

IV.6. BEAD COUPLING

IV.6.1. Amine-modified beads

4.5×10^8 freshly sonified amine-modified fluorescent beads (Molecular Probes, 1 μm in diameter) were incubated with purified 200 kDa glycans in CMFTSW (1.5 mg/ml) and 2 mg of 5,5'-dithiobis-(2-nitrobenzoic acid) (DTNB, SE, Molecular Probes) overnight at RT. Afterwards, beads were washed 5x in CMFTSW and stored in 1 ml CMFTSW. Coupling efficiency was determined by dotting a bead aliquot on a Zeta probe membrane and Alcian staining (see IV.4.), and by measuring the glycan concentration (by staining with 1% Toluidine Blue) on the beads after reversing the DTNB crosslinking with the disulfide-reducing agent DTT.

IV.6.2. Carboxylate-modified beads

3.6×10^8 freshly sonified fluorescent carboxylate-modified beads (Molecular Probes, 1 μm in diameter) were incubated with 200 kDa glycans in CMFTSW (1.5 mg/ml), 3 mg of water-soluble 1-ethyl-3-(3-dimethylaminopropyl)carbodiimide (EDAC, Molecular Probes), and 1 mg of N-hydroxysulfosuccinimide (Molecular Probes) overnight at RT, pH 6.0. Afterwards, beads were washed 5 times in CMFTSW and stored in 1 ml CMFTSW. Coupling efficiency was determined by dotting a bead aliquot on a Zeta probe membrane and Alcian staining (see IV.4.).

IV.7. BEAD AGGREGATION ASSAY

9×10^7 glycan-coated amine-modified beads, or 7×10^7 glycan-coated carboxylate-modified beads were diluted in artificial seawater: CMFTSW (20 μl beads / 400 μl CMFTSW) in wells constructed by mounting a conical plastic ring (1.5 cm in diameter) onto a coverslip. 10 mM $CaCl_2$ was added and aggregation was allowed to proceed on a rotary shaker at 60 rpm for 4 h. Images of bead aggregates were acquired with a confocal laser-scanning microscope (Leica Lasertechnik, Heidelberg,

Germany) equipped with an argon/krypton laser and a 10x objective (PL Fluotar, N.A. 0.3). The size of the scanned area was 1000 x 1000 μm (512 x 512 pixels). Image processing was performed using Adobe Photoshop version 6.0. Quantifications were performed using UTHSCSA Image Tool version 2.00 Alpha.

IV.8. ESTIMATION OF CA^{2+} UPTAKE DURING CELL-CELL AND GLYCAN-COATED BEAD-BEAD AGGREGATIONS

The calcium uptake was estimated for cell-cell and glycan-coated bead-bead aggregation. 5 x 10^3 cells or 9 x 10^7 glycan-coated amine-modified beads were allowed to aggregate on a rotary shaker at 60 rpm for 10 h in CMFTSW containing 10 mM CaCl$_2$ labeled with calcium-45 (74 MBq, 2 mCi, AmershamPharmaciaBiotech). Every certain time, cells or glycans were spun down (1'000g / 5 min.) and the radioactivity of the calcium-45 left in the suspension was determined to obtain the non-taken Ca^{2+}. The radioactivity was determined in Liquid Scintillation Cocktail (Beckman) in a Beckmann LS 3801 reader. The radioactivity of non-taken Ca^{2+} was deduced from the radioactivity of the overall Ca^{2+} added to obtain the quantity of Ca^{2+} taken by aggregating cells or glycans coated on beads.

IV.9. BINDING TO COATED PLATES

IV.9.1. Preparation of coated plates

Solutions of purified proteoglycans (5 mg/ml) or purified 200 kDa glycans (2 mg/ml) in CMFTSW were appropriately diluted and placed in duplicates in wells of a 96-well flat bottom plastic plate (Falcon, 0.3 ml/well volume). After 2 h, each well was washed with CMFTSW to remove non-bound proteoglycans and glycans.

The quantity of proteoglycans or glycans adhered to plates was determined by staining with 0.1 % Toluidine Blue and measuring the absorbance at 630 nm.

IV.9.2. Binding of cells to proteoglycan-coated plates

Solutions of purified proteoglycans in CMFTSW (0.01 μg/ml - 1 μg/ml) were coated in duplicates in wells. 100 μl of live cells (5 x 10^3) in CSW were added to each proteoglycan-coated well, supplemented with 200 μl CMFTSW containing 10 mM $CaCl_2$ and incubated for 2h at RT. Non-bound cells were washed off by gradient washing in CMFTSW containing 10 mM $CaCl_2$. Namely, plates were immersed in CSW with 10 mM $CaCl_2$ in a large container, suspended upside down for 10 min with gentle shaking to allow non-adherent cells to sediment out of plates. Bound cells were lysed for 10 min in 2 M NaCl, 20 mM Tris-HCl, pH 7.5. 200 ng Hoechst in 20 mM Tris-HCl, pH 7.5 was added to cell lysates and the fluorescence was measured at λ_{ex}=360 nm and λ_{em}=450 nm.

IV.9.3. Binding of glycans, glycan-coated beads, and cells to glycan-coated plates

Solutions of 200 kDa glycans in CMFTSW (0.01 μg/ml - 8 μg/ml) were coated in duplicates in wells. One set of wells with coated glycans was left to serve as a control. 100 μl of glycans in CMFTSW (0.1 mg/ml) were added to the second set of coated wells and incubated for 2 h at RT, after addition of 10 mM $CaCl_2$. Afterwards, non-bound glycans were washed off with CMFTSW containing 10 mM $CaCl_2$. Bound glycans and control glycans (the coat) were stained with 0.1 % Toluidine Blue and absorbance was measured at 630 nm. The absorbance of glycans used as a coat (control) was deducted from the total absorbance measured after the addition of glycans to coated wells to give the absorbance of bound glycans.

200 μl of glycan-coated amine-modified beads (9 x 10^7), or glycan-coated carboxylate-modified beads (7 x 10^7) in CMFTSW were added to each glycan-coated well, and incubated for 2 h at RT. Afterwards, non-bound glycan-coated beads were washed off with CMFTSW containing 10 mM $CaCl_2$. Images of adhered glycan coated-beads were acquired with a confocal laser-scanning microscope (Leica Lasertechnik, Heidelberg, Germany) as before (see IV.7.).

100 µl of live mature or larval cells (5 x 10^3) in CSW were added to each glycan-coated well, supplemented with 200 µl CMFTSW containing 10 mM $CaCl_2$ and incubated for 2h at RT. Non-bound cells were washed off by gradient washing in CMFTSW containing 10 mM $CaCl_2$, and lysed as before. Treatment with Hoechst and fluorescent measurements were done as in binding of cells to proteoglycan-coated plates (see IV.9.2.).

IV.10. ATOMIC FORCE MICROSCOPY (AFM)

IV.10.1. Support and tip preparation

Force measurements were performed with a commercial Nanoscope III AFM (from Digital Instruments, Santa Barbara, CA, USA) equipped with a 162 µm scanner (J-scanner) and oxide-sharpened Si_3N_4 cantilevers with a thickness of 400 nm and a length of 100 µm (k = 0.1 N/m; Olympus Ltd., Tokyo, Japan).

Cantilever spring constants k measured for a series of cantilevers from the same region of the wafer revealed on average k=0.085 N/m and a standard deviation of SD=0.002 N/m. We observed a variation of <15% for k-values from different cantilever batches. All measurements were done with cantilevers from the same batch.

Surface clustering of 200 kDa glycans was determined by fluorescence imaging. Glycans were labeled through their amino groups of the amino acid portion with 5(6)-Carboxyfluorescein-N-hydroxysuccinimidester (Boehringer, Mannheim). Labeled glycans were separated from free labeling substance via a P-6 sizing column (Pharmacia) in 100 mM pyridine-acetate buffer (pH 5.0).

IV.10.2. Force measurements

AFM supports were built as described[113]. The mica was cleaved using scotch tape, masked using a plastic ring mask with an inner diameter of 5 mm, and immediately brought into the vacuum chamber of the gold sputter coater (Bal-Tec SCD 050). A vacuum of 10^{-2} mbar was generated and the pressure was then adjusted to 5 x 10^{-2} mbar with argon. A 20 nm gold layer was deposited on the mica surface and the tip controlled by a quartz thickness and deposition rate monitor (Bal-Tec QSG 050). Both the support and the tip were overlaid with CMFTSW containing 10 mM $CaCl_2$ and the gold-gold-interaction was measured. Afterwards, the support and the tip were incubated for 15 min at RT with isolated 200 kDa glycans (1 mg/ml) and glycan-glycan force measurements were performed in CMFTSW containing 10 mM $CaCl_2$. The AFM stylus approached and retracted from the surface approximately 100 times with a speed of 200 nm/s. The tip was moved laterally by 50 nm after recording 5 force-distance curves. All measurements were conducted at RT.

IV.11. ANALYTICAL METHODS

IV.11.1. Carbohydrate analysis

For carbohydrate composition, proteoglycans were hydrolyzed in 4 M TFA at 100ºC for 4 h. Remaining TFA was removed by methanol-aided evaporation. Carbohydrates were analyzed by high performance anion exchange chromatography using a Dionex BioLC system and a CarboPac PA1 column. The column was equilibrated with 16 mM NaOH and eluted with linear gradients from 16 mM NaOH to 0.1 M NaOH/50mM Na-acetate, and from 0.1 M NaOH/180 mM Na-acetate. Pulsed amperometric detection was done by using PAD 2 cell with E1 = +0.05 V, 480 ms, E2 = +0.75 V, 180 ms, and E3 = -0.20 V, 360 ms. Relative amounts were calculated using relative response factors from standard samples containing 2 nM of the respective monosaccharides, and treated the same way as the polysaccharide samples.

IV.11.2. *Amino acid analysis*

For amino acid analyses, dry glycan samples were diluted in 1 ml UP water and the aliquots of 25 µl were lyophilized and hydrolyzed during 24 h. After hydrolysis, the black residues were suspended in 100 µl of 50 mM HCl containing 50 pmol/µl Sarcosine (Sar) and L-norvaline (Nva) each while ultrasonicated for 15 min. After 15-min centrifugation, the transparent solutions were transferred into new reagent tubes and analyzed on a Hewlett-Packard AminoQuant II analyzer.

V. RESULTS

V.1. GLYCANS OBTAINED BY PRONASE DIGESTION

Proteoglycan molecules from four different species were subjected to an extensive pronase digestion in order to obtain protein-free glycans from the core structures. The total 200 kDa glycans were separated from free amino acids and peptides by gel filtration (see IV.4). This protocol is a general and routinely used method for obtaining protein-free carbohydrates[110]. Two approaches were used for obtaining glycans: 1) pronase digestion of the whole proteoglycan molecules or 2) EDTA-dissociation of proteoglycans into two subunits: arm fragments and core structures, followed by pronase digestion of each subunit.

In the first approach, after pronase digestion of proteoglycan molecules, glycans were separated on Sephadex G-75 sizing column. Two major peaks could bee seen after separation of glycans from each species (Fig. 15*A*). Fractions from each peak were collected and PAGE in a Tris-borate-EDTA buffer (TBE) was used to estimate the size of the glycans[108]. There were always two main glycans obtained from different surface proteoglycans: 6 kDa and 200 kDa (Fig. 15*B*). 200 kDa glycans were obtained from fractions collected from the first peak, and 6 kDa glycans were obtained from fractions collected from the second peak. The big glycan obtained from *Cliona celata* appeared to be slightly smaller than the ones from other species. The molecular weight of the glycan, as observed on TBE-gels, was around 170 kDa.

In the second approach, proteoglycans from all four species were first dissociated by prolonged EDTA treatment. The resulting subunits were separated on an A-15m column (Fig. 16*A*). The first peak of big volume is considered to contain the central core protein and the second peak of small volume is considered to contain arm fragments[57]. Upon pronase digestion, the first peak consisted of 200 kDa glycans and small amount of 6 kDa glycans (Fig. 16*B*). The peak of arm fragments consisted of

only 6 kDa glycans. Farther separation of 200 kDa and 6 kDa glycans from the first peak had to be performed on Sephadex G-75 column to obtain pure glycan fractions.

The second approach was time consuming and was not used for obtaining 200 kDa glycan. Only 200 kDa glycans obtained from the first approach were used for experiments.

There have been essentially no losses of carbohydrates during the purification procedures since the carbohydrate yield of the glycan fractions was ~97%. Amino acid analysis of glycans from the four sponge species used showed that there was from 0.7 (*Cliona celata*) to 1.1 (*Microciona prolifera*) mol of linker aspartate/mol of glycan (Table 4). Only trace amounts of a few other amino acids were detected. This indicates that the digestion was complete and that the purification procedure for the 200 kDa glycans led to essentially pure glycan fractions, free of any protein contaminations.

The carbohydrate compositions of purified proteoglycans from four different sponge species were analyzed by high performance anion exchange chromatography. All proteoglycans contained galactose (Gal), fucose (Fuc), mannose (Man), N-acetylglucosamine (GlcNAc), N-acetylgalactosamine (GalNAc), and glucuronic acid (GlcUA). The carbohydrate makeup of proteoglycans from different individuals of the same species was very similar, while proteoglycans from different species showed large differences (Table 5). *Microciona* proteoglycan was characterized by high fucose, while *Halichondria* proteoglycan had threefold less. *Microciona* and *Halichondria* proteoglycans showed high galactose, while *Cliona* proteoglycans had three- to fourfold less. The latter was the only species with significant amounts of GalNAc. On the other hand, only *Microciona* proteoglycan contained significant amounts of GlcUA.
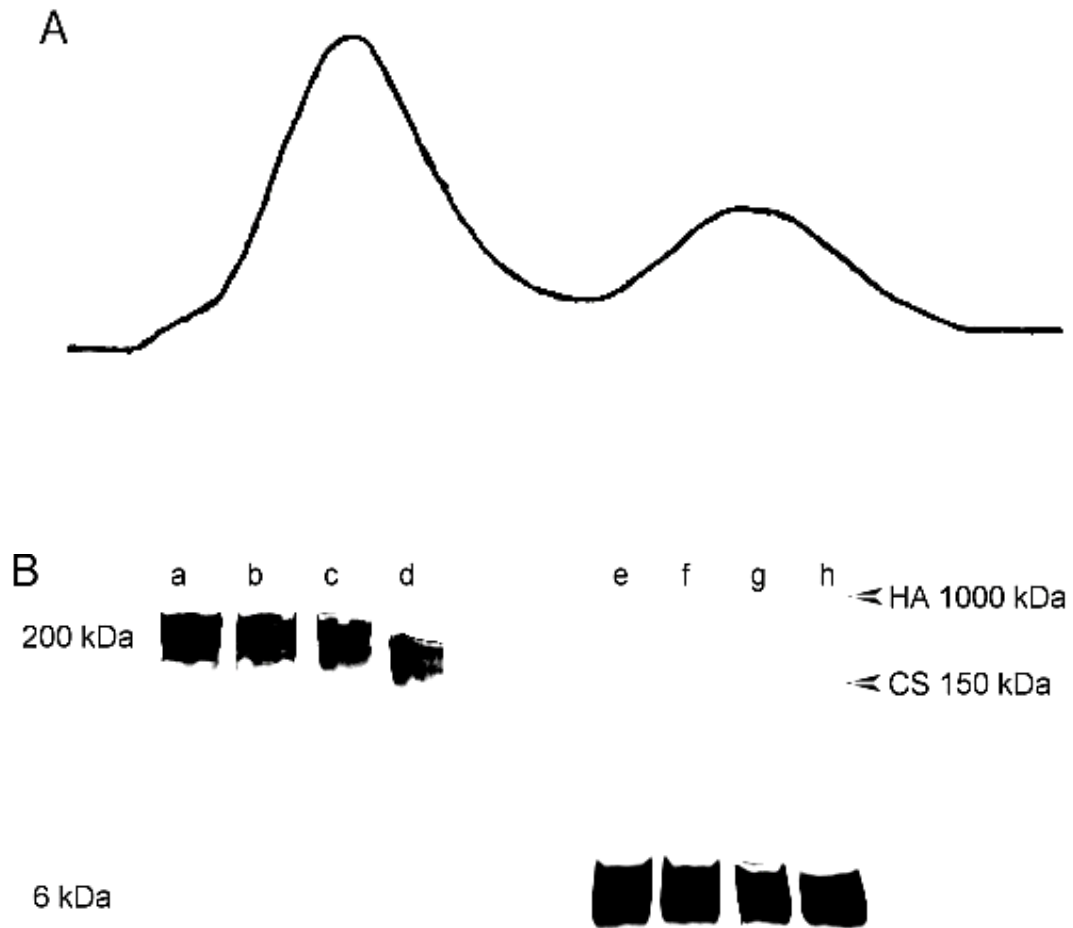
Fig. 15. Separation of glycans obtained by pronase digestion of the whole proteoglycan molecules from different sponge species. *A*, Separation of glycans on Sephadex G-75 sizing column from a pronase digestion of the whole proteoglycan molecule (see IV.4.). *B*, PAGE electrophoresis of glycans obtained from both peaks. *a-d* 200 kDa glycans obtained from the first peak; *e-h*, 6 kDa glycans obtained from the second peak. *a* and *e*, *Microciona prolifera* glycans; *b* and *f*, *Halichondria panicea* glycans; *c* and *g*, *Suberites fuscus* glycans; *d* and *h*, *Cliona celata* glycans. Molecular weight standards: HA, hyaluronic acid; CS, chondroitin sulfate.
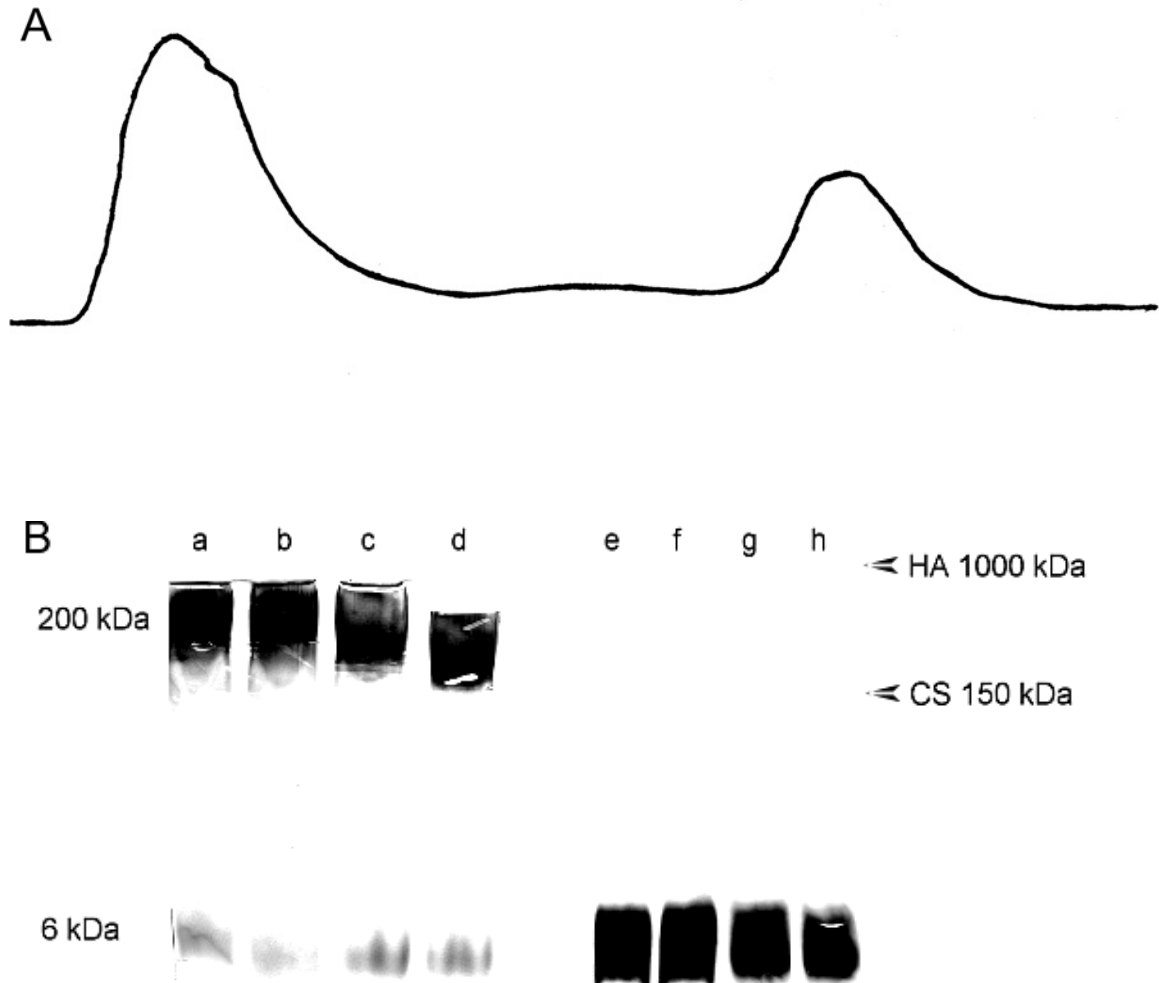
Fig. 16. Separation of glycans obtained by pronase digestion of subunits of different surface proteoglycans after EDTA-treatment. *A*, Separation of proteoglycan fragments on A-15m sizing column after prolonged EDTA-treatment of proteoglycan molecules (see IV.3.). ***B***, PAGE electrophoresis of glycans obtained from both peaks by pronase digestion. ***a-d*** 200 and 6 kDa glycans obtained from the first peak; ***e-h***, 6 kDa glycans obtained from the second peak. ***a*** and ***e***, *Microciona prolifera* glycans; ***b*** and ***f***, *Halichondria panicea* glycans; ***c*** and ***g***, *Suberites fuscus* glycans; ***d*** and ***h***, *Cliona celata* glycans. Molecular weight standards: HA, hyaluronic acid; CS, chondroitin sulfate.

Table 4. Trace amino acid composition of 200 kDa glycans. The values are the average of 4 determinations. Cys was not determined.

	Microciona	*Halichondria*	*Suberites*	*Cliona*
	mol amino acid/mol glycan			
Asp	1.1	0.9	0.9	0.7
Glu	0.4	0.3	0.4	0.2
Ser	0.2	0.1	0.2	0
His	0	0	0	0
Gly	0.3	0.3	0.2	0.3
Thr	0.4	0.1	0	0.1
Ala	0.2	0.1	0.1	0
Arg	0	0	0	0
Tyr	0	0	0	0
Val	0	0	0	0
Met	0	0	0	0
Phe	0	0.1	0	0
Ile	0	0	0	0
Leu	0	0.1	0.1	0
Lys	0	0	0	0
Pro	0	0	0	0
Asn	0	0	0	0
Gln	0	0	0	0
Trp	0	0	0	0
Ca	0	0	0	0
Total	2.6	2.0	1.9	1.3

Table 5. Comparison of the carbohydrate composition of proteoglycans from two sponge species. The average values were obtained from 4 sponge individuals of each species.

	Microciona	*Halichondria*	*Suberites*	*Cliona*
	carbohydrates (mol %)			
Fuc	30.2	8.2	15.0	22.1
Gal	33.5	40.9	25.0	10.8
Man	9.7	15.2	12.4	14.0
GalNAc	3.7	1.2	2.0	10.1
GlcNAc	18.3	14.1	34.2	27.5
GlcUA	9.1	3.0	1.9	4.5

V.2. AGGREGATION ASSAYS

V.2.1. CELL-CELL AGGREGATION IS SPECIES-SPECIFIC

In the classical assay for specific cell-cell recognition, mechanically dissociated live sponge cells can recognize its own kind and form big homogenous aggregates on a rotary shaker at the right shear forces, i.e. rotor speed, in the presence of physiological 10 mM Ca^{2+} in artificial seawater. At too high rotation speed no cell aggregates are formed since shear forces are too high. At too low rotation speed unspecific, faulty initial contacts will remain since such cells do not get a second or third chance to form higher affinity adhesions with other cells. At the optimal speed of the shaker (60 rpm) a sufficient shear force was implied and species-specific cell aggregates could consistently be observed after 4 h in seawater with 10 mM $CaCl_2$.

Dissociated cells from the same sponge aggregated species-specifically in the presence of physiological 10 mM Ca^{2+} (Fig. 17*A-B*). Large homotypic aggregates of cells with red (*Microciona prolifera*) and yellow (*Suberites fuscus*) natural pigment could be observed. The mixture of cells from two different sponge species did not mix but formed separate aggregates (Fig. 17*C-D*). Red (*Microciona*) and yellow (*Suberites*) cells (*C*), as well as red (*Microciona*) and grey (*Halichondria panicea*) cells (*D*), formed separate clumps according to the species of origin.

This homotypic (between cells from the same species) and heterotypic (between cells from two different species) cell-cell interactions could be abolished in the absence of Ca^{2+} (Fig. 17*E-F*). The antibody directed against the carbohydrate epitope of *Microciona* surface proteoglycan could only inhibit the specific cell-cell recognition between *Microciona* red cells (Fig. 17*G*). The antibody had no visible effect on homotypic aggregations between cells from any other sponge species, as shown for aggregation between *Suberites* yellow cells (Fig. 17*H*).
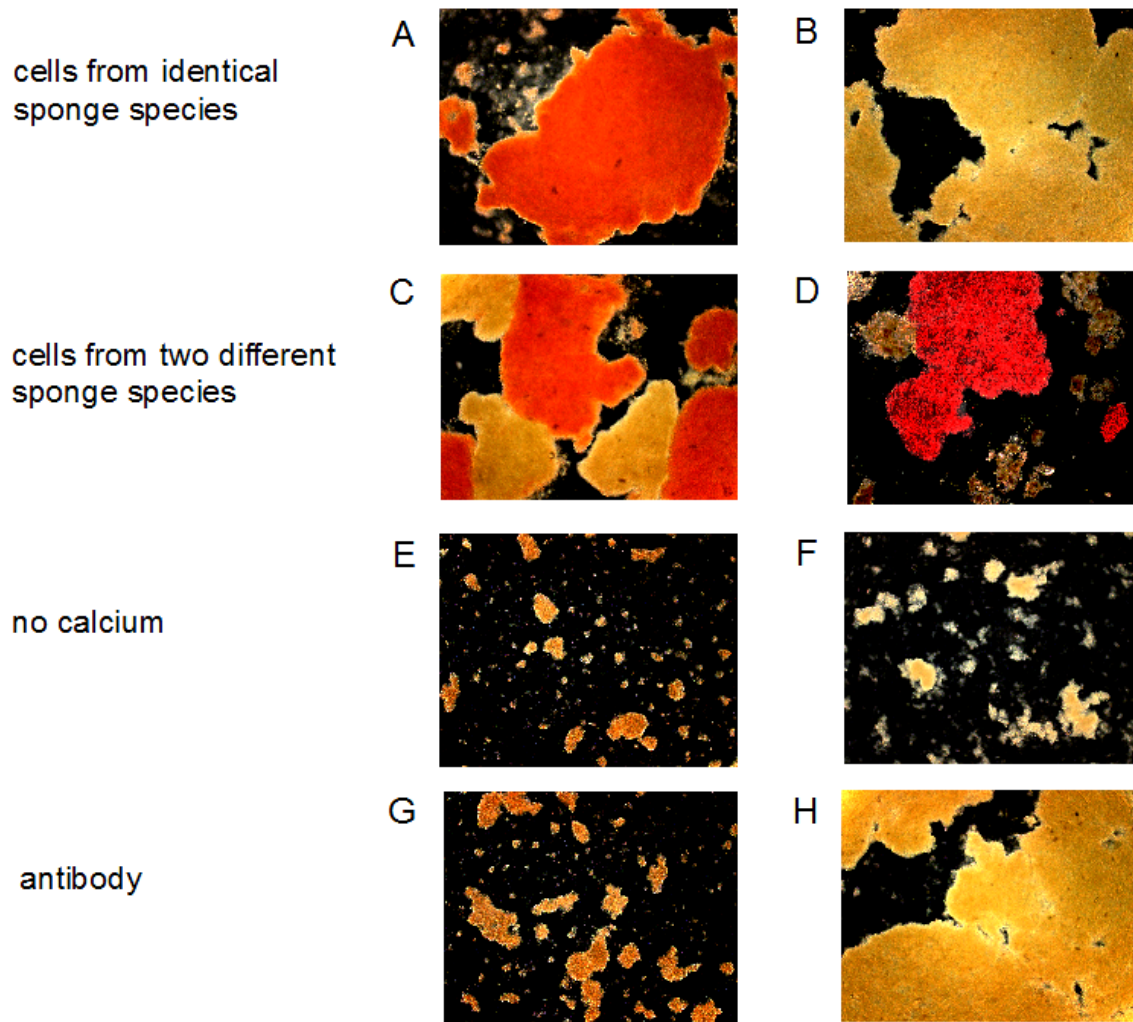
cells from identical sponge species

cells from two different sponge species

no calcium

antibody

Fig. 17. Species-specific recognition between live cells. Rotation-mediated cell-cell recognition was monitored for 4 h in artificial seawater with physiological 10mM Ca^{2+}. *A*, Homotypic aggregation between *Microciona prolifera* red cells. *B*, Homotypic aggregation between *Suberites fuscus* yellow cells. *C*, Species-specific sorting between red (*Microciona*) and yellow (*Suberites*) cells. *D*, Species-specific sorting between red (*Microciona*) and grey (*Halichondria panicea*) cells. *E*, Inhibition of the homotypic aggregation between red (*Microciona*) cells in the absence of Ca^{2+}. *F*, Inhibition of the heterotypic aggregation between red (*Microciona*) and grey (*Halichondria*) cells in the absence of Ca^{2+}. *G*, Inhibition of the homotypic aggregation between red (*Microciona*) cells by the antibody directed against the carbohydrate epitope of *Microciona* proteoglycan. *H*, No inhibition of the homotypic aggregation between yellow (*Suberites*) cells by the antibody directed against the carbohydrate epitope of *Microciona* proteoglycan. Pictures were taken by phase-contrast microscope at 10x magnification.

V.2.2. BINDING OF GLYCANS TO BEADS

The binding efficiency of 200 kDa glycans to beads and its impact on bead-bead aggregation was studied. Fig. 18 shows the binding efficiency of 200 kDa glycans purified from *Microciona prolifera* and *Cliona celata* surface proteoglycans to red and green amine-modified fluorescent beads (1 μm in diameter). The DTNB crosslinking of glycans to amine-modified beads could be easily reversed by treatment with the disulfide-reducing agent DTT and the glycan concentration on the beads could be estimated (see IV.6.1.).

Applied coupling method resulted in very high binding efficiency of both *Microciona* and *Cliona* 200 kDa glycans to amine beads (Fig. 18). 0.19 nM (*Cliona*) to 0.21 nM (*Microciona*) glycans were immobilized onto beads when 0.25 nM glycans were added to 4.5×10^8 amine beads. However, the size of bead aggregates after 4 h of rotation-mediated homotypic aggregations between *Microciona* glycan-coated beads and between *Cliona* glycan-coated beads was small (Fig. 18*A*). When 5 nM glycans were added to 4.5×10^8 amine beads, 3.5 nM (*Cliona*) and 3.75 nM (*Microciona*) glycans were bound, and the resulting bead aggregates were much bigger in size. The system was saturated when 25 nM glycans were added to beads for coupling (Fig. 18*B*). The size of bead aggregates was only slightly bigger than of those when 5 nM glycans were added for coupling. Therefore, 5 nM glycans were always used for coupling of 200 kDa glycans to amine-modified beads.

Very similar results were obtained when binding efficiency of 200 kDa glycans to carboxylate-modified beads was studied (data not shown). The optimal amount of glycans used for coupling to carboxylate-modified beads was also 5 nM.
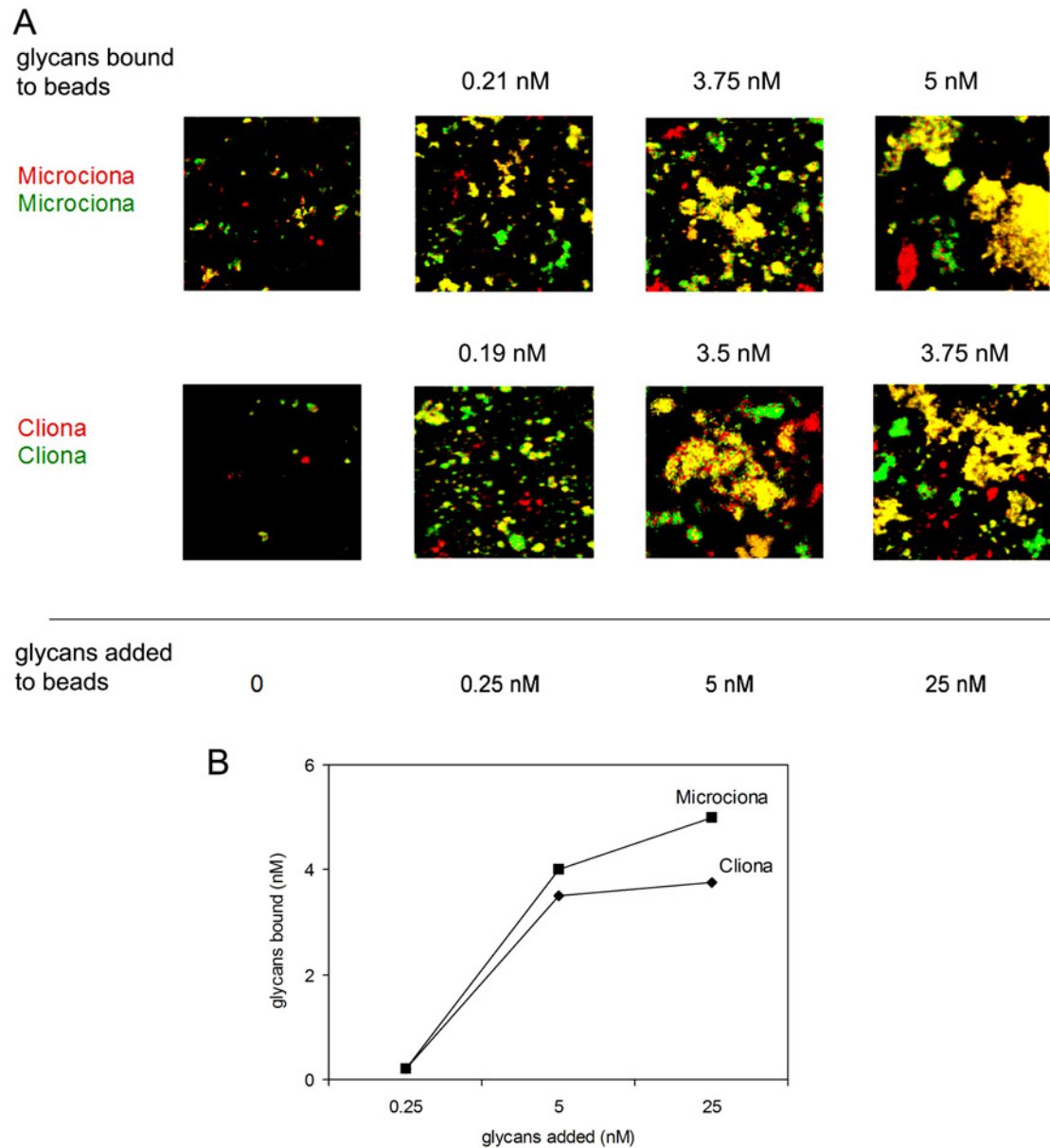
Fig. 18. Relationship between glycan binding to beads and glycan-coated bead-bead aggregation. The binding efficiency of 200 kDa glycans from two different sponge species: *Microciona prolifera* and *Cliona celata* to red and green amine-modified beads was determined (see IV.6.1.). The moles of glycans bound to beads is given as compared to the initial moles of glycans added to 4.5×10^8 amine beads for coupling. *A*, Homotypic aggregation between beads coated with *Microciona* glycan and between beads coated with *Cliona* glycan. Pictures were taken with a confocal microscope at 10x magnification. Yellow areas depict clumps of mixed red and green beads. Red and green areas reflect clumps of separated beads. *B*, Graph indicating relationship between the amount of glycans added and glycans bound to the beads.

The aggregation experiments were designed to allow reaching almost identical density of glycans on the bead surface as compared to glycan density on sponge cell surface required for cell-cell aggregation. It has previously been reported that the average amount of surface proteoglycans associated with each *Microciona prolifera* cell *in vivo* is around 28'000 molecules[75]. The number of 200 kDa glycan copies per proteoglycan molecule was determined from the mass of total carbohydrate recovered in 200 kDa glycan fractions either after gel electrophoresis or gel filtration[74]. Since 37% of the total carbohydrate content of the proteoglycan molecule occurred in the form of 200 kDa glycan (~70% of the proteoglycan mass is carbohydrate; proteoglycan $M_r = 2 \times 10^7$), one proteoglycan carries ~26 copies of this glycan. Therefore, ~10'400 glycan molecules (400 proteoglycan molecules) per cell cause living cells to aggregate.

In our studies, binding measurements indicated that ~2500 molecules of 200 kDa glycan glycan molecules per amine- or carboxylate-modified bead were sufficient to aggregate species-specifically glycan-coated beads. The number was calculated from the specific absorbance of stained glycans after reversing the binding to beads and Avogadro's number, and was divided by the number of beads. Surface areas of the cell and the bead were calculated from diameters, and they were 12.56 μm^2 and 3.14 μm^2 accordingly. This led to the final assessment that the glycan density necessary for specific glycan-coated bead (~810 molecules/μm^2) and for specific live cell (828 molecules/μm^2) recognition is very similar.

Calculations of the glycan density on the cell surface:

- 10400 glycan molecules required for **cell-cell aggregation**

- surface area of the cell is 12.56 μm^2 calculated from $4pi\ r^2$, where r = 1 μm

- that makes **828.025 glycan molecules / μm^2**

Calculations of the glycan density on the bead surface:

- required glycan concentration for **amine-modified bead-bead aggregation**:

0.3845 x 10^{-3} mg per 4.5 x 10^8 beads   */ 4.5 x 10^8*

- that gives 0.08544 x 10^{-11} mg per 1 bead   */200 x 10^3*

- that gives 0.0004272 x 10^{-17} M per 1 bead   *x Avogadro's number: 6.022 x 10^{23}*

- that gives 0.002573 x 10^6 glycan molecules per 1 bead   */ 3.14*

  (surface area of the bead is 3.14 μm^2, where r = 0.5 μm)

- that gives **819.426 glycan molecules / μm^2**

- required glycan concentration for **carboxylate-modified bead-bead aggregation**:

0.30034 x 10^{-3} mg per 3.6 x 10^8 beads   */ 3.6 x 10^8*

- that gives 0.083428 x 10^{-11} mg per 1 bead   */200 x 10^3*

- that gives 0.00041714 x 10^{-17} M per 1 bead   *x Avogadro's number: 6.022 x 10^{23}*

- that gives 0.002512 x 10^6 molecules per 1 bead   */ 3.14*

(surface area of the bead is 3.14 μm^2, where r = 0.5 μm)

- that gives **800.001 glycan molecules / μm^2**

V.2.3. CELL-GLYCAN AGGREGATION IS SPECIES-SPECIFIC

In a cell-glycan recognition assay, live cells were allowed to aggregate with different 200 kDa glycans coated on red amine-modified beads (1 µm in diameter) similar in size to small sponge cells (2 µm in diameter). The same shear forces, i.e. rotor speed, were provided as in cell-cell aggregation.

Cells specifically recognized beads coated with their own 200 kDa during aggregation in the presence of physiological Ca^{2+} and formed homogeneous aggregates (Fig. 19*A-C*). Red *Microciona prolifera cells* (*A*), yellow *Suberites fuscus* cells (*B*), and grey *Halichondria panicea* cells (*C*) formed mixed aggregates with their own glycans coated on red beads.

In stark contrast, the same cells did not mix with beads coated with glycans from different sponge species during aggregation in the presence of Ca^{2+} (Fig. 19*D-F*). *Microciona* red cells separated from aggregates of red beads coated with *Halichondria* glycan (*D*). Also *Suberites* yellow cells species-specifically sorted out and formed their own aggregates separated from aggregates of red beads coated with *Microciona* glycan (*E*). Finally, *Halichondria* grey cells did not mix but separated from clumps of red beads coated with *Cliona celata* cells.

The species-specific cell-glycan aggregation occurred only in the presence of Ca^{2+} in artificial seawater (Fig. 19*G-I*). Pretreatment of *Microciona prolifera* cells with the antibody directed against the carbohydrate epitope of the *Microciona* surface proteoglycan inhibited the aggregation of these cells with beads coated with their own glycan (Fig. 19*J*). Pretreatment of cells from other sponge species with the antibody had no visible effect on the aggregation between these cells and their glycans coated on beads (data not shown).
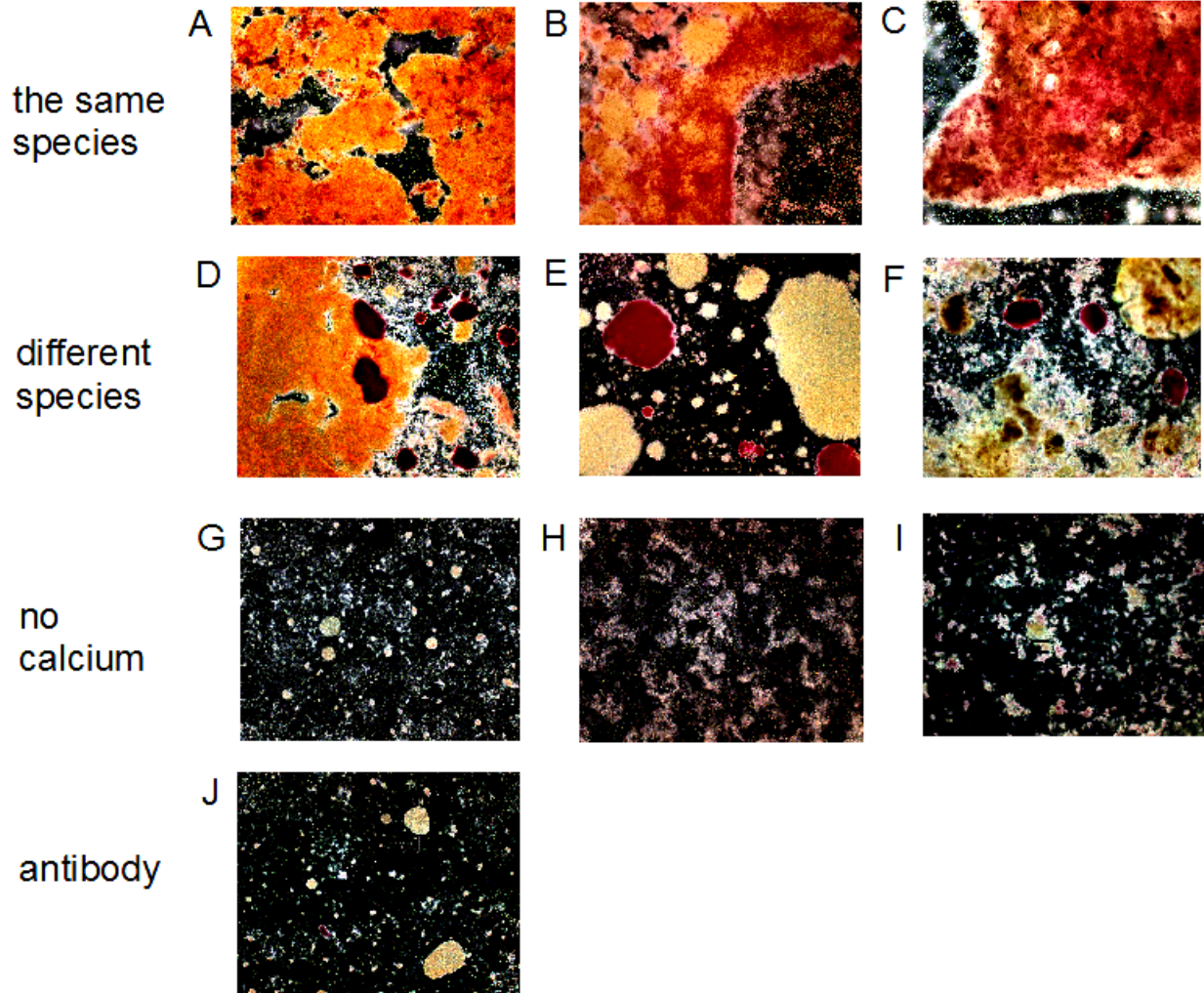
Fig. 19. Species-specific recognition between live cells and glycans coated on red beads. Rotation-mediated cell-glycan recognition was monitored for 4 h in artificial seawater with physiological 10 mM Ca^{2+}. ***A***, Homotypic aggregation between *Microciona prolifera* red cells and their glycans on red beads. ***B***, Homotypic aggregation between *Suberites fuscus* yellow cells and their glycans on red beads. ***C***, Homotypic aggregation between *Halichondria panicea* grey cells and their glycans on red beads. ***D***, Species-specific sorting between red (*Microciona*) cells and *Halichondria* glycans on red beads. ***E***, Species-specific sorting between yellow (*Suberites*) cells and *Microciona* glycans on red beads. ***F***, Species-specific sorting between grey (*Halichondria*) cells and *Cliona celata* glycans on red beads. ***G***, Inhibition of the homotypic aggregation between red (*Microciona*) cells and their glycan on red beads in the absence of Ca^{2+}. ***H***, Inhibition of the homotypic aggregation between yellow (*Suberites*) cells and their glycan on red beads in the absence of Ca^{2+}. ***I***, Inhibition of the homotypic aggregation between and (*Halichondria*) cells and their glycan on red beads in the absence of Ca^{2+}. ***J***, Inhibition of the homotypic aggregation between red (*Microciona*) cells and their glycan on red beads by the antibody directed against the carbohydrate epitope of *Microciona* proteoglycan. Pictures were taken by phase-contrast microscope at 10x magnification.

V.2.4. GLYCAN-GLYCAN AGGREGATION IS SPECIES-SPECIFIC

The glycan-coated bead-bead aggregation assay was designed to mimic the classical assay for specific recognition between live sponge cells. Amine- and carboxylate modified beads (1.0 μm in diameter) of two different colors: red and green, were coated with 200 kDa glycans derived from four different species of surface proteoglycans. Aggregation was monitored for 4 h, under identical shear forces, i.e. rotor speed, as provided for cell-cell and cell-glycan recognition assays (60 rpm), in artificial seawater with physiological 10 mM Ca^{2+}.

When glycans from the same species were coated on red and green amine-modified beads, they mixed and formed from 63% (*Cliona*) to 79% (*Microciona*) of yellow aggregates, which are the result of intermingling of red and green (Fig. 20). In stark contrast, beads coated with glycans derived from different species did separate into red and green aggregates showing species-specific sorting. In this case yellow aggregates, i.e. heterogeneous mixtures of glycans originating from different species, never formed more than 12% of patches.

As in cell-cell and cell-glycan aggregation assays, the absence of Ca^{2+}-ions inhibited the specific glycan-glycan recognition. The antibody directed against the carbohydrate epitope of the *Microciona* proteoglycan inhibited only the homotypic interaction between *Microciona* glycans coated on red and green beads (Fig. 20). There was no visible effect of the antibody on homotypic aggregations between glycans from other than *Microciona* species coated on beads (data not shown).

Very similar results were obtained during aggregation between 200 kDa glycans coated onto red and green carboxylate-modified beads. The glycan coupling chemistry was different than this for coupling onto amine-modified beads (see IV.6.), which allowed to test glycan-coated bead-bead recognition in different
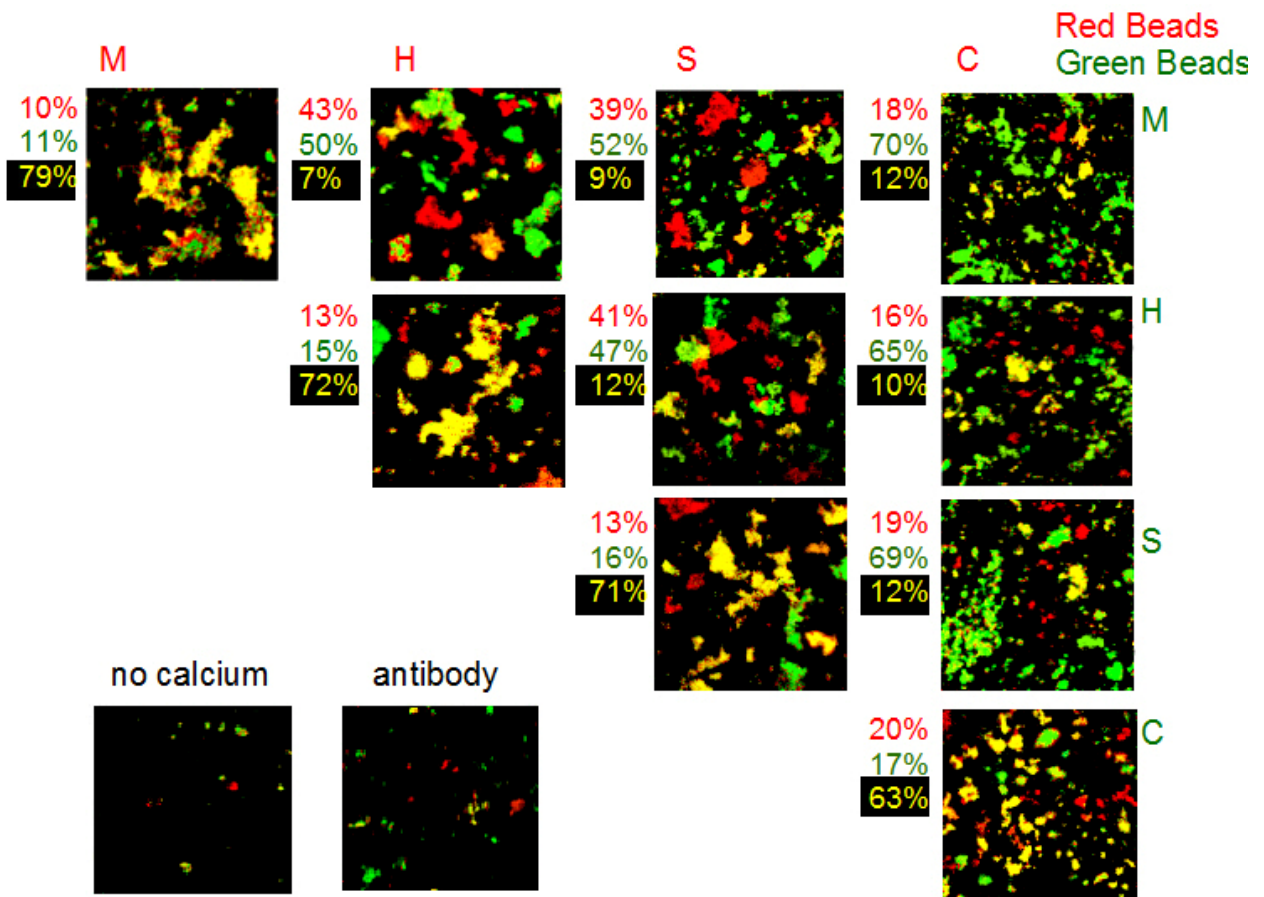
Fig. 20. Species-specific recognition between glycan-coated amine-modified beads. Red and green glycan-coated amine-modified beads sorted out specifically during 4 h rotation-mediated aggregation in seawater with physiological 10 mM Ca^{2+} (see IV.7.). Yellow areas depict clumps of mixed red and green beads coated with identical glycans. Red and green areas reflect clumps of separated beads coated with different species of glycans. The colored numbers on the left side of each picture represent the percentage of clumps of the respective color. The glycan-glycan recognition could be inhibited by the absence of Ca^{2+}-ions. The antibody directed against the carbohydrate epitope of *Microciona prolifera* proteoglycan inhibited homotypic aggregation between *Microciona* glycans coated on red and green beads. Pictures were taken with a confocal microscope at 10x magnification.

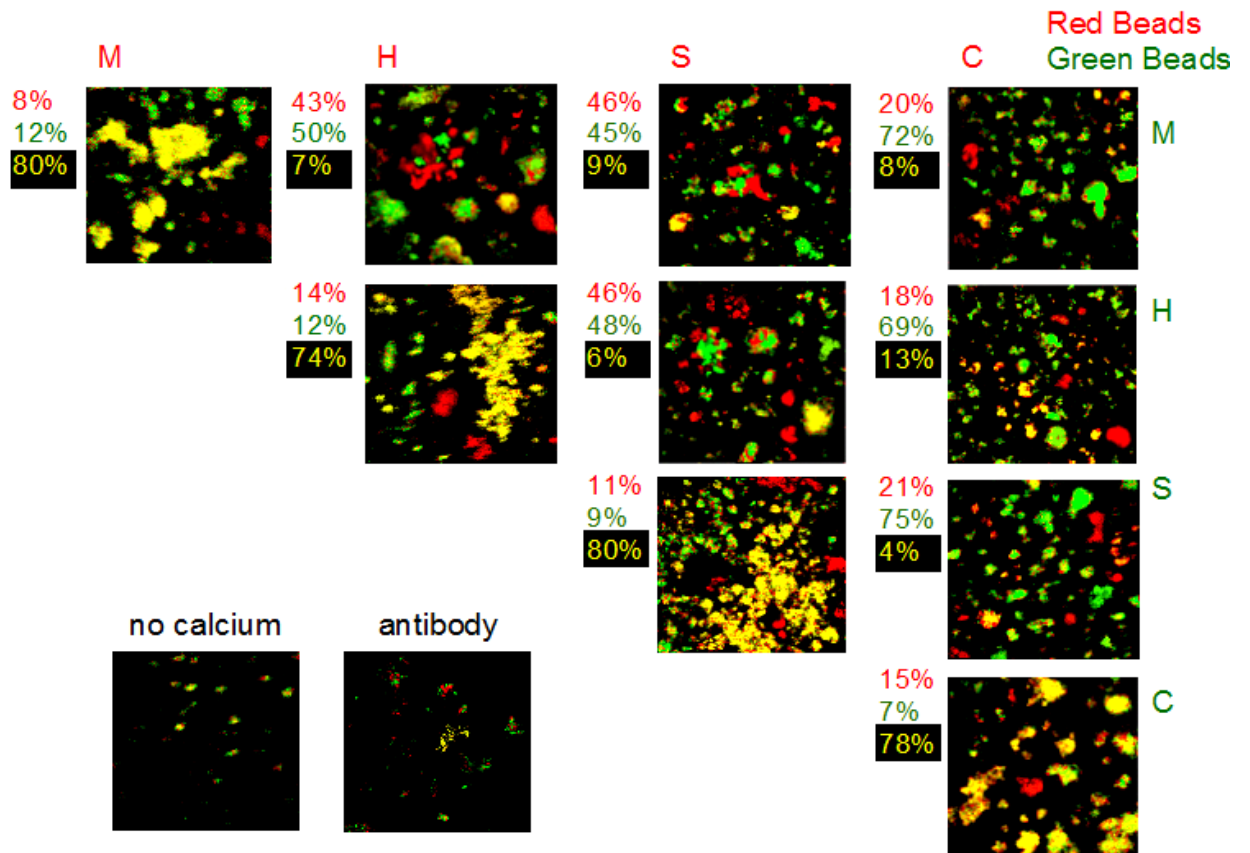M – *Microciona*, H – *Halichondria*, S – *Suberites*, C - *Cliona*.

Fig. 21. Species-specific recognition between glycan-coated carboxylate-modified beads. Red and green glycan-coated carboxylate-modified beads sorted out specifically during 4 h rotation-mediated aggregation in seawater with physiological 10 mM Ca^{2+} (see IV.7.). Yellow areas depict clumps of mixed red and green beads coated with identical glycans. Red and green areas reflect clumps of separated beads coated with different glycans. The colored numbers on the left side of each picture represent the percentage of clumps of the respective color. The glycan-glycan recognition could be inhibited by the absence of Ca^{2+}-ions. The antibody directed against the carbohydrate epitope of *Microciona* proteoglycan inhibited homotypic aggregation between *Microciona* glycans coated on red and green beads. Pictures were taken with a confocal microscope at 10x magnification.
M – *Microciona*, H – *Halichondria*, S – *Suberites*, C - *Cliona*.

system. Carboxylate-modified beads were the same size as the amine-modified beads (1.0 μm in diameter) and the same conditions for aggregation were provided.

Red and green carboxylate beads coated with 200 kDa glycans from the same species mixed and formed from 74% (*Halichondria*) to 80% (*Microciona* and *Suberites*) of homogenous yellow aggregates (Fig. 21). Combinations of beads coated with 200 kDa glycans from different species specifically sorted out and formed separate red and green aggregates. Heterogeneous mixtures of glycans originating from different species never formed more than 13% of yellow clusters. As previously, the absence of Ca^{2+}-ions inhibited the specific aggregation between glycan-coated carboxylate-modified beads, and the antibody directed against the carbohydrate epitope of the *Microciona prolifera* proteoglycan inhibited only the homotypic aggregation between beads coated with *Microciona* 200 kDa glycan (Fig. 21).

There were two possible modes for the color distribution in the glycan-coated bead-bead aggregation: either it was random or species-specific. Random distribution applied to the homotypic glycan-coated bead-bead aggregation, i.e. between glycans from the same species, and the color distribution in these homotypic aggregations could be explained by statistics: the binomial coefficients and Pascal's triangle (Fig. 22).

A binomial is a polynomial expression with two terms, such as (x + y). The terms in Pascal's triangle can be used to write the expansion of any binomial $(x + y)^n$. The numbers in the rows of Pascal's triangle are the same as the coefficients generated by raising the binomial (x + y) to a power. Here, x represents one green bead (g), and y represents one red bead (r), so it could be written $(g + r)^n$. n stands for the average number of beads in each aggregate. For example, if there would be on the average 4 beads in each formed aggregate (n = 4) the expansion, according to the row nr 4 in the Pascal's triangle, would be as shown in Fig. 22:

$$(g + r)^4 = 1g^4 + 4g^3r + 6g^2r^2 + 4gr^3 + 1r^4.$$

It means that there would be one aggregate consisting of only green beads; one aggregate consisting mostly of green beads with small number of red (seen in overlap as orange); one aggregate consisting in half of green and red beads (seen in overlap as yellow); one aggregate consisting mostly of red beads with small amount of green (seen as orange); one aggregate consisting of only red beads. Accordingly, the size of aggregates and color distribution will change with the n number. When n number, i.e. average number of beads in aggregates, is low the size and number of formed aggregates is low as well. It can be also predicted, how many mixed (seen as yellow) and separated (seen as green and red) aggregates will be present. When n number is high, more and bigger aggregates will be present. It can be also predicted that more mixed (yellow) aggregates will form. Nevertheless, there will always be some small red and green clusters present as explained by the distribution in Pascal's triangle.

The average number of amine beads in single aggregates (n number) in all homotypic aggregations performed here, i.e. between *Microciona* glycans, between *Halichondria* glycans, between *Suberites* glycans, and between *Cliona* glycans is given in Fig. 22. It can be seen, that the highest n number was for homotypic *Microciona* aggregates (6×10^3) and the lowest n number was for *Cliona* aggregates (1.5×10^3). In summary, the biggest homotypic aggregates formed in glycan-coated bead-bead aggregation (Fig. 20) were seen for beads coated with *Microciona* (M-M), with the highest percentage of yellow clumps (79%). Moderate number of yellow clumps was recorded for *Halichondria* (H-H) and *Suberites* (S-S) bead aggregates: ~70%, which were characterized by the same n number. Finally, the lowest number of yellow aggregates: 63%, was observed for *Cliona* (C-C), characterized by the lowest n number.
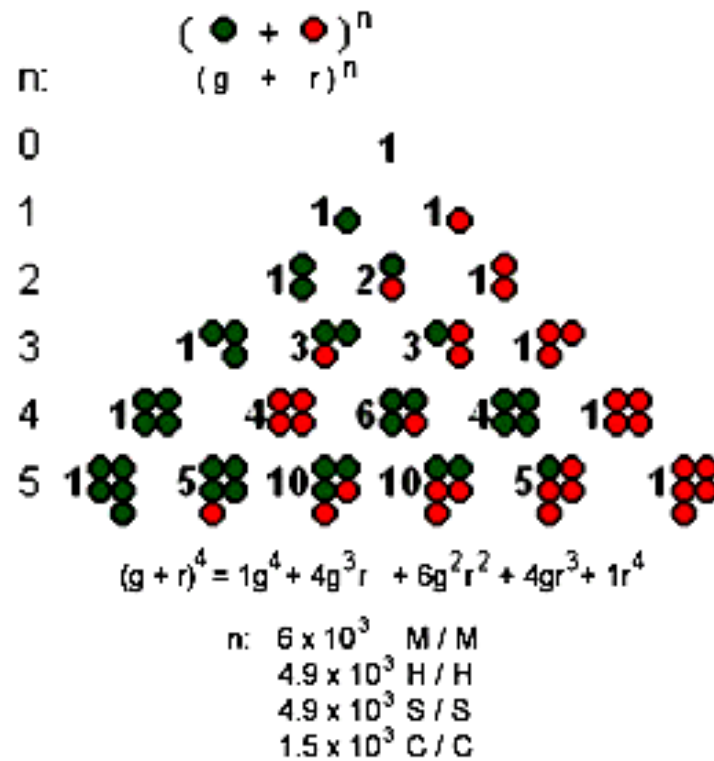
Fig. 22. Pascal's triangle for color distribution in the homotypic glycan-coated bead-bead aggregation. Binomial expansion of the formula (g + r) rose to a power *n*. The numbers in the rows of Pascal's triangle refer to coefficients generated by raising the binomial (g + r) to a power. The example of the expansion of binomial formula (g + r) when n = 4. Average numbers of single beads (*n*) in homotypic glycan-coated bead aggregates are given. *n*, the average number of single beads in aggregates. *g*, a green bead. *r*, a red bead. M – *Microciona*, H – *Halichondria*, S – *Suberites*, C - *Cliona*.

Pascal's triangle analysis of the color distribution in the heterotypic glycan-coated bead-bead aggregation, i.e. between glycans from two different species, proved the species-specific and not random character of the aggregation. Red and green beads coated with glycans from two different species were species-specifically sorting out into separate red and green aggregates. This aggregation did not simply apply to statistics but depended on biological properties of sorting such as density of glycans on a bead surface, shear forces and differences in the strength of the heterotypic vs. homotypic glycan-glycan interactions.

V.2.5. CALCIUM UPTAKE IN CELL-CELL AND GLYCAN-GLYCAN AGGREGATION

Specific interactions between mechanically dissociated live sponge cells, surface proteoglycans, and glycans are dependent on Ca^{2+}-ions. Physiological concentration of Ca^{2+}, i.e. 10 mM, has to be always added to initiate these specific interactions.

The calcium uptake in the homotypic aggregation between *Microciona prolifera* cells and between *Cliona celata* cells was studied (Fig. 23*A*). 10 mM $CaCl_2$ labeled with Ca-45 was added to artificial seawater and cells were allowed to aggregate for 12 h (see IV.8.). The presence of Ca-45 left in the buffer was monitored to estimate the quantity of calcium that went into cell aggregates and was involved in cell-cell interactions. *Microciona* cells take Ca^{2+}-ions from the artificial seawater buffer much faster than *Cliona* cells (Fig. 23*A*). ~ 70% of calcium went from the buffer into *Microciona* cell aggregates within the first 30 min of aggregation process, while only ~40% of total calcium went into *Cliona* cell aggregates. At the end, after 4 h of aggregation, ~90% of the total calcium went into *Microciona* cell aggregates. The saturation point for aggregation between *Cliona* cells was reached after 6 h of the process, and ~85% of the total added calcium went into *Cliona* cell aggregates.

Similarly, 10 mM $CaCl_2$ labeled with Ca-45 was added to artificial seawater to initiate 12 h-aggregation between *Microciona* 200 kDa glycans and between *Cliona* 200 kDa glycans coated on beads. Monitoring of Ca-45 revealed that, as in cell-cell aggregation, *Microciona* glycans take calcium from the buffer much faster than *Cliona* glycans (Fig. 23*B*). Differences are even more distinct than those observed during cell-cell aggregation. After 30 min of the aggregation process, almost half of the calcium was involved in forming and stabilizing *Microciona* glycan aggregates, whereas only ~20% of calcium was involved in forming *Cliona* glycan aggregates. After 5 h of aggregation, the saturation point in *Microciona* bead-bead aggregation was reached and ~80% of the total added calcium went from the buffer into *Microciona* glycan aggregates. The saturation point for *Cliona* glycan-coated bead-

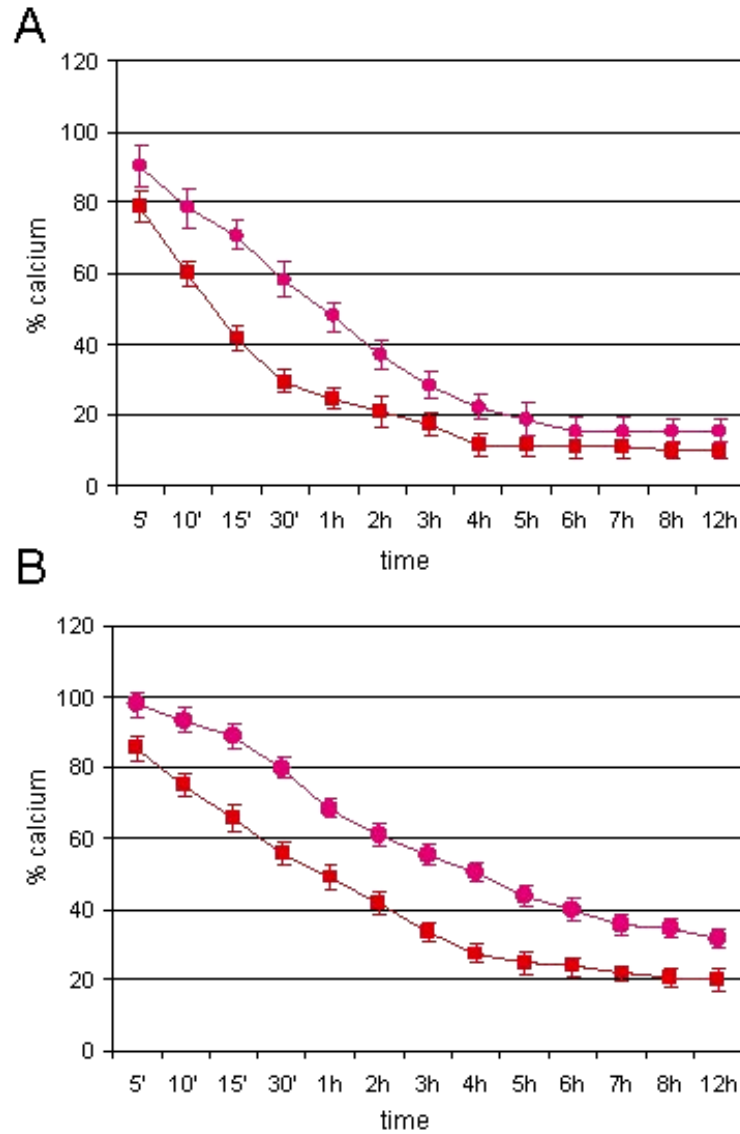bead aggregation was reached after 7 h, and ~75% of the total calcium went into *Cliona* glycan aggregates.

Fig. 23. Calcium uptake in cell-cell and glycan-glycan aggregation. Calcium uptake in 12h-rotation mediated aggregation in artificial seawater with physiological 10 mM labeled calcium (see IV.8.) *A*, Calcium uptake in homotypic *Microciona-Microciona* (■) and *Cliona-Cliona* (●) cell-cell aggregation. *B*, Calcium uptake in homotypic *Microciona-Microciona* (■) and *Cliona-Cliona* (●) glycan-coated bead-bead aggregation.

V. 3. ADHESION TO GLYCAN-COATED PLATES

V.3.1. BINDING TO PLASTIC SURFACES

Cell surface proteoglycans and purified 200 kDa glycans were used as a coat in binding experiments to coated plates. Therefore, the ability of purified cell surface proteoglycans and 200 kDa glycans to bind to a plastic surface of 96-well flat bottom plates was tested. Proteoglycans and glycans from different sponge species adsorbed on polystyrene wells without any derivatization (see IV.9.1.).

The ability of proteoglycans to adhere to polystyrene wells was rather high when 0.02-0.6 µg proteoglycans were added to wells, and it was between 60 and 80% (Fig. 24*A*). The percentage of proteoglycans bound to a plastic surface dropped down to 22-45%, when more than 1.25 µg proteoglycans were added to wells. *Cliona celata* proteoglycan showed the best ability to bind to plastic surfaces. Binding ability of *Microciona prolifera* proteoglycan molecules was the worst, especially when the amount of added proteoglycans was above 1.25 µg.

In experiments studying cell adhesion to proteoglycan-coated surfaces, the amount of proteoglycans added as a coat to plastic wells was high enough to reach the final amount in the range of 0.01-1 µg proteoglycans bound to plastic surfaces.

Adsorption of glycans on polystyrene wells is usually low, and the approximate percentage of glycans bound to a plastic surface was 40-58% (Fig. 24*B*). These values are lower than these for binding of proteoglycans to plastic surfaces. Moreover, binding of glycans to a plastic surface was not dependent on the amount of glycans added to wells of 96-well plates. There were also almost no differences in binding abilities between different species of glycans.

67

In all experiments studying glycan and cell adhesion to glycan-coated plates, the concentration of glycans added as a coat to plastic wells was high enough to reach the final amount in the range of 0.025-5 µg glycans bound to plastic surfaces.
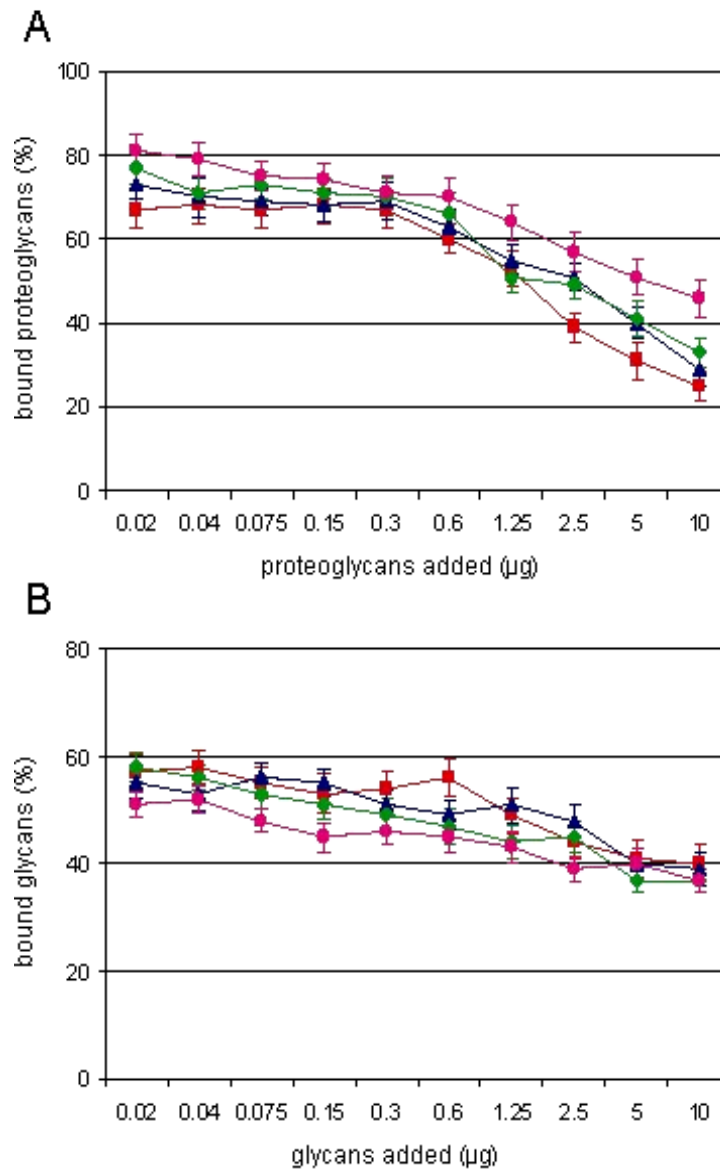

Fig. 24. Binding of proteoglycans and glycans to plastic surfaces. Isolated µ proteoglycans and glycans in artificial seawater were added to 96-well flat bottom polystyrene plastic plates for 2 h and non-bound molecules were washed off with artificial seawater (see IV.9.1.). *A*, Binding of proteoglycan molecules to a plastic surface. *B*, Binding of 200 kDa glycan molecules to a plastic surface. (■) *Microciona,* (▲) *Halichondria*, (◆) *Suberites*, (●) *Cliona.*

68

V.3.2. ADHESION OF LIVE CELLS TO PROTEOGLYCAN - COATED PLATES IS SPECIES-SPECIFIC

Surface proteoglycans from four different sponge species were coated on plastic surfaces. Mechanically dissociated cells were added to wells and the ability and specificity of live sponge cells to adhere to different surface proteoglycans coated onto a solid phase was studied. Cells adhered strongly to their own surface proteoglycans in the presence of physiological Ca^{2+}-ions in artificial seawater (Fig. 25*A-D*). The amount of cells that adhered specifically to their own proteoglycans was the highest for *Microciona prolifera*, moderate for *Halichondria panicea and Suberites fuscus*, and the lowest for *Cliona celata*.

Adhesion of cells to proteoglycans from other sponge species was reduced, i.e. it was 3-5 times lower. The difference between strong adhesion of cells to their own proteoglycans and much reduced to proteoglycans from other species could be clearly observed above 0.2 μg of surface-bound proteoglycans. *Microciona* cells, along the best ability for homotypic binding to their own proteoglycans, were characterized by the highest ability of heterotypical binding to surfaces coated with proteoglycans from other species. Nevertheless, it was still 3 times lower than binding to surfaces coated with their own proteoglycan. On the contrary, *Cliona* cells, characterized by the lowest ability for homotypic binding to their own proteoglycan, showed the best species-specific recognition and bound 5 times less to surfaces coated with other species of proteoglycans.

The adhesion of sponge cells to surfaces coated with their own surface proteoglycans was clearly dependent on the quantity of the proteoglycan coated and could be abolished in the absence of Ca^{2+}-ions in artificial seawater. The antibody directed against the carbohydrate epitope of the *Microciona* surface proteoglycan almost completely inhibited the adhesion of *Microciona* cells to their surface proteoglycans (M-M) (Fig. 25*E*). Little cross-reactivity of the antibody[108] could be detected and it
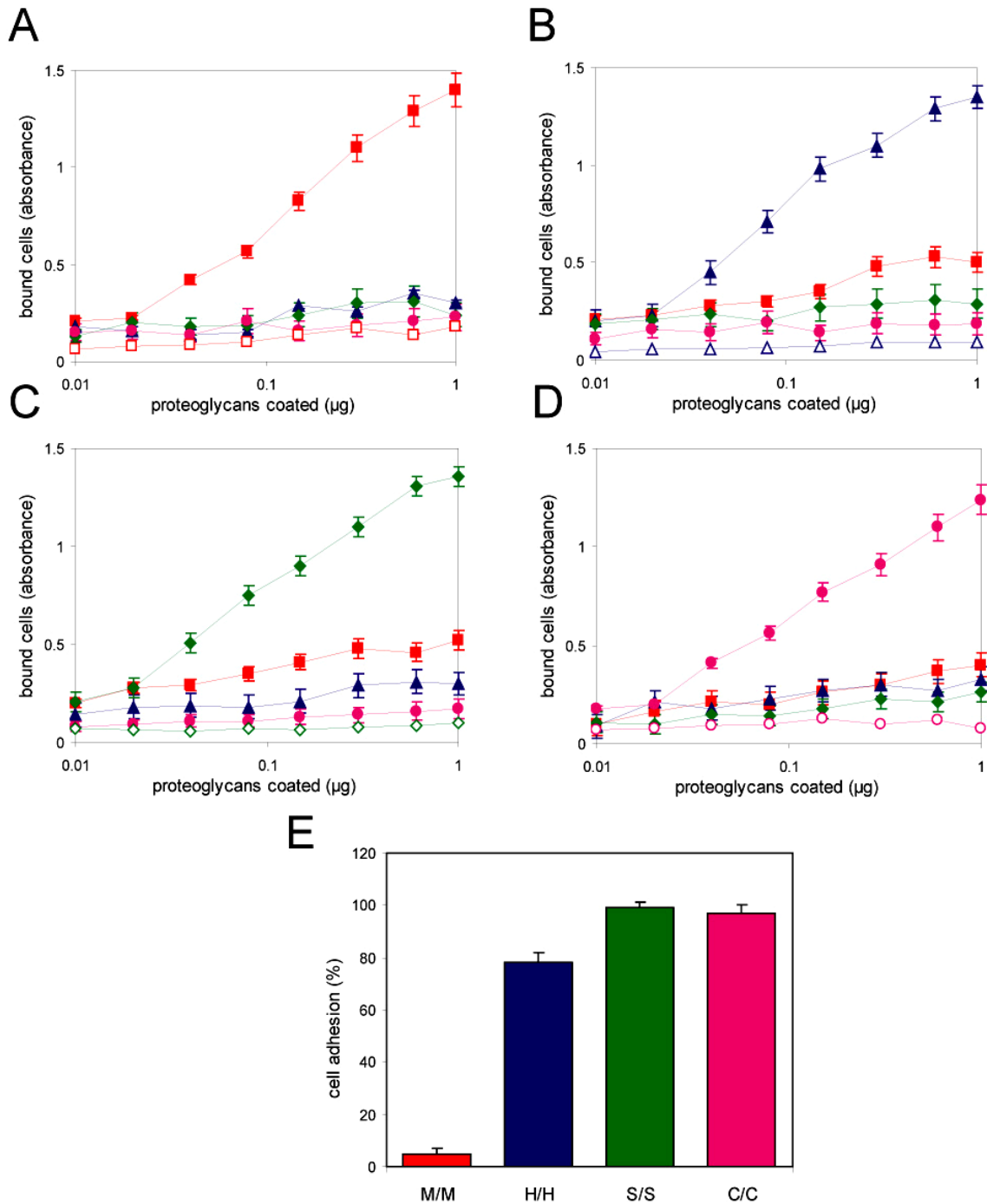
Fig. 25. Adhesion of live cells to proteoglycan-coated plates. 2h-adhesion of live cells to 96-well flat bottom polystyrene plastic plates coated with proteoglycans from different sponges in artificial seawater with physiological 10 mM Ca^{2+} (see IV.9.2.). *A*, *Microciona*, *B*, *Halichondria*, *C*, *Suberites*, and *D*, *Cliona* cells adhered to *Microciona* (■), *Halichondria* (▲), *Suberites* (◆), and *Cliona* (●) proteoglycans coated on a surface. (□,△,◇,○) Binding of the respective cells to their glycans coated on plates without the presence of Ca^{2+}. *E*, Effect of the antibody directed against the carbohydrate epitope of *Microciona* proteoglycan on cell adhesion to proteoglycan-coated plates.

blocked 12% of the homotypic adhesion between *Halichondria* cells and their surface proteoglycans (H-H). The antibody did not block homotypic adhesions between *Suberites* (S-S) and *Cliona* (C-C) cells and their surface proteoglycans.

V.3.3. ADHESION OF LIVE CELLS TO GLYCAN-COATED PLATES IS SPECIES-SPECIFIC

In the second cellular adhesion system, the adhesion of live cells to 200 kDa glycans from four different surface proteoglycans coated onto plastic surfaces was investigated. As in cell adhesion to the whole proteoglycan molecules coated onto a solid phase, cells adhered specifically to surfaces coated with 200 kDa glycans from their own surface proteoglycans (Fig. 26*A-D*). The highest amount of cells that adhered to surfaces coated with their own glycans was again for *Microciona prolifera* cells, and the lowest for *Cliona celata* cells.

Heterotypic adhesion of cells to glycans from other sponge species was 2.5 to 5.5 times lower. The difference between strong adhesion of cells to their own glycans and much lower to glycans from other species could be clearly observed above 0.5 µg of surface-bound glycans. As in binding to proteoglycan-coated surfaces, *Microciona* cells showed the highest ability for cross-specific adhesion to glycans from other species. However, *Microciona* cells still bound to surfaces coated with glycans from other species 2.5 - 3 times less than to surfaces coated with their own glycan. *Cliona* cells bound to glycans from other species 5.5 times less than to their own, showing the highest ability for species-specific recognition of glycans.

Cell adhesion was dependent on the quantity of glycans coated, and could be abolished in the absence of Ca^{2+}-ions in artificial seawater. Pretreatment of *Microciona* cells with the antibody directed against the carbohydrate epitope of their surface proteoglycan inhibited 86% of these cells from adhesion to their own 200
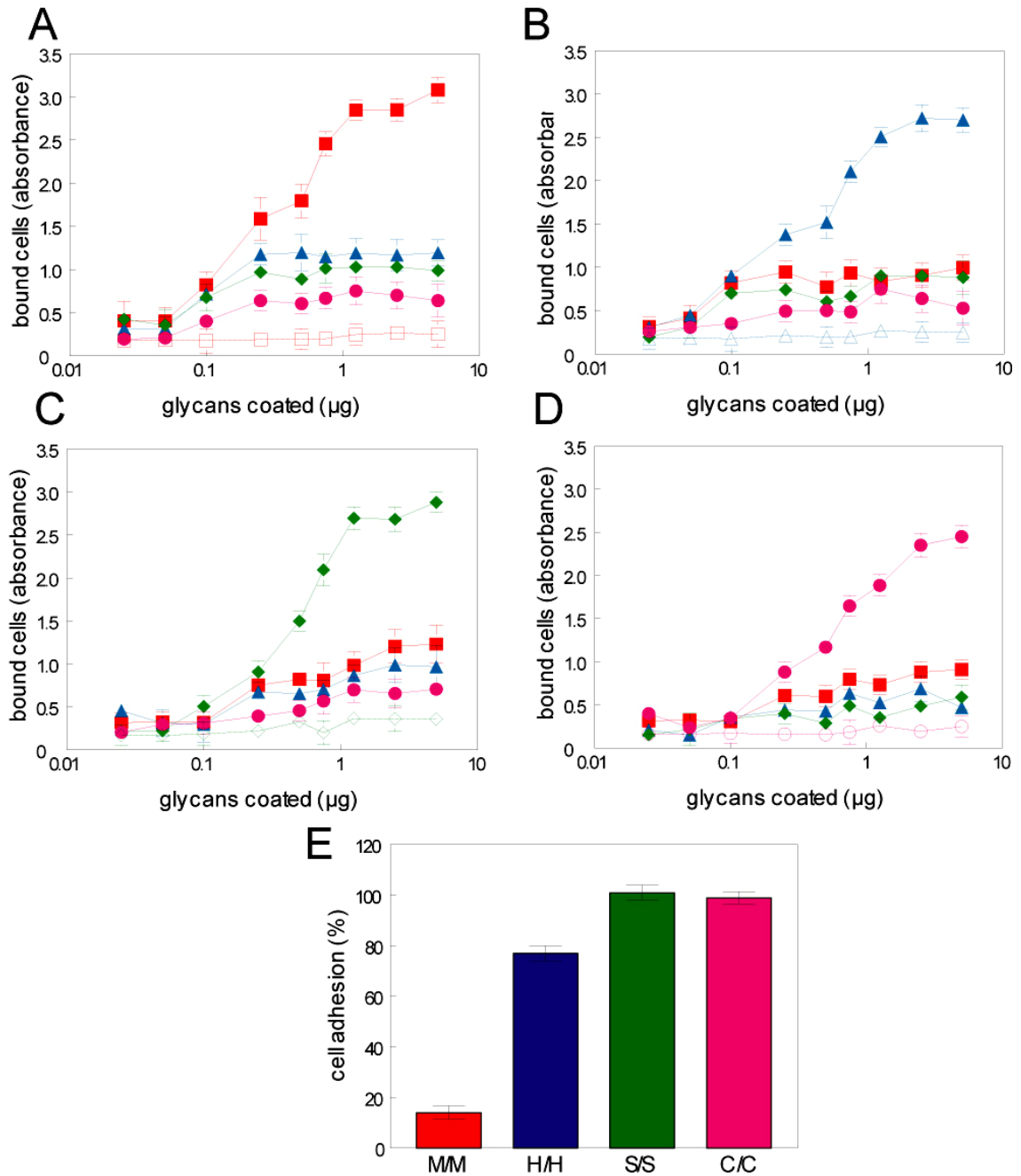
Fig. 26. Adhesion of live cells to glycan-coated plates. 2h-adhesion of live cells to 96-well flat bottom polystyrene plastic plates coated with glycans from different proteoglycans in artificial seawater with physiological 10 mM Ca^{2+} (see IV.9.3.). **A**, *Microciona*, **B**, *Halichondria*, **C**, *Suberites*, and **D**, *Cliona* cells adhered to *Microciona* (■), *Halichondria* (▲), *Suberites* (♦), and *Cliona* (●) glycans coated on a surface. (□,△,◇,○) Binding of the respective cells to their glycans coated on plates without the presence of Ca^{2+}. **E**, Effect of the antibody directed against the carbohydrate epitope of *Microciona* proteoglycan on cell adhesion to glycan-coated plates.

kDa glycan (M-M) (Fig. 26*E*). As previously, the antibody showed little cross-reactivity[108] and could reduce the adhesion between *Halichondria* cells and their glycans (H-H) by 23%, while not having an effect on other homotypic adhesions (S-S, C-C).

V.3.4. ADHESION OF LIVE CELLS TO GLYCAN-COATED PLATES PROMOTES CELL DIFFERENTIATION

Some sponge cells differentiate irreversibly, such as those committed to reproduction, or specialized for secretory activity and skeleton production[114,115]. Other cells retain differentiative capacity and can change their function. After the primary differentiation in development, the reservoir of cells with the capacity for later differentiations remains to establish the histological system characteristic of the adult sponge. Mechanically dissociated sponge cells could reform functional sponge organism by e.g. differentiation of archaeocyte cells, which can give rise to all cell types of a mature sponge.

Mechanically dissociated *Microciona prolifera* cells were added to plates coated with their own 200 kDa glycan and to plates not coated with any 200 kDa glycans. A great enhancement of cell differentiation was observed in *Microciona* cells adhered to glycan-coated plates (Fig. 27*A-C*). After 60 h, the formation of spicule skeleton was observed. Spicules are the most common type of a mineral skeleton[114]. Their primarily function is supporting and maintenance of the sponge structure.

In contrast, no cell differentiation and spicules formation could be observed when *Microciona* cells were added to non-coated plates (Fig. 27*D-F*). No skeleton formation could be seen after 60 h of cell adhesion to plastic surfaces not coated with the glycan. Only after 84 h, cell differentiation slowly occurred and also the formation of mineral skeleton in the form of spicules slowly started.
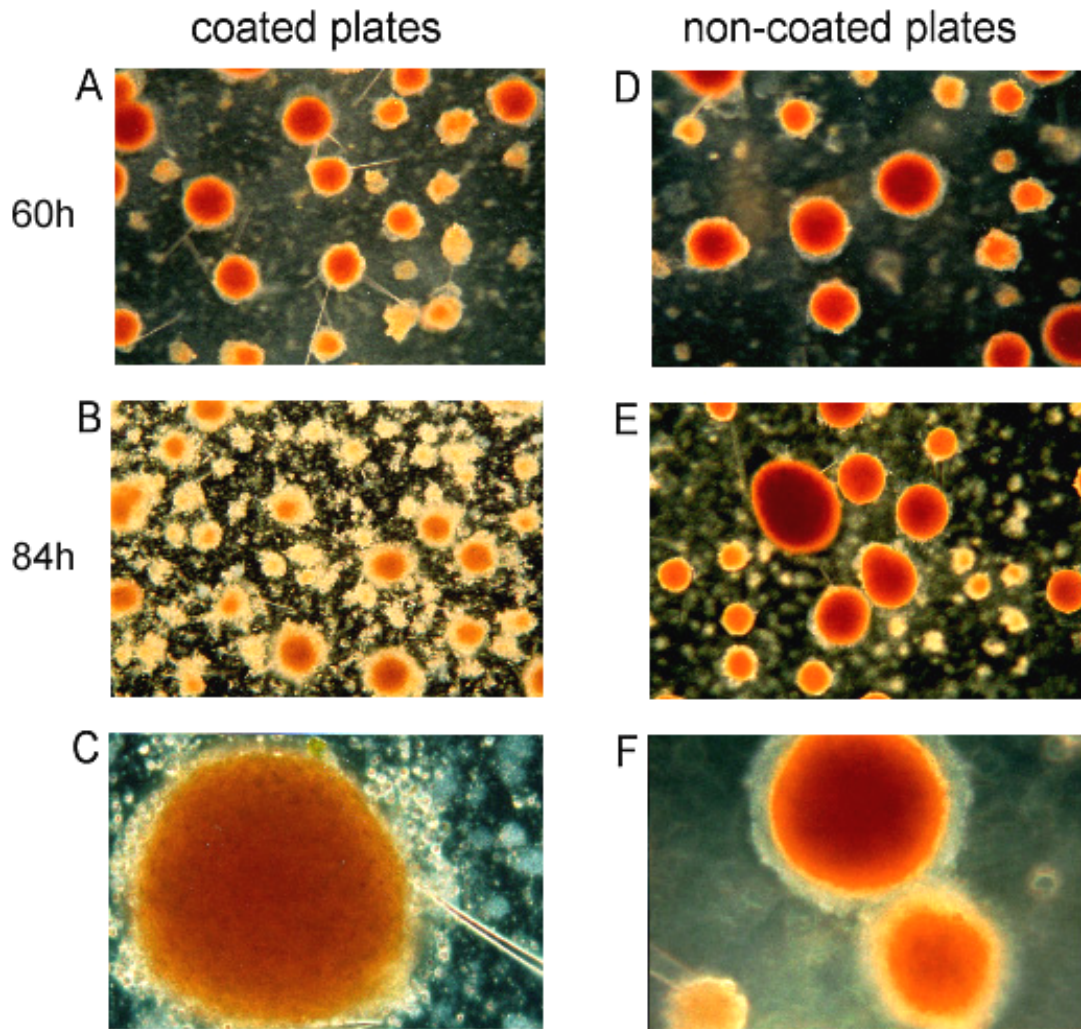
Fig. 27. Cell differentiation and formation of the spicule skeleton. *Microciona prolifera* cells were added to plastic surfaces coated with their own 200 kDa glycans (*A-C*) and to non-coated plastic surfaces (*D-F*) in artificial seawater with physiological 10 mM Ca^{2+}. *A*, Formation of spicules after 60-h adhesion of *Microciona* cells to glycan-coated surface. *B*, Further differentiation of *Microciona* cells after 84-h adhesion to glycan-coated surface. *C*, Differentiating *Microciona* cell with formed spicules after 84-h adhesion. *D*, *Microciona* cells after 60-h adhesion to non-coated surface. *E*, Slow differentiation and formation of spicules after 84-h adhesion. *F*, *Microciona* cells after 84h-adhesion to non-coated surface. Pictures were taken by phase-contrast microscope at 32x magnification for *A, B, D, E*, and at 40x magnification for *C, F*.
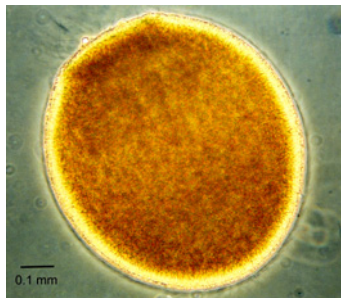
V.3.5. ADHESION OF LARVAL CELLS TO GLYCAN-COATED PLATES IS SPECIES-SPECIFIC

Sometimes, after settlement and spreading of sponge larvae, highly species-specific fusion of individual larvae can occur[114]. To mimic the natural behavior of larvae and their ability to recognize and adhere to surface glycans, larval cells of *Microciona prolifera* and *Halichondria panicea* were obtained (Fig. 28) and investigated for binding to surfaces coated with 200 kDa glycans purified from proteoglycans from cells of "mother sponges".

Larval cells specifically recognized and strongly adhered to their own surface glycans (Fig. 29*A-B*). The amount of *Microciona* larval cells that adhered to their own glycan was higher than the amount of *Halichondria* cells that adhered to their glycan. The binding of larval cells to 200 kDa glycans from other species was 3.5 - 6 times lower.

Adhesion of larval cells to surfaces coated with 200 kDa glycans was observed only in the presence of Ca^{2+}-ions. The antibody directed against the carbohydrate epitope of *Microciona* surface proteoglycan blocked 84% of the adhesion of *Microciona* larval cells to their 200 kDa glycan and reduced the adhesion of *Halichondria* cells to their glycan by 16% (Fig. 29*C*).

Microciona prolifera larvae   *Halichondria panicea* larvae
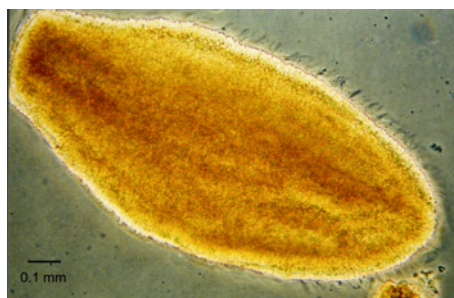
Fig. 28. Pictures of larvae obtained from two different sponge species. Swimming larvae were obtained as described in IV.1.
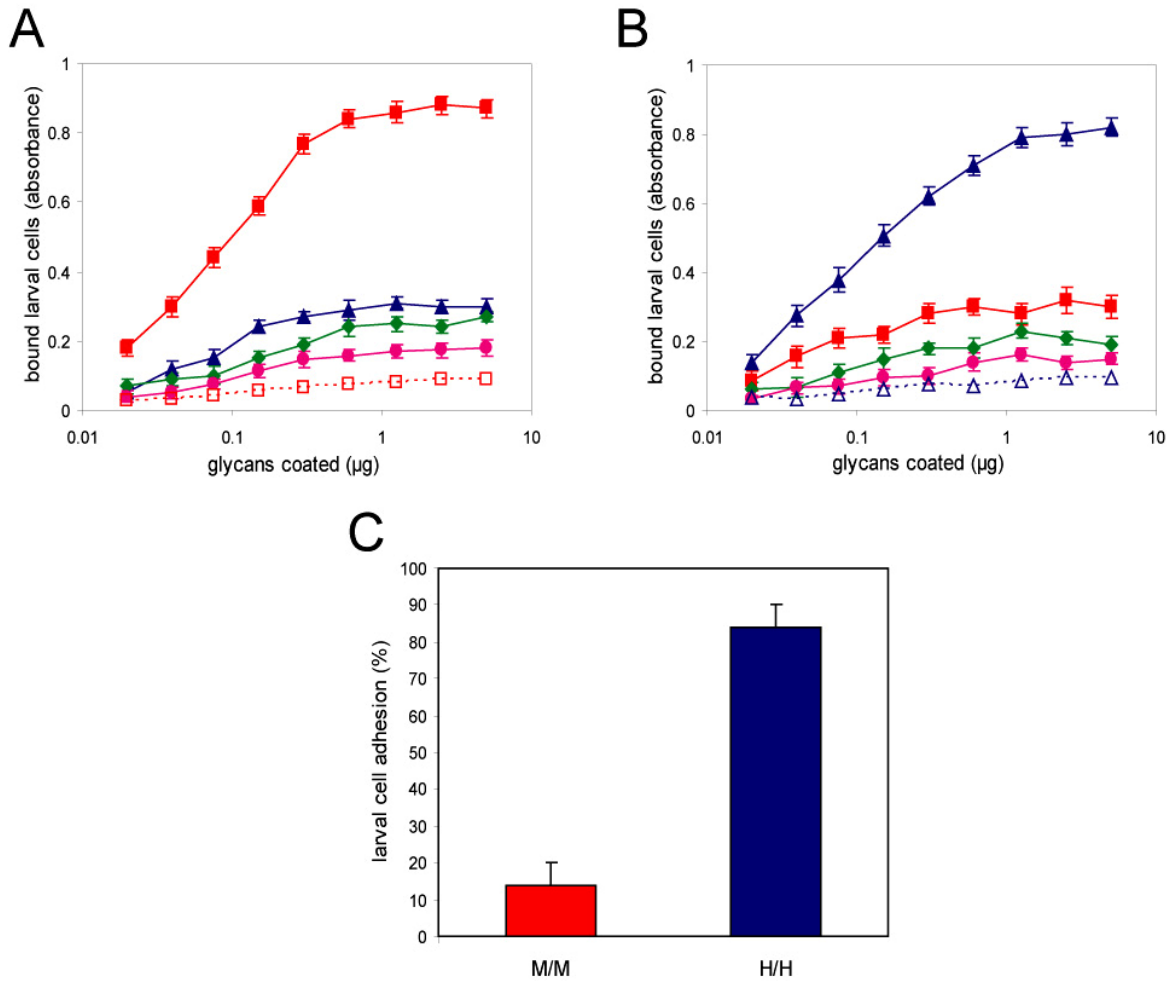
Fig. 29. Adhesion of larval cells to glycan-coated plates. 2h-adhesion of larval cells to 96-well flat bottom polystyrene plastic plates coated with glycans from mother sponges in artificial seawater with physiological 10 mM Ca^{2+} (see IV.9.3.). **A**, *Microciona*, **B**, *Halichondria*, **C**, *Suberites*, and **D**, *Cliona* cells adhered to *Microciona* (■), *Halichondria* (▲), *Suberites* (◆), and *Cliona* (●) glycans coated on a surface. (□,△) Binding of the respective cells to their glycans coated on plates without the presence of Ca^{2+}. **E**, Effect of the antibody directed against the carbohydrate epitope of *Microciona* proteoglycan on cell adhesion to glycan-coated plates.

V.3.6. ADHESION OF GLYCAN-COATED BEADS TO GLYCAN-COATED PLATES IS SPECIES-SPECIFIC

The behavior and aggregation of glycan-coated beads resembled the behavior and aggregation of live sponge cells. The size of beads (1 µm in diameter) is similar to the size of small sponge cells (2 µm in diameter). Most importantly, the density of 200 kDa glycan molecules on the bead surface (810 molecules/μm^2) required for glycan-coated bead-bead aggregation was almost identical to the density of 200 kDa glycan molecules on cell surface (828 molecules/μm^2) required for cell-cell aggregation (see IV.2.2.). These allow quantitative comparisons between experiments with adhesion of live cells and beads coated with 200 kDa glycans to glycan-coated surfaces.

The same red amine-modified beads coated with different 200 kDa glycans as in the cell-glycan aggregation (see IV.2.3.) were used to study glycan-coated beads adhesion to glycan-coated plates. Glycan-coated beads adhered strongly to the surface coated with the identical glycan as on beads (Fig. 30). There was almost no adhesion to the surface coated with glycans different than these on beads.

As in all previous adhesion experiments, the species-specific adhesion of glycan-coated beads to surfaces coated with glycans was strictly dependent on the presence of physiological Ca^{2+}-ions in artificial seawater (10 mM). The carbohydrate epitope of *Microciona* proteoglycan-directed antibody abolished the homotypic adhesion of red beads coated with *Microciona* 200 kDa glycans to the surface coated with the same glycan, while having no visible effect on homotypic adhesions of red beads coated with other studied species of glycans.
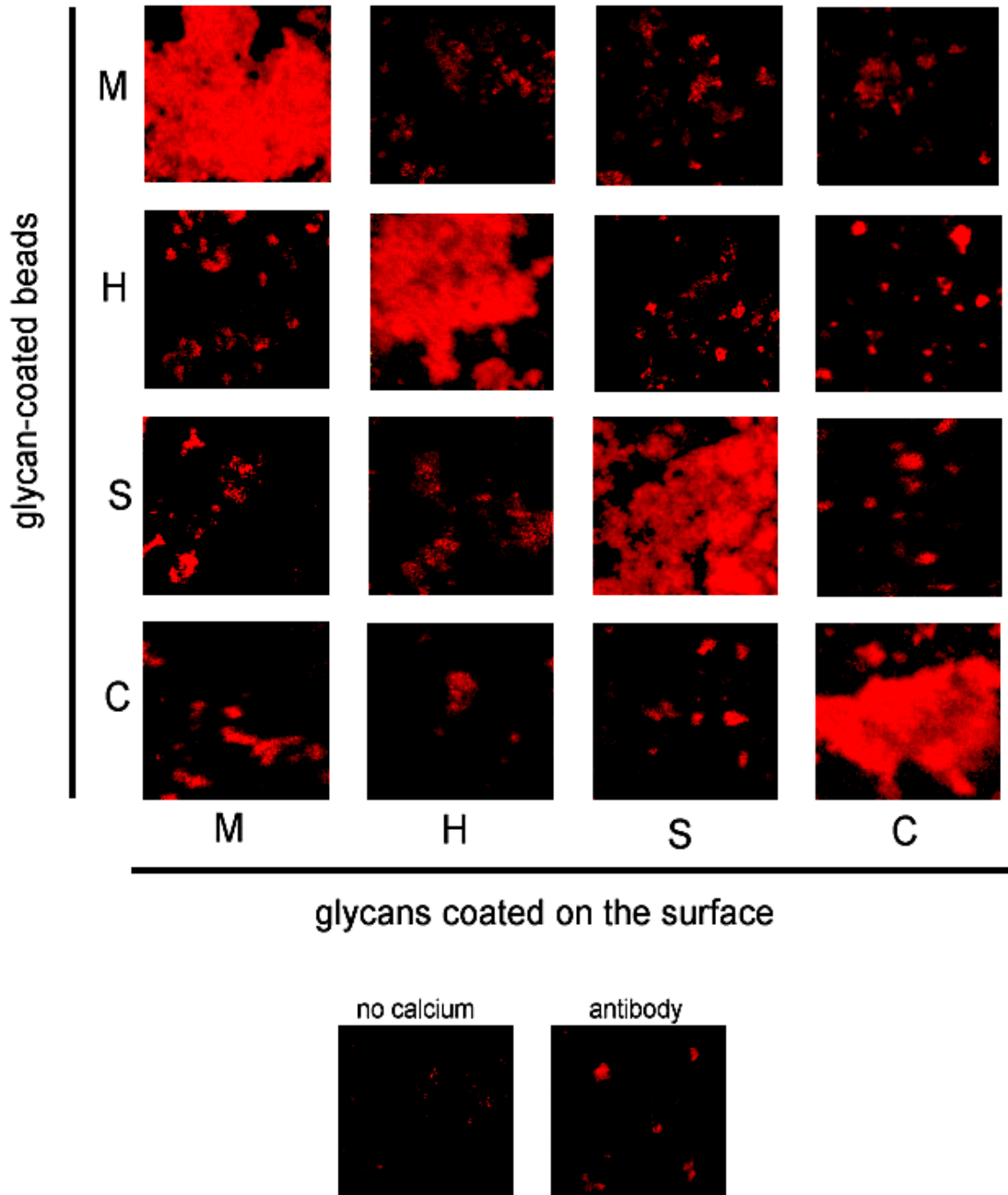
Fig. 30. Adhesion of glycan-coated beads to glycan-coated plates. 2h-adhesion of glycan-coated red amine-modified beads to 96-well flat bottom polystyrene plastic plates coated with glycans from different proteoglycans in artificial seawater with physiological 10 mM Ca^{2+} (see IV.9.3.). The adhesion could be inhibited by the absence of Ca^{2+}-ions. The antibody directed against the carbohydrate epitope of *Microciona* proteoglycan inhibited homotypic adhesion of *Microciona* glycan-coated green beads to the surface coated with the same glycans. Pictures were taken with a confocal microscope at 10x magnification. M – *Microciona*, H – *Halichondria*, S – *Suberites*, C - *Cliona*.

V.3.7. ADHESION OF GLYCANS TO GLYCAN-COATED PLATES IS SPECIES-SPECIFIC

Equal quantities of 200 kDa glycans purified from various surface proteoglycans were added to 96-well plates pre-coated with different 200 kDa glycans, and left to adhere for 2h in artificial seawater with physiological 10 mM Ca^{2+}.

200 kDa glycans adhered strongly, and in a dose-dependent manner, to identical glycans coated on a solid phase (Fig. 31*A-D*). The amount of glycans bound to surfaces coated with the glycan from the same species was distributed exactly the same as in the adhesion between matured cells and their surface glycans. The highest amount of bound glycans was for homotypic binding between *Microciona* glycans, moderate between *Halichondria* and *Suberites* glycans, and the lowest between *Cliona* glycans.

Heterotypic adhesions between glycans from two different species were much reduced. There was from 2.5 to 4.5 times less heterotypic adhesion between different glycans when compared to homotypic adhesion between glycans from the same species. Differences between high adhesion of glycans to the same glycans coated on the surface and much lower adhesion to glycans from other species coated on the surface could be clearly observed above 0.6 μg of coated glycans. Similarly to results from adhesion of live cells to glycan-coated plates, *Microciona* glycan showed the highest ability for cross-specific adhesion to surfaces coated with glycans from other species. However, *Microciona* glycan still bound to surfaces coated with glycans from other species 2.5 times less than to surfaces coated with another *Microciona* glycan. *Cliona* glycan showed the highest ability for species-specific recognition and bound to surfaces coated with glycans from other species 4.5 times less than to surfaces coated with another *Cliona* glycan.
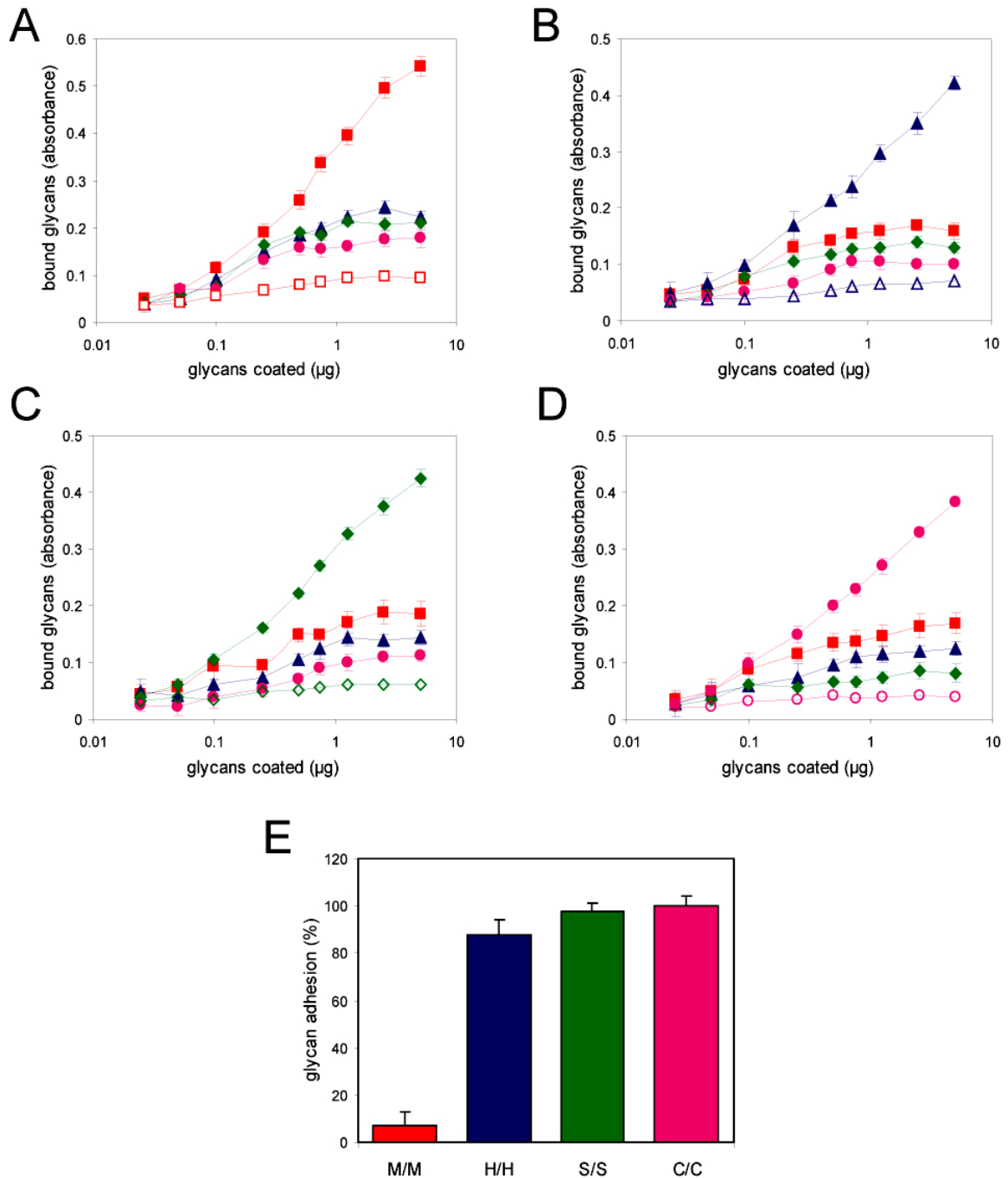
Fig. 31. Adhesion of glycans to glycan-coated plates. 2h-adhesion of 200 kDa glycans to 96-well flat bottom polystyrene plastic plates coated with glycans from different proteoglycans in artificial seawater with physiological 10 mM Ca^{2+} (see IV.9.3.). *A*, *Microciona*, *B*, *Halichondria*, *C*, *Suberites*, and *D*, *Cliona* glycans adhere to *Microciona* (■), *Halichondria* (▲), *Suberites* (◆), and *Cliona* (●) glycans coated on a surface. (□,△,◇,○) Binding of the respective glycans to the same glycans coated on plates without the presence of Ca^{2+}. *E*, Effect of the antibody directed against the carbohydrate epitope of *Microciona* proteoglycan on a glycan adhesion to glycan-coated plates.

Adhesion occurred only in the presence of Ca^{2+}-ions. The antibody directed against the carbohydrate epitope of *Microciona* proteoglycan blocked 93% of the homotypic adhesion between *Microciona* glycans. The antibody showed little cross-reactivity by blocking 12% of the homotypic adhesion between *Halichondria* glycan[108], while having almost no effect on other homotypic interactions (Fig. 31*E*).

V.4. ATOMIC FORCE MICROSCOPY MEASUREMENTS OF ADHESION FORCES BETWEEN SINGLE GLYCAN MOLECULES

Atomic force microscopy (AFM) has the precision and sensitivity to study molecular recognition under native conditions at the level of single events at forces down to the piconewton (pN) range[116,117]. 200 kDa glycan molecules from different sponge species were coated on an AFM tip and a surface. Gold coated Si_3N_4 tips and gold coated micas allowed covalent chemisorption of the naturally sulfated 200 kDa glycans (Fig. 32). Intermolecular adhesion force measurements between single glycan molecules were performed in artificial seawater with physiological 10 nM Ca^{2+}.

V.4.1. SINGLE CARBOHYDRATE-CARBOHYDRATE ADHESION FORCE IS IN THE PICONEWTON RANGE

Figure 32 shows the AFM set up for measuring the forces between single 200 kDa molecules. During retraction of the tip the glycan structure was lifted, stretched and finally non-covalent bonds between two molecules were being broken one by one. The existence of multiple non-covalent bonds between carbohydrates of glycan molecules is suggested by the presence of multiple peaks on force curves, as recorded in the presence of Ca^{2+} (Fig. 32, *line 3-9*). Monitored cantilever deflection was a direct measure for the forces between interacting glycan molecules. There was no interaction measured during the surface approach. On retraction, the sensor tip

detected strong multiple interactions between 200 kDa glycans from the same species. The single non-covalent bond between two interacting glycan molecules from the same species was ruptured at the forces between 190 (*Cliona* glycan-glycan interaction) and 310 pN (*Microciona* glycan-glycan interaction) (Fig. 33 and 34).

There was no interaction recorded between gold-gold (Fig. 32, *line 1*) or in the absence of Ca^{2+}-ions (*line 2*). Force measurements taken directly at the surface (<10 nm) were due to non-specific interactions between the cantilever tip and the surface[118], e.g. the first peak in Fig 32, *lines 3, 6, 8* and the first two in Fig. 32, *line 5*. Only those measured at distances >10 nm from the surface were considered as a direct binding force between interacting glycan molecules.
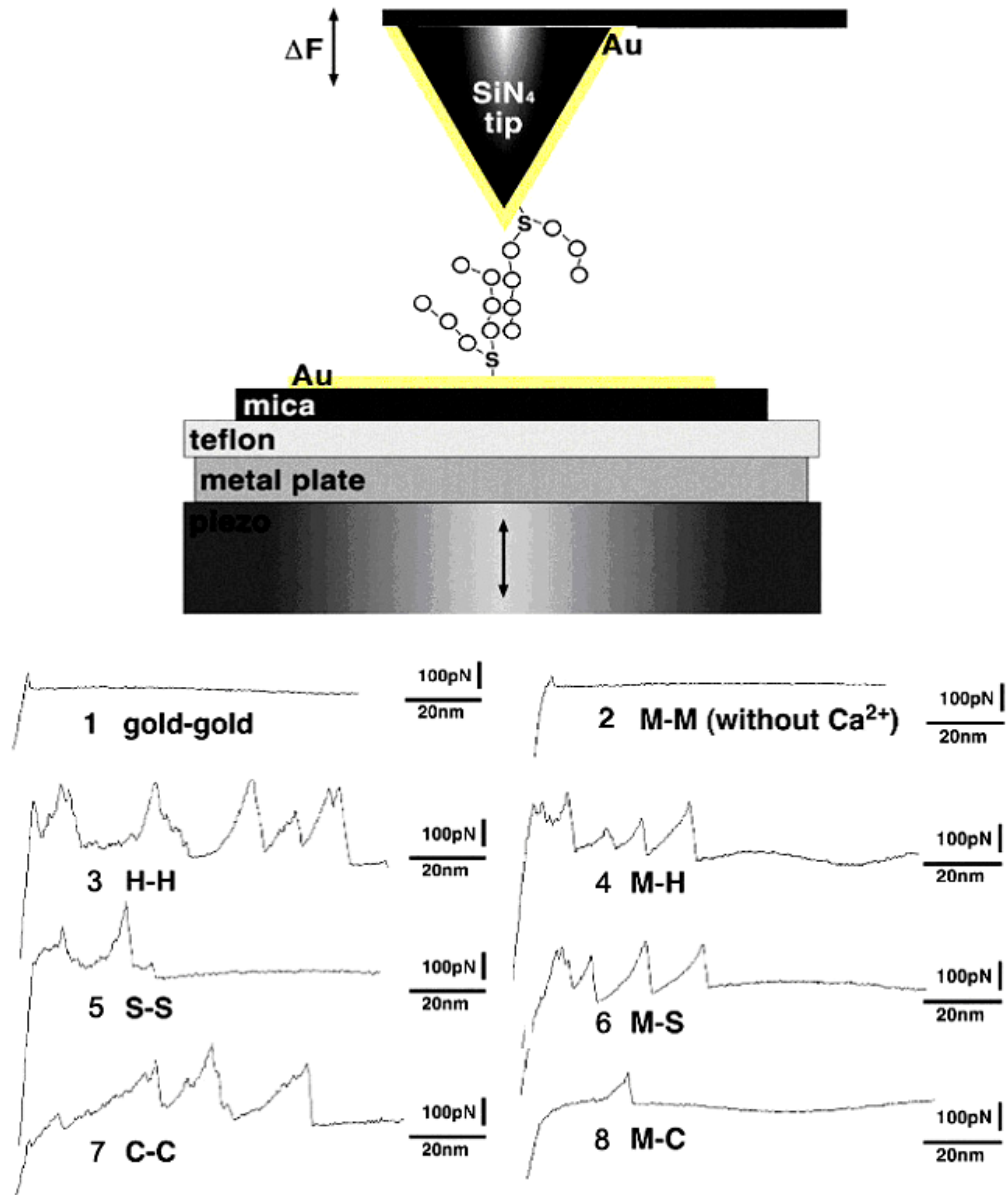
Fig. 32. Scheme of AFM set-up for the measurement of the intermolecular forces between glycan molecules. AFM measurements were performed in artificial seawater with physiological 10 mM Ca^{2+} (see IV.10.). Examples of AFM force curves: *line 1* and *2*, control curves: (*1*) gold-gold and (*2*) glycan-glycan interaction in seawater without Ca^{2+}; *lines 3, 5, 7,* interaction curves between glycans from the same species; *lines 4, 6, 8*, interaction curves between glycans from different species. M - *Microciona*, H - *Halichondria*, S - *Suberites*, C - *Cliona*.

V.4.2. SINGLE CARBOHYDRATE-CARBOHYDRATE INTERACTION IS SPECIES-SPECIFIC

The species-specific character of interactions between single glycans was investigated by coating *Microciona* glycan on the mica and three other studied sponge species, i.e. *Halichondria*, *Suberites*, and *Cliona* on AFM tips, and measuring heterotypic interactions in artificial seawater with physiological 10 mM Ca^{2+}.

In stark contrast to strong binding forces between identical glycans, clearly reduced ones were recorded between glycans from different species (Fig. 33). The single non-covalent bond between two interacting glycan molecules from two different species was ruptured at the forces between 110 and 210 pN. Heterotypic interaction between *Cliona* and *Microciona* glycans was the weakest measured interaction (110 pN). Heterotypic interactions between *Halichondria* and *Microciona*, and between *Suberites* and *Microciona* were stronger and they were 220 and 210 pN respectively.

In a statistical analysis, the binding forces between glycans from the same species of proteoglycans (Fig. 33 *panelA*) were always stronger than those between glycans from different species of proteoglycans (Fig. 33 *panelB*). P values from the Mann-Whitney test were calculated to study the difference between the strength of homotypic vs. heterotypic interactions. The Mann-Whitney test, also called the rank sum test, is a nonparametric test to compare two unpaired groups. P value is the key result. If it is < 0.05, the difference between compared groups is not a coincidence, and concludes that the populations have different medians. If it is < 0.01, the difference between two groups is significant. Here, P values for the difference in adhesion force between homotypic and heterotypic glycan-glycan interactions were clearly below 0.01 and showed that the difference is statistically significant.
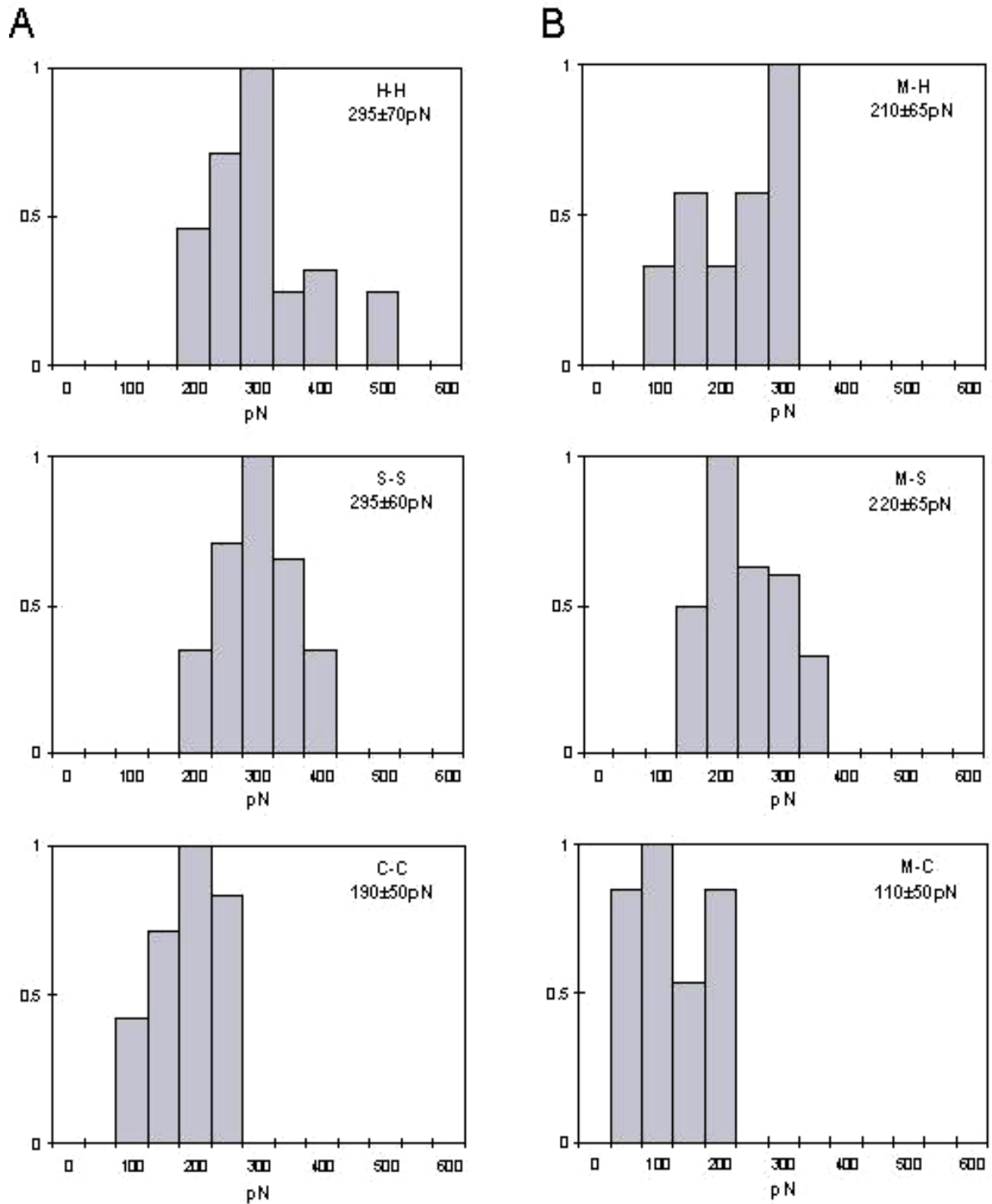
Fig. 33. Quantitative evaluation of species-specific vs. non-specific adhesion forces between glycan molecules. *panel A*, Adhesion force values of interactions between glycans from the same species. *panel B*, Adhesion force values of interactions between glycans from two different species. On the ordinate number of rupture events are provided normalized to 1.0 for the category of the highest number of events. M - *Microciona* glycan, H - *Halichondria* glycan, S - *Suberites* glycan, C - *Cliona* glycan.

V.4.3. SPECIES-SPECIFICITY OF THE CARBOHYDRATE-CARBOHYDRATE INTERACTION IS REFLECTED IN THE POLYVALENCE

The characteristic feature of the carbohydrate-carbohydrate interaction is the repetition of interactive sites along the carbohydrate chain, which further increases the strength of the interaction. The distance between the peak numbers 1 and 2 (2 and 3, etc) on AFM force curves was measured to produce a histogram of the peak periodicity (Fig. 34).

60-70 % of force curves between glycans from the same species showed more than one interaction peak (Fig. 34 *panelA*). It indicates a repetition of the binding motif along the carbohydrate chain and therefore a polyvalent character of the interaction. Most of AFM curves showed a distance between binding motifs of 10-20 nm. Only in the case of *Halichondria* glycan was the distance between binding motifs 10-30 nm.

In contrast, less than 35% of force curves between glycans from different species showed multiple interaction peaks, demonstrating the preference for one rather unspecific binding event during the interaction (Fig. 34 *panelB*). The periodicity was named 'single rupture peak' when there was only one interaction event on a force curve. More than 50 % of force curves between glycans from different species, and for *Microciona-Cliona* (M-C) up to 75 %, were 'single rupture peaks' indicating the high presence of only one interaction site and, therefore, much less polyvalent character of binding in comparison with homotypic interactions.

200 kDa glycan molecules have chain-like structures of an average folded length of ~40 nm as imaged by AFM[57], whereas the extended structure has a length of up to 180 nm[76,119]. The AFM sensor tip detected forces between single glycan molecules at distances from 0 nm up to 130 nm above the surface. 75% of the total lengths of the force curves for glycans from the same species were 20-50 nm, and in some cases

the curves showed extensions up to 130 nm (Fig. 35 *panelA*). This indicates that the interaction sites were located along the carbohydrate chain and not only at its end. In stark contrast, 70% of the force curves for heterotypic mixtures of glycans from different species showed total interaction lengths of 10-30 nm only (Fig. 35 *panelB*).
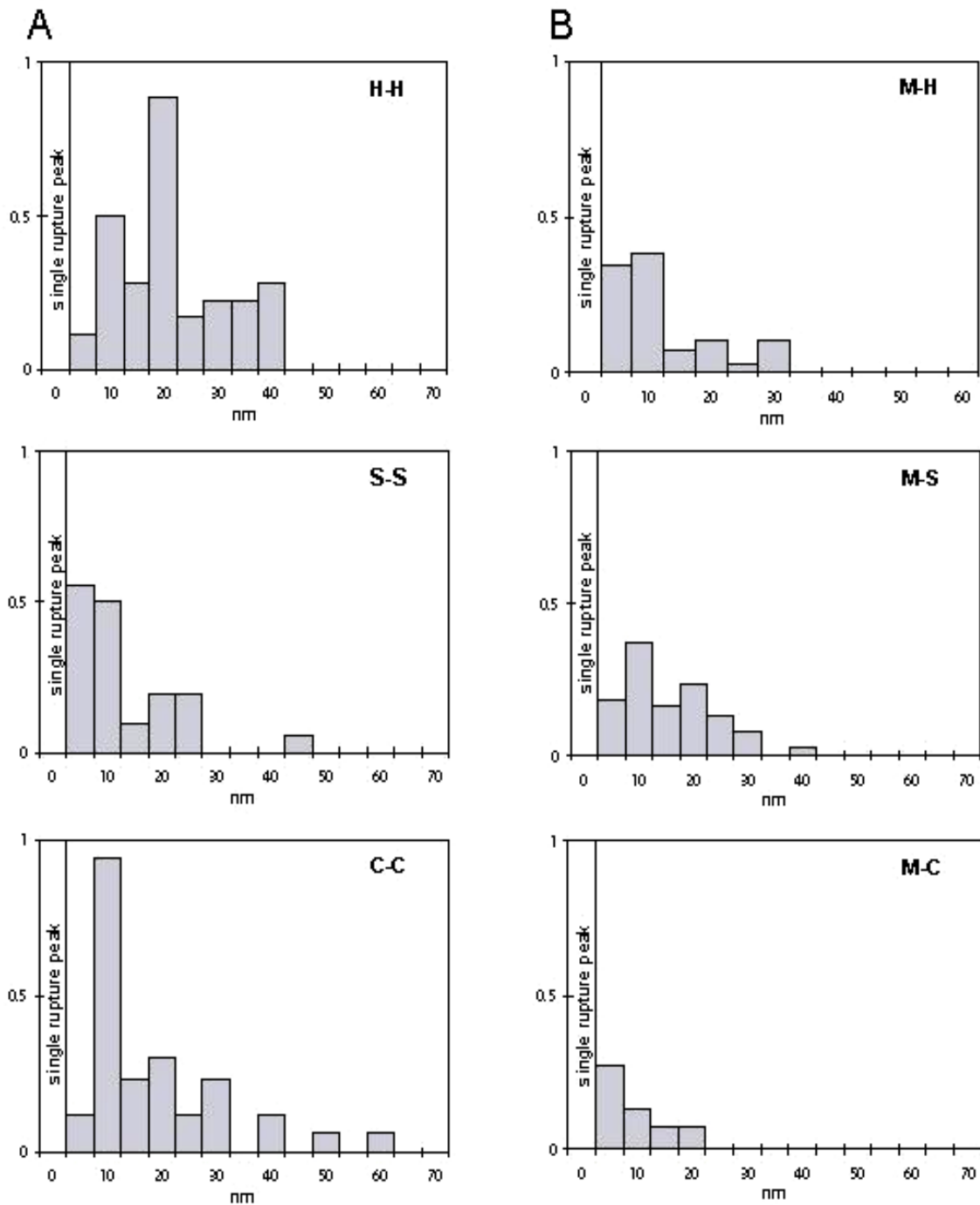
Fig. 34. Periodicity measurements of distances between AFM rupture peaks. Periodicity measurements indicate the distances between binding motifs on the carbohydrate chain of the glycan molecule. *panel A*, Periodicity measurement between rupture peaks of AFM curves recorded between interacting glycans from the same species. *panel B*, Periodicity measurement between rupture peaks of AFM curves recorded between interacting glycans from two different species. "Single rupture peaks" bar reflects the number of probe lift events where only one rupture event could be registered. M - *Microciona* glycan, H - *Halichondria* glycan, S - *Suberites* glycan, C - *Cliona* glycan.

88
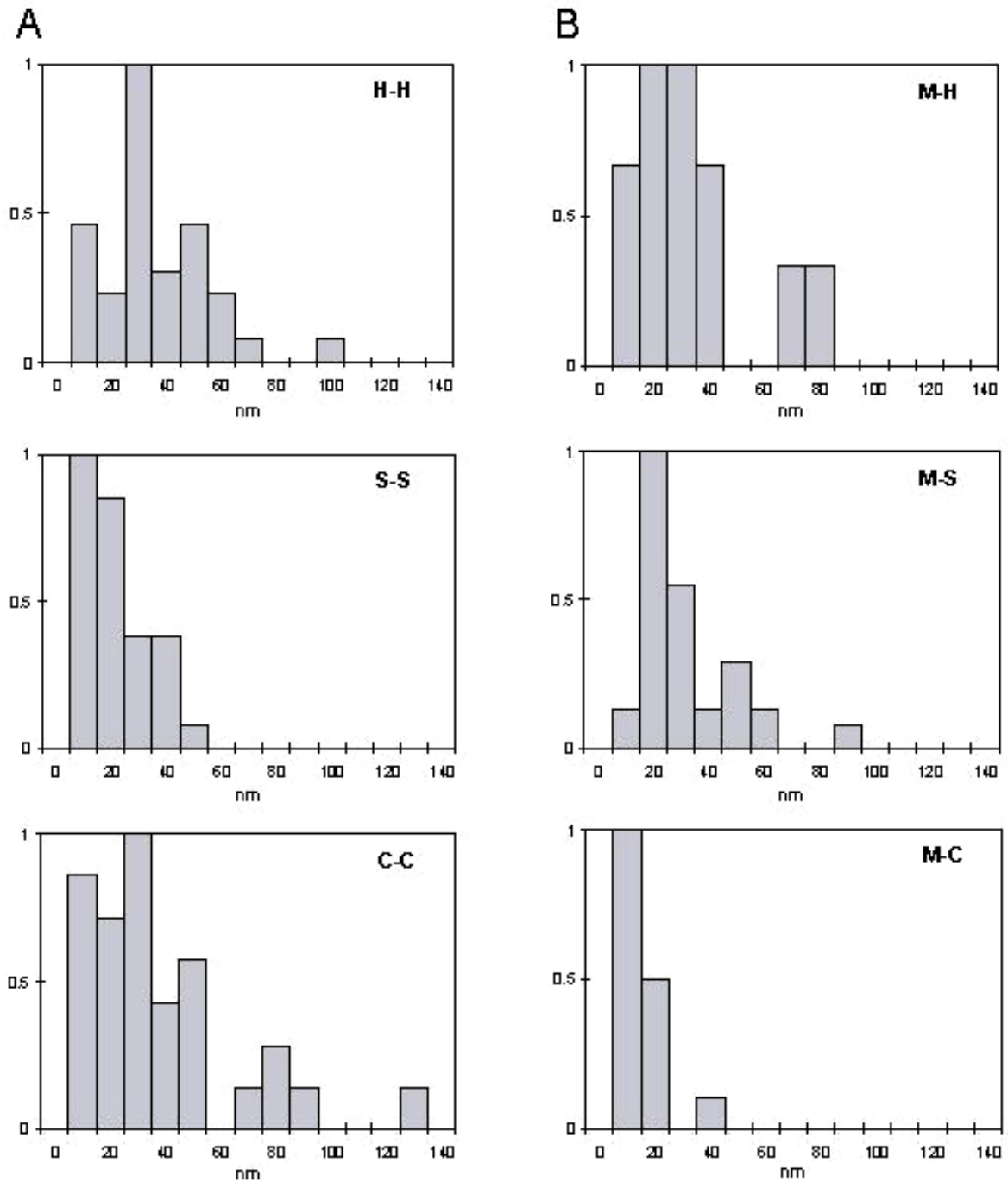
Fig. 35. The total length of the interacting carbohydrate chain. The total length of the interacting carbohydrate chain of the glycan molecule is indicated by the length of the force curves measured from the lift-off point to the last peak. *panel A*, The length of the carbohydrate chain in homotypic interactions between glycans from the same species. *panel B*, The length of the carbohydrate chain in heterotypic interactions between glycans from two different species. M - *Microciona* glycan, H - *Halichondria* glycan, S - *Suberites* glycan, C - *Cliona* glycan.

V.4.4. CALCIUM ENHANCES THE STRENGTH OF THE CARBOHYDRATE-CARBOHYDRATE INTERACTION

The role of Ca^{2+}-ions in carbohydrate-carbohydrate interactions was studied by increasing the calcium concentration in artificial seawater from physiological 10 mM to 100 mM during AFM measurements of the adhesion force between single *Microciona prolifera* 200 kDa glycans. A non-covalent bond (one peak on the force curve) between two interacting *Microciona* glycan molecules was ruptured at the force of 310 pN when AFM measurements were performed in 10 mM Ca^{2+} (Fig. 36*A*). The adhesion force increased when the Ca^{2+} concentration was increased from 10 to 100 mM. The adhesion force per binding site between two glycan molecules went up to 375 pN (Fig. 36*D*).

The occurrence of polyvalent interactions between single glycan molecules was higher in 100 than in 10 mM Ca^{2+}. In 100 mM Ca^{2+}, up to 85% of force curves showed the presence of multiple interaction sites indicating the repetition of binding sites along the interacting carbohydrate chain of the glycan molecule (Fig. 36*B*). The distance between binding motifs was 10-20 nm. In 10 mM Ca^{2+}, ~70% of force curves showed multiple peaks (Fig. 36*E*). The distance between binding motifs did not change. This had an effect on both the strength and the specificity of the glycan-glycan interaction.

The total length of the interacting carbohydrate chain did not change with the enhancement of Ca^{2+} concentration. In both cases, the longest extensions of the interacting carbohydrate chain were up to 120 nm (Fig. 36*C,F*). Most of the force curves were mainly 20-50 nm long in 10 and 100 mM Ca^{2+}. However, appearance of longer curves, i.e. longer carbohydrate chains, was more frequent for glycan-glycan interaction in the presence of 100 mM Ca^{2+} as compared to 10 mM Ca^{2+}. Up to 13% of curves were above 80 nm long in 100 mM Ca^{2+} when only ~3% of curves were above 80 nm long in 10 mM Ca^{2+}.
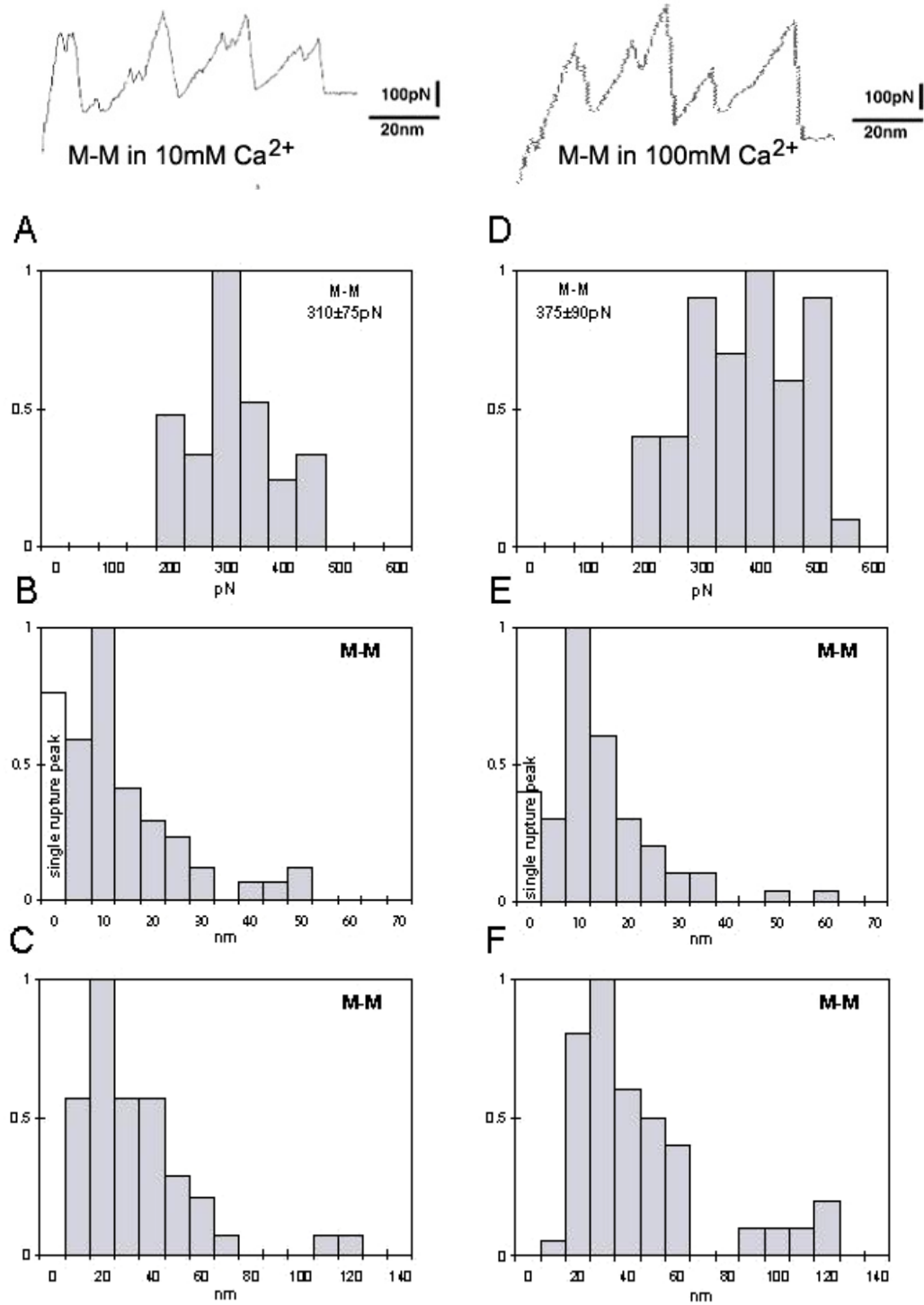
Fig. 36. Quantitative evaluations of interactions between single glycan molecules in physiological 10 mM Ca^{2+} (*A-C*) vs. interactions in 100 mM Ca^{2+} (*D-F*). Examples of interaction curves between *Microciona prolifera* glycans measured in artificial seawater with 10 and 100 mM Ca^{2+}. Adhesion force values for glycan-glycan interactions in *A*, 10 mM Ca^{2+} and *D*, 100 mM Ca^{2+}. Periodicity measurements of distances between rupture peaks in *B*, 10 mM Ca^{2+} and *E*, 100 mM Ca^{2+}. The length of the carbohydrate chain in glycan-glycan interactions in *C*, 10 mM Ca^{2+} and *E*, 100 mM Ca^{2+}. *M-Microciona prolifera* glycan.

VI. SUMMARY AND DISCUSSION

The importance of proteoglycans as key players in different physiological and pathophysiological cellular events[120,121], especially in adhesive properties of cells with regard to invasiveness of tumor cells and proliferation[122,123], is now emerging. Nevertheless, there is still little known about the carbohydrate moiety of the proteoglycan molecule and its role in cellular interactions. Carbohydrates are the most exposed structures on the cell surface[124], but their role in cellular interactions[125] is still neglected. It is well established that many biologically important interactions occur between proteins[126] and between proteins and carbohydrates[127]. For example, the molecular structure of the carbohydrate-protein linkage region from connective tissue proteoglycans has been characterized[128]. Direct carbohydrate-carbohydrate interactions are in general considered as very weak due to weak association constant[24,82], as compared for example to protein-carbohydrate interactions[129], and therefore not able to provide required specificity for cellular recognition. However, direct measurements of the forces between individual surface oligosaccharides of proteoglycan molecules have not yet been performed. Moreover, possible species-specificity of direct carbohydrate-carbohydrate interaction has never been investigated in any biological system.

Therefore, the aim of this thesis was to:
- measure the strength of the interaction between single glycan molecules isolated from cell surface proteoglycans,
- characterize the possible species-specific character of the glycan-glycan interaction,
- study the role of the glycan-glycan interaction in cellular recognition and adhesion events.

200 kDa glycans from core structures of cell surface proteoglycans from four different sponge species were purified and interactions between glycan molecules

and its possible role in cell-cell recognition were investigated. Compared with knowledge of other organisms, information on sponges has an extra added value because sponges as a group are the oldest Metazoans alive, and contribute more to our understanding of life on earth than similar knowledge of other animal groups[130]. Sponges, as the earliest multicellular organisms, evolved by developing cell recognition and adhesion processes. Remarkably, dissociated sponge cells from two different species can reaggregate through surface proteoglycans by species-specific associations that approach the selectivity of the evolutionarily advanced Ig superfamily. Consequently, this simple and highly specific cellular recognition phenomenon has been used for almost a century as a model system to study specific cellular recognition and adhesion during tissue and organ formation in multicellular organisms.

This thesis presents the first comparative data on species-specificity and strength of self-interactions between glycans derived from cell surface proteoglycans[131] (Table 6, 7):

1. Adhesive forces between single glycan molecules are in the range of 200-300 pN and compare well with other biologically relevant forces,

2. Carbohydrate-carbohydrate interaction is species-specific,

3. Carbohydrate-carbohydrate interaction is polyvalent,

4. Ca^{2+} probably reinforces the contact between the interacting oligosaccharides of glycan molecules,

5. Adhesion of live cells to glycan-coated surfaces promotes cell differentiation and formation of mineral skeleton.

Table 6. A summary of experiments performed to detect and characterize cell-glycan interactions.

experiment type	conditions	results
aggregation of cells with glycan-coated amine-modified beads	mechanically dissociated live sponge cells aggregate with 200 kDa glycans coated on red amine-modified beads similar in size to small cells; artificial seawater with physiological 10 mM Ca^{2+}; rotor speed 60 rpm; 4-h aggregation	species-specific aggregation; separation of cell aggregates from aggregates of beads coated with glycans from different species; mixing of cells and beads coated with their own glycans
cell adhesion to glycan-coated plates	equal quantities of live cells from four different species added to glycan-coated plates; artificial seawater with physiological 10 mM Ca^{2+}; 2-h adhesion; non-adhered cells washed off	species-specific adhesion of cells to glycan-coated plates; strong cell adhesion to surfaces coated with their own glycan; greatly reduced cell adhesion to surfaces coated with glycans from other species; greatly enhanced cell differentiation and formation of mineral skeleton in cells adhered to their own glycans
larval cell adhesion to glycan-coated plates	equal quantities of larval cells from two different species added to glycan-coated plates; artificial seawater with physiological 10 mM Ca^{2+}; 2-h adhesion; non-adhered cells washed off	species-specific adhesion of larval cells to glycan-coated plates; strong larval cell adhesion to surfaces coated with their own glycan; greatly reduced larval cell adhesion to surfaces coated with glycans from other species

Table 7. A summary of experiments performed to detect and characterize glycan-glycan interactions.

experiment type	conditions	results
aggregation of glycan-coated amine-modified beads	200 kDa glycans from four different species coated on red and green amine-modified beads (1 μm in diameter); artificial seawater with physiological 10 mM Ca^{2+}; rotor speed 60 rpm; 4-h aggregation	species-specific aggregation; separation of red and green beads coated with two different species of glycans; mixing of red and green beads coated with glycans from the same species
aggregation of glycan-coated carboxylate-modified beads	200 kDa glycans from four different species coated on red and green carboxylate-modified beads (1 μm in diameter); artificial seawater with physiological 10 mM Ca^{2+}; rotor speed 60 rpm; 4-h aggregation	species-specific aggregation; separation of red and green beads coated with two different species of glycans; mixing of red and green beads coated with glycans from the same species
glycan adhesion to glycan-coated plates	equal quantities of 200 kDa glycans from four different species added to glycan-coated plates; artificial seawater with physiological 10 mM Ca^{2+}; 2-h adhesion; non-adhered glycans washed off	species-specific adhesion of glycans to glycan-coated plates; strong glycan adhesion to surfaces coated with the same glycan; greatly reduced glycan adhesion to surfaces coated with glycans from other species
AFM measurements of adhesion forces between two single glycan molecules	covalent chemisorption of naturally sulfated 200 kDa glycans from four different species to gold-coated AFM tip and gold-coated mica; artificial seawater with physiological 10 mM Ca^{2+}	adhesion forces between glycans from the same species in the range of 190–310 pN; reduced adhesion forces between glycans from two different species in the range of 110-210 pN; statistically significant difference between the same species of glycans vs. different species of glycans adhesion forces

The examination of carbohydrate-carbohydrate interactions at the atomic level is critical in understanding the nature of these interactions and their biological role. Measured adhesive forces between identical glycans from surface proteoglycans varied from 190 to 310 pN[131] and they compare well with the range of other biologically relevant forces measured with AFM. Forces between the entire proteoglycan molecules vary from 50 to 400 pN, depending on the number of binding sites ruptured[119]. Similar values are also reported for single protein-glycan interactions when the interaction of P-selectin from leukocytes with its carbohydrate ligand from endothelial cells was measured (165pN)[132,133], or for single antibody-antigen recognition with unbinding forces of 244 pN[134,135]. Single molecule AFM measurements were also used to characterize binding strength (unbinding force) of a vascular endothelial (VE)-cadherin[136], which revealed relatively low unbinding forces (35-55 pN). Unbinding forces increased with interaction time and indicated association of cadherins into complexes with cumulative binding strength. These observations favor a model by which weak binding strength and affinity of cadherins require clustering and cytoskeletal immobilization for amplification. The smallest value of adhesion force reported to date is the interaction force between individual molecules of Le^x-determinant, which is 20 pN[137]. The two latter examples may support the opinion that carbohydrate-carbohydrate interactions are too weak to manifest themselves in biologically relevant cellular recognition. However, carbohydrate molecules offer multivalent presence of oligosaccharide chains on cell surfaces, which can easily enhance weak binding forces to forces seen with biologically relevant interactions, e.g. organization of GSLs as clusters on plasma membrane[16,17,18].

The AFM measurements of the forces per binding site between single glycan molecules originating from two different sponge species were performed to quantitatively characterize species-specificity of the glycan-glycan interaction. Adhesion forces measured between different glycans were lower than forces between glycans from the same species, and the statistical significance of the difference was confirmed by p values below 0.01. Moreover, homotypic carbohydrate-carbohydrate

interactions between glycans of the same species showed polyvalent binding characteristics with interaction sites located along the chain, while it was not favored in heterotypic interactions between different glycans. Most of heterotypic interactions arisen from the existence of only one binding site between two molecules. On the contrary, homotypic interactions were created through at least three separate binding sites between two glycan molecules. This involvement of several binding sites located along the carbohydrate chain in the glycan-glycan interaction offered an easy way to increase the overall adhesion force between two interacting molecules.

The exact number of single rupture events recorded during AFM measurements of forces between two interacting glycan molecules is difficult to define with certainty since it cannot be excluded that a so called "single event" may be a composite of more than one bond rupture. Nevertheless, since the overall lengths of the longest AFM force curves (130 nm) match roughly the extended length of the glycan molecule (160-180 nm)[76,119], it can be assumed that single glycan molecule and not multiple glycan molecule interactions were here measured.

Not only the adhesion force per binding site and the enhancement of the forces through polyvalence can guarantee the specificity of carbohydrate-carbohydrate interaction. Sugar sequences between glycans from different sponge surface proteoglycans vary a lot. The carbohydrate composition (Fuc, GalN, GlcN, Gal, Man and GlcA) was highly conserved between individuals of the same sponge species, whereas large differences were seen between different species. Detailed structural analyses of different sponge proteoglycans have revealed species-specific structures[138]. This diversity of polysaccharide primary structure affords diversity in higher order structure, and the specificity of the carbohydrate-carbohydrate interaction may be provided also by the three dimensional spatial relationships of the sugars.

Architectural and compositional differences between carbohydrate chains could even be gradual, allowing cells test surrounding surfaces and first create weak random contacts before releasing or reinforcing adhesion[96]. Therefore, interactions between two different species of glycans could still be recorded in AFM measurements, though of lower stability than these between two glycans from the same species. The gradual adhesion was also seen in glycan-coated beads aggregation, where heterotypic aggregates consisting of glycans from different species were present in high number at the beginning of 4-h aggregation process. More time was required for glycan-coated beads to species-specifically sort out according to their species of origin and form homotypic aggregates consisting of beads coated with glycans from the same species only.

Ca^{2+}-ions or other divalent cations are crucial in carbohydrate-carbohydrate interactions[30,75,106,139]. In species-specific cell-cell recognition in sponges only Ca^{2+}-ions are essential. No interaction between cells, cells and surface glycans, and between surface glycans could be here observed in the absence of Ca^{2+}. Also no adhesion forces between single glycan molecules could be detected during AFM measurements. Ca^{2+} probably reinforces the contact between the interacting oligosaccharides of glycan molecules since an increase in Ca^{2+} in the buffer led to an increase in adhesion forces and in polyvalent interactions. Similarly, corneal epithelial cell-cell adhesion through the Le[x] determinant is highly dependent on the presence of Ca^{2+}-ions[106]. Also self-aggregation of Le[x] molecules in aqueous solution, where the molecules move freely, occurs only in the presence of Ca^{2+}-ions[107]. However, it has been reported that the presence of Ca^{2+}-ions did not contribute significantly to the adhesion force in Le[x]-Le[x] interactions measured by AFM[137]. There is also no Ca^{2+} in the Le[x] crystal[100]. Therefore, it has been implied that Ca^{2+} is only responsible for the approach and organization of the carbohydrates in the cell membrane. The role of Ca^{2+} in carbohydrate-carbohydrate interactions is still not well understood. Ca^{2+}-ions could be responsible for the approach and organization of the sugar moieties providing the surfaces for interaction, or they could enhance directly the adhesion force between complementary surfaces, acting as a bridge

between specific hydroxy groups. Further experimental evidence is needed before any of these proposals could be considered as a model.

Selective recognition of glycans by live cells confirmed the existence of carbohydrate-carbohydrate recognition system in biologically relevant situations (Table 6). The aggregation of live cells with glycan-coated beads imitated the ability of sponge cells to species-specifically aggregate after mechanical dissociation to finally reconstitute a functional sponge with canals, spicules (mineral skeleton), and collagen fibrils and fibres[50,51,114,115]. Importantly, only live cells that adhered to surfaces coated with their own surface glycans showed an enhanced capacity for cell differentiation and formation of spicules.

Glycan-coated bead-bead aggregation perfectly mimicked the species-specific cell-cell aggregation. Glycan-coated beads sorted out specifically into aggregates consisting of beads coated with the same glycan. In heterotypic aggregations between *Cliona* glycans coated on red beads and any other species of glycans coated on green beads (C-M, C-H, and C-S combinations in Fig 20 and 21), the percentage of total red clumps (consisting of beads coated only with *Cliona* glycan) was always very small as compared to the percentage of total green clumps (consisting of beads coated with the glycan from another species: *Microciona, Halichondria* and *Suberites*). After 4h of sorting out, only 15-20% of red aggregates were seen in all heterotypic aggregations when there were 65-75% of green aggregates present. This can be explained by differences in binding forces between glycans measured by AFM. The stronger the binding force between glycan molecules, the lower the off rate and the faster formation of bead aggregates. The binding forces between *Cliona* glycans were the weakest among all measured (190 pN), while the binding forces between *Microciona* glycans were the strongest of all (310 pN). The binding forces between *Halichondria* and between *Suberites* glycans were 295 pN. Moreover, the measurements of Ca^{2+} that went from the buffer into glycan-coated bead aggregates revealed that the Ca^{2+} uptake was the slowest in homotypic *Cliona-Cliona* aggregations as compared to homotypic aggregations between other species.

Therefore, during heterotypic aggregations between *Cliona* glycan coated on red beads and other three species glycans coated on green beads, most of the total Ca^{2+} present in the buffer probably went first into aggregates formed by other species and not enough Ca^{2+} was left in the buffer to form *Cliona* aggregates.

Similarly, in homotypic glycan-coated bead-bead aggregations, aggregates formed by beads coated with *Cliona* glycan (C-C in Fig. 20 and 21) were always much smaller than aggregates formed by beads coated with glycans from other species (M-M, H-H and S-S). The possible explanation could also lie in differences in binding forces between different glycans measured by AFM. This would lead to lower off rate and faster formation of glycan-coated bead aggregates for stronger glycan-glycan interactions. Therefore, beads coated with *Cliona* glycan formed smaller clusters than these formed, e.g. by *Microciona* glycan after 4h of aggregation process.

Inhibition of sponge cell recognition and aggregation by species-specific carbohydrate epitope antibodies as shown in previous studies[74,108] do not prove glycan-glycan interactions to be relevant but of course leave the option of glycan-protein interactions. The same interpretation holds for two of the approaches presented here: species-specificity for the glycan-coated bead aggregation with live sponge cells (Fig. 19) and for matured and larval cells binding to glycan-coated plastic surfaces (Fig. 26, 29). The specificity found here for glycan-coated bead sorting (Fig. 20, 21), for glycan-glycan interaction (Fig. 31), and for the force and specificity shown in the AFM measurements (Fig. 33) make, however, a role for carbohydrate-carbohydrate in sponge cell recognition and adhesion likely.

The fact that the outermost cell surface is made up primarily of a dense layer of hydrophilic glycans supports the notion that upon first contact between cells such reversible and flexible glycan-glycan interactions may play a pivotal role in the early steps of cellular recognition and adhesion processes[141], where strong single covalent bonds[140] would be counter productive, both at the molecular and the cellular level.

Better methods for the synthesis and characterization of carbohydrates are creating numerous opportunities for elucidation of the biological roles of these outermost cell surface structures[141]. If carbohydrate-carbohydrate interactions may ensure adequate cell behavior during the formation, maintenance, and pathogenesis of tissues a thorough understanding of the chemical and molecular nature of specific carbohydrate-carbohydrate recognition will be a prerequisite for the development of strategies to modify it and to progress thereby in an understanding of its biological relevance.

VII. REFERENCES

[1] Stipp, C. S., Hemler, M. E. Transmembrane-4-superfamily proteins CD151 and CD81 associate with α3β1 integrin, and selectively contribute to α3β1-dependent neurite outgrowth. *J. Cell Science* **113**, 1871-1882 (2000).

[2] Hakomori, S. Structure and function of sphingoglycolipids in transmembrane signalling and cell-cell interactions. *Biochem. Soc. Trans.* **21**, 583-595 (1993).

[3] Bernimoulin, M. P., *et al*. Molecular basis of leukocyte rolling on PSGL-1. Predominant role of core-2 O-glycans and of tyrosine sulfate residue 51. *J. Biol. Chem.* **278**, 37-47 (2003).

[4] Karlsson, K. A. Microbial recognition of target-cell glycoconjugates. *Curr. Opin. Struct. Biol.* **5**, 622-635 (1995).

[5] Feizi, T., Loveless, R. W. Carbohydrate recognition by *Mycoplasma pneumoniae* and pathologic consequences. *Am. J. Respir. Crit. Care Med.* **154**, 133-136 (1996).

[6] Rostand, K. S., Esko, J. D. Microbial adherence to and invasion through proteoglycans. *Infect. Immun.* **65**, 1-8 (1997).

[7] Hakomori, S. Glycosylation defining cancer malignancy: new wine in an old bottle. *Proc. Natl. Acad. Sci. USA* **99**, 10231-10233 (2002).

[8] Hynes, R. O., Zhao, Q. The evolution of cell adhesion. *J. Cell Biol.* **150**, 89-96 (2000).

[9] Feizi, T. Progress in deciphering the information content of the 'glycome'--a crescendo in the closing years of the millennium. *Glycoconj. J.* **17**, 553-565 (2000).

[10] Hakomori, S. Structure, organization, and function of glycosphingolipids in membrane. *Curr. Opin. Hematol.* **10**, 16-24 (2003).

[11] Hakomori, S. Cancer-associated glycosphingolipid antigens: their structure, organization, and function. *Acta Anatomica* **161**, 79-90 (1998).

[12] Hakomori, S., Handa, K. Glycosphingolipid-dependent cross-talk between glycosynapses interfacing tumor cells with their host cells: essential basis to define tumor malignancy. *FEBS Letters* **531**, 88-92 (2002).

[13] Fantini, J., Maresca, M., Hammache, D., Yahi, N., Delézay, O. Glycosphingolipid (GSL) microdomains as attachment platforms for host pathogens and their toxins on intestinal epithelial cells: activation of signal transduction pathways and perturbations of intestinal absorption and secretion. *Glycoconj. J.* **17**, 173-179 (2000).

[14] Kasahara, K., Sanai, Y. Functional roles of glycosphingolipids in signal transduction via lipid rafts. *Glycoconj. J.* **17**, 153-162 (2000).

[15] Hakomori, S. Cell adhesion/recognition and signal transduction through glycosphingolipid microdomain. *Glycoconj. J.* **17**, 143-151 (2000).

[16] Hoekstra, D., *et al.* Membrane dynamics and cell polarity: the role of sphingolipids. *J. Lipid Res.* **44**, 869-877 (2003).

[17] Simons, K., Ikonen, E. Functional rafts in cell membranes. *Nature* **387**, 569-572 (1997).

[18] Kurzchalia, T. V., Parton, R. G. Membrane microdomains and caveolae. *Curr. Opin. Cell Biol.* **11**, 11424-11431 (1999).

[19] Hakomori, S., Handa, K., Iwabuchi, K., Yamamura, S., Prinetti, A. New insights in glycosphingolipid function: "glycosignaling domain," a cell surface assembly of glycosphingolipids with signal transducer molecules, involved in cell adhesion coupled with signaling. *Glycobiology* **8**, xi-xix (1998).

[20] Ilangumaran, S., Hoessli, D. C. Effects of cholesterol depletion by cyclodextrin on the sphingolipid microdomains of the plasma membrane. *Biochem. J.* **335**, 433-440 (1998).

[21] Keller, P., Simons, K. Cholesterol is required for surface transport of influenza virus hemagglutinin. *J. Cell Biol.* **140**, 1357-1367 (1998).

[22] Strömber, N., *et al.* Saccharide orientation at the cell surface affects glycolipid receptor function. *Proc. Natl. Acad. Sci. USA* **88**, 9340-9344 (1991).

[23] Buccoliero, R., Futerman, A. H. The roles of ceramide and complex sphingolipids in neuronal cell function. *Pharmacol. Res.* **47**, 409-419 (2003).

[24] Varki, A. Selectin ligands. *Proc. Natl. Acad. Sci. USA* **91**, 7390-7397 (1994).

[25] Kannagi, R., Kanamori, A. Glycobiology of sialyl 6-sulfo Lewis x, a new carbohydrate ligand for selectins. *Trends Glycosci. Glycotechnol.* **11**, 329-344 (1999).

[26] Crocker, P. R., Varki, A. Siglecs in the immune system. *Immunology* **103**, 137-145 (2001).

[27] Feizi, T. Demonstration by monoclonal antibodies that carbohydrate structures of glycoproteins and glycolipids are onco-developmental antigens. *Nature* **314**, 53-57 (1985).

[28] Fenderson, B. A., Zehavi, U., Hakomori, S. A multivalent lacto-N-fucopentaose III-lysyllysine conjugate decompacts preimplantation mouse embryos, while the free oligosaccharide is ineffective. *J. Exp. Med.* **160**, 1591-1596 (1984).

[29] Fenderson, B. A., Andrews, P. W., Nudelman, E., Clausen, H., Hakomori, S. Glycolipid core structure switching from globo- to lacto- and ganglio-series during retinoic acid-

induced differentiation of TERA-2-derived human embryonal carcinoma cells. *Dev. Biol.* **122**, 21-34 (1987).

[30] Eggens, I. *et al*. Specific Interaction between Le[x] and Le[x] determinants. *J. Biol. Chem.* **264**, 9476-9484 (1989).

[31] Shevinsky, L. H., Knowles, B. B., Damjanov, I., Solter, D. Monoclonal antibody to murine embryos defines a stage-specific embryonic antigen expressed on mouse embryos and human teratocarcinoma cells. *Cell* **30**, 697-705 (1982).

[32] Willison, K. R., Karol, R. A., Suzuki, A., Kundu, S. K., Marcus, D. M. Neutral glycolipid antigens as developmental markers of mouse teratocarcinoma and early embryos: an immunologic and chemical analysis. *J. Immunol.* **129**, 603-609 (1982).

[33] Song, Y., Withers, D. A., Hakomori, S.-I. Globoside-dependent adhesion of human embryonal carcinoma cells, based on carbohydrate-carbohydrate interaction, initiates signal transduction and induces enhanced activity of transcription factors AP1 and CREB. *J. Biol. Chem.* **273**, 2517-2525 (1998).

[34] Kojima, N., Hakomori, S. Specific interaction between gangliotriaosylceramide (Gg3) and sialosyllactosylceramide (GM3) as a basis for specific cellular recognition between lymphoma and melanoma cells. *J. Biol. Chem.* **264**, 20159-20162 (1989).

[35] Iwabuchi, K., Yamamura, S., Prinetti, A., Handa, K., Hakomori, S. GM3-enriched microdomain involved in cell adhesion and signal transduction through carbohydrate-carbohydrate interaction in mouse melanoma B16 cells. *J. Biol. Chem*. **273**, 9130-9138 (1998).

[36] Kojima, N., Hakomori, S. Cell adhesion, spreading, and motility of GM3-expressing cells based on glycolipid-glycolipid interaction. *J. Biol. Chem.* **266**, 17552-17558 (1991).

[37] Kojima, N., Hakomori, S. Synergistic effect of two cell recognition systems: glycosphingolipid-glycosphingolipid interaction and integrin receptor interaction with pericellular matrix protein. *Glycobiology* **1**, 623-630 (1991).

[38] Kojima, N., Shiota, M., Sadahira, Y., Handa, K., Hakomori S. Cell adhesion in a dynamic flow system as compared to static system. Glycosphingolipid-glycosphingolipid interaction in the dynamic system predominates over lectin- or integrin-based mechanisms in adhesion of B16 melanoma cells to non-activated endothelial cells. *J. Biol. Chem.* **267**, 17262-17270 (1992).

[39] Hardingham, T. E., Fosang, A. J. Proteoglycans: Many forms and many functions. *FASEB J.* **6**, 861-870 (1992).

[40] Selva, E. M., Perrimon, N. Role of heparan sulfate proteoglycans in cell signaling and cancer. *Adv. Cancer Res.* **83**, 67-80 (2001).

[41] Iozzo, R. V. Matrix proteoglycans: From molecular design to cellular function. *Annu. Rev. Biochem.* **67**, 609-652 (1998).

[42] Truant, S., *et al.* Requirement of both mucins and proteoglycans in cell-cell dissociation and invasiveness of colon carcinoma HT-29 cells. *Int. J. Cancer* **104**, 683-694 (2003).

[43] Casu, B., Lindahl, U. Structure and biological interactions of heparin and heparan sulfate. *Adv. Carbohydr. Chem. Biochem.* **57**, 159-206 (2001).

[44] Huang, W., *et al.* Crystal structure of Proteus vulgaris chondroitin sulfate ABC lyase I at 1.9A resolution. *J. Mol. Biol.* **328**, 623-634 (2003).

[45] Shirk, R. A., *et al.* Altered dermatan sulfate structure and reduced heparin cofactor II-stimulating activity of biglycan and decorin from human atherosclerotic plaque. *J. Biol. Chem.* **275**, 18085-18092 (2000).

[46] Funderburgh, J. L. Keratan sulfate: structure, biosynthesis, and function. *Glycobiology* **10**, 951-958 (2000).

[47] Ward, P. D., Thibeault, S. L., Gray, S. D. Hyaluronic acid: its role in voice. *J. Voice* **16**, 303-309 (2002).

[48] Vynios, D. H., Karamanos, N. K., Tsiganos, C. P. Advances in analysis of glycosaminoglycans: its application for the assessment of physiological and pathological states of connective tissues. *J. Chromatogr. B. Analyt. Technol. Biomed. Life Sci.* **781**, 21-38 (2002).

[49] Humphreys, T. Chemical dissolution and *in vitro* reconstruction of sponge cell adhesions. Isolation and functional demonstration of the components involved. *Dev. Biol.* **8**, 27-47 (1963).

[50] Wilson, H. V. On some phenomena of coalescence and regeneration in sponges. *J. Exp. Zool.* **5**, 245-258 (1907).

[51] Galtsoff, P. S. Regeneration after dissociation: An experimental study on sponges. *J. Exp. Zool.* **42**, 223-251 (1925).

[52] Férnandez-Busquets, X., Burger, M. M. Circular proteoglycans from sponges: first members of the spongican family. *Cell Mol. Life Sci.* **60**, 88-112 (2003).

[53] Henkart, P., Humphreys, S., Humphreys, T. Characterization of sponge aggregation factor. A unique proteoglycan complex. *Biochemistry* **12**, 3045-3050 (1973).

[54] Cauldwell, C. B., Henkart, P., Humphreys, T. Physical properties of sponge aggregation factor. A unique proteoglycan complex. *Biochemistry* **12**, 3051-3055 (1973).

[55] Müller, W. E., Beyer, R., Pondeljak, V., Müller, I., Zahn, R. K. Species-specific aggregation factor in sponges. XIII. Entire and core structure of the large circular proteid particle from *Geodia cydonium*. *Tissue Cell* **10**, 191-199 (1978).

[56] Müller, W. E., Conrad, J., Pondeljak, V., Steffen, R., Zahn, R. K. Electron microscopical characterization of sponge aggregation factors. *Tissue Cell* **14**, 219-223 (1982).

[57] Jarchow, J. *et al*. Supramolecular structure of a new family of circular proteoglycans mediating cell adhesion in sponges. *J. Struct. Biol*. **132**, 95-105 (2000).

[58] Edelman, G. M., Crossin, K. L. Cell adhesion molecules: Implications for a molecular histology. *Annu. Rev. Biochem.* **60**, 155-190 (1991).

[59] Takeichi, M. The cadherins: Cell-cell adhesion molecules controlling animal morphogenesis. *Development* **102**, 639-655 (1988).

[60] Varner, J. A., Burger, M. M., Kaufman, J. F. Two cell surface proteins bind the sponge *Microciona prolifera* aggregation factor. *J. Biol. Chem.* **263**, 8498-8508 (1988).

[61] Varner, J. A. Cell adhesion in sponges: potentiation by a cell surface 68 kDa proteoglycan-binding protein. *J. Cell. Sci.* **108**, 3119-3126 (1995).

[62] Varner, J. A. Isolation of a sponge-derived extracellular matrix adhesion protein. *J. Biol. Chem.* **271**, 16119-16125 (1996).

[63] Müller, W. E. G., Müller, I., Zahn, R. K., Kurelec, B. Species-specific aggregation factor in sponges. VI. Aggregation receptor from the cell surface. *J. Cell Sci.* **21**, 227-41 (1976).

[64] Müller, W. E. G., *et al*. Ubiquitin and ubiquitination in cells from the marine sponge *Geodia cydonium*. *Biol. Chem. Hoppe Seyler* **375**, 53-60 (1994).

[65] Pfeifer, K. Cloning of the polyubiquitin cDNA from the marine sponge *Geodia cydonium* and its preferential expression during reaggregation of cells. *J. Cell Sci.* **106**, 545-553 (1993).

[66] Rottmann, M., *et al*. Specific phosphorylation of proteins in pore complex-laminae from the sponge *Geodia cydonium* by the homologous aggregation factor and phorbol ester. Role of protein kinase C in the phosphorylation of DNA topoisomerase II. *EMBO J.* **6**, 3939-3944 (1987).

[67] Schröder, H. C., *et al*. Induction of *ras* gene expression by homologous aggregation factor in cells from the sponge *Geodia cydonium*. *J. Biol. Chem.* **263**, 16334-16340 (1988).

[68] Férnandez-Busquets, X., Gerosa, D., Hess, D., Burger, M. M. Accumulation in marine sponge grafts of the mRNA encoding the main proteins of the cell adhesion system. *J. Biol. Chem.* **273**, 29545-29553 (1998).

[69] Müller, W. E. G., *et al.* Aggregation of sponge cells. XX. Self aggregation of the circular proteid particle. *Biochim. Biophys. Acta* **551**, 363-367 (1979).

[70] Müller, W. E. G., Zahn, R. K., Kurelec, B., Müller, I. Species specific aggregation factor in sponges. Transfer of a species specific aggregation receptor from *Suberites domuncula* to cells of *Geodia cydonium. Differen.* **10**, 55-60 (1978).

[71] Férnandez-Busquets, X., Burger, M. M. The main protein of the aggregation factor responsible for species-specific cell adhesion in the marine sponge *Microciona prolifera* is highly polymorphic. *J. Biol. Chem.* **272**, 27839-27847 (1997).

[72] Férnandez-Busquets, X., Kammerer, R. A., Burger, M. M. A 35-kDa protein is the basic unit of the core from the $2x10^4$-kDa aggregation factor responsible for species-specific cell adhesion in the marine sponge *Microciona prolifera*. *J. Biol. Chem.* **271**, 23558-23565 (1996).

[73] Misevic, G. N., Burger, M. M. The species-specific cell-binding site of the aggregation factor from the sponge *Microciona prolifera* is a highly repetitive novel glycan containing glucuronic acid, fucose and mannose. *J. Biol. Chem.* **265**, 20577-20584 (1990).

[74] Misevic, G. N., Burger M. M. Carbohydrate-carbohydrate interactions of a novel acidic glycan can mediate sponge cell adhesion. *J. Biol. Chem.* **268**, 4922-4929 (1993).

[75] Jumblatt, J. E., Schlup, V., Burger M. M. Cell-cell recognition: Specific binding of Microciona sponge aggregation factor to homotypic cells and the role of calcium ions. *Biochemistry* **19**, 1038-1042 (1980).

[76] Cowman, M. K., Li, M., Balazs, E. A. Tapping mode atomic force microscopy of hyaluronan: Extended and intramolecularly interacting chains. *Biophys. J.* **75**, 2030-2037 (1998).

[77] Turner, S. R., Burger, M. M. Involvement of carbohydrate group in the active site for surface guided reassociation of animal cells. *Nature* **244**, 509-510 (1973).

[78] Spillmann, D. *et al.* Characterization of a novel sulfated carbohydrate unit implicated in the carbohydrate-carbohydrate-mediated cell aggregation of the marine sponge *Microciona prolifera*. *J. Biol. Chem.* **270**, 5089-5097 (1995).

[79] Spillmann, D. *et al*. Characterization of a novel pyruvylated carbohydrate unit implicated in the cell aggregation of the marine sponge *Microciona prolifera*. *J. Biol. Chem.* **268**, 13378-13387 (1993).

[80] Haseley, S. R., Vermeer, H. J., Kamerling, J. P., Vliegenthart, J. F. G. Carbohydrate self-recognition mediates marine sponge cellular adhesion. *PNAS* **98**, 9419-9424 (2001).

[81] Jarchow, J., Burger, M. M. Species-specific association of the cell-aggregation molecule mediates recognition in marine sponges. *Cell Adhes. Commun.* **6**, 405-414 (1998).

[82] Spillman, D., Burger, M. M. Carbohydrate-carbohydrate interactions in adhesion. *J. Cellul. Biochem.* **61**, 562-568 (1996).

[83] Spillmann, D. Carbohydrates in cellular recognition: from leucine-zipper to sugar-zipper? *Glycoconj. J.* **11**, 169-171 (1994).

[84] Fukuda, M. Cell surface glycoconjugates as onco-differentiation markers in hematopoietic cells. *Biochim. Biophys. Acta* **780**, 119-150 (1985).

[85] Iwabuchi, K., Yamamura, S., Prinetti, A., Handa, K., Kakomori, S. Separation of "glycosphingolipid signaling domain" from caveolin-containing membrane fraction in mouse melanoma B16 cells and its role in cell adhesion coupled with signaling. *J. Biol. Chem.* **273**, 9130-9138 (1998).

[86] Kobayashi, T., Hirabayashi, Y. Lipid membrane domains in cell surface and vacuolar systems. *Glycoconj. J.* **17**, 163-171 (2000).

[87] Brown, D. A., Rose, J. K. Sorting of GPI-anchored proteins to glycolipid-enriched membrane subdomains during transport to the apical cell surface. *Cell* **68**, 533-544 (1992).

[88] Tillack, T. W., Allietta, M., Moran, R. E., Young, W. W. J. Localization of globoside and Forssman glycolipids on erythrocyte membranes. *Biochim. Biophys. Acta* **733**, 15-24 (1983).

[89] Sorice, M., *et al.* Evidence for the existence of ganglioside-enriched plasma membrane domains in human peripheral lymphocytes. *J. Lipid Res*. **38**, 969-980 (1997).

[90] Sorice, M., *et al.* Association between GM3 and CD4-Ick complex in human peripheral blood lymphocytes. *Glycoconj. J.* **17**, 247-252 (2000).

[91] Yohe, H. C., *et al.* The major gangliosides of human peripheral blood monocytes/macrophages: absence of ganglio series structures. *Glycobiology* **11**, 831-841 (2001).

[92] Stroud, M. R., *et al.* Monosialogangliosides of human myelogenous leukemia HL60 cells and normal human leukocytes. 1. Separation of E-selectin binding from nonbinding

gangliosides, and absence of sialosyl-Le(x) having tetraosyl to octaosyl core. *Biochemistry* **35**, 758-769 (1996).

[93] Stroud, M. R., *et al.* Monosialogangliosides of human myelogenous leukemia HL60 cells and normal human leukocytes. 2. Characterization of E-selectin binding fractions, and structural requirements for physiological binding to E-selectin. *Biochemistry* **35**, 770-778 (1996).

[94] Misevic, G. N., Burger, M. M. Reconstitution of high cell binding affinity of a marine sponge aggregation factor by cross-linking of small low affinity fragments into a large polyvalent polymer. *J. Biol. Chem.* **261**, 2853-2859 (1986).

[95] Stewart, R. J., Boggs, J. M. A carbohydrate-carbohydrate interaction between galactosylceramide-containing liposomes and cerebroside sulfate-containing liposomes: dependence on the glycolipid ceramide composition. *Biochemistry* **32**, 10666-10674 (1993).

[96] Burger, M. M. Early events of encounter at the cell surface. *In Nicholls JG (ed): "The role of Intercellular Signals: Navigation, Encounter, Outcome." Berlin: Verlag Chemie*, 119-134 (1979).

[97] Scheiner, S., Kar, T., Gu, Y. Strength of the Calpha H..O hydrogen bond of amino acid residues. *J. Biol. Chem.* **276**, 9832-9837 (2001).

[98] Modig, K., Pfrommer, B. G., Halle, B. Temperature-dependent hydrogen-bond geometry in liquid water. *Phys. Rev. Lett.* **90**, 075502 (2003).

[99] Perez, C., *et al.* Controlled incorporation of water molecules into carboxy hydrogen-bond networks: a designed approach. *Org. Lett.* **5**, 641-644 (2003).

[100] Pérez, S., *et al.* Crystal and molecular structure of a histo-blood group antigen involved in cell adhesion: the Lewis x trisaccharide. *Glycobiology* **6**, 537-542 (1996).

[101] Scott, J. E. Secondary structures in hyaluronan solutions: chemical and biological implications. *Ciba Foundation Symposium* **143**, 6-20 (1989).

[102] Almond, A., Brass, A., Sheehan, J. K. Dynamic exchange between stabilized conformations predicted for hyaluronan tetrasaccharides: comparison of molecular dynamics simulations with available NMR data. *Glycobiology* **8**, 973-980 (1998).

[103] Lemieux, R. U. *Acc. Cem. Res.* **29**, 373-380 (1996).

[104] Dagastine, R. R., Prieve, D. C., White, L. R. The dielectric function for water and its application to van der Waals forces. *J. Colloid Interface Sci.* **231**, 351-358 (2002).

[105] Kojima, N., *et al.* Further studies on cell adhesion based on Le(x)-Le(x) interaction, with new approaches: embryoglycan aggregation of F9 teratocarcinoma cells, and adhesion of various tumour cells based on Le(x) expression. *Glycoconj. J.* **11**, 238-248 (1994).

[106] Cao, Z., *et al.* Role of the Lewis^x glycan determinant in corneal epithelial cell adhesion and differentiation. *J. Biol. Chem.* **276**, 21714-21723 (2001).

[107] de la Fuente, J. M., *et al.* Gold glyconanoparticles as water-soluble polyvalent models to study carbohydrate interactions. *Angew. Chem. Int. Ed. Engl.* **40**, 2257-2261 (2001).

[108] Misevic, G. N., Finne, J., Burger, M. M. Involvement of carbohydrates as multiple low affinity interaction sites in the self-association of the aggregation factor from the marine sponge *Microciona prolifera. J. Biol. Chem.* **262**, 5870-5877 (1987).

[109] Humphreys, S., Humphreys, T., Sano, J. Organization and polysaccharides of sponge aggregation factor. *J. Supramol. Struct.* **7**, 339-351 (1977).

[110] Finne, J., Krusius, T. Preparation and fractionation of glycopeptides. *Methods. Enzymol.* **83**, 269-277 (1982).

[111] Misevic, G. N. Immunoblotting and immunobinding of acidic polysaccharides separated by gel electrophoresis. *Methods Enzymol.* **179**, 95-104 (1989).

[112] Min, H., Cowman, M. K. Combined alcian blue and silver staining of glycosaminoglycans in polyacrylamide gels: application to electrophoretic analysis of molecular weight distribution. *Anal. Biochem.* **155**, 275-285 (1986).

[113] Müller, D. J., Baumeister, W., Engel, A. Controlled unzipping of a bacterial surface layer with atomic force microscopy. *Proc. Natl. Acad. Sci. USA* **96**, 13170-13174 (1999).

[114] Hooper, J. N. A., van Soest, R. W. M. Systema Porifera. A guide to the classification of sponges. *Kluwer Academic/Plenum, New York* (2002).

[115] Bergquist, P. R. Sponges. *Hutchinson & Co Ltd* (1978).

[116] Alonso, J. L., Goldmann, W. H. Feeling the forces: atomic force microscopy in cell biology. *Life Sci.* **72**, 2553-2560 (2003).

[117] Hooton, J. C., *et al.* Characterization of particle-interactions by atomic force microscopy: effect of contact area. *Pharm. Res.* **20**, 508-514 (2003).

[118] M. Carrion-Vazquez *et al.* Mechanical design of proteins studied by single-molecule force spectroscopy and protein engineering. *Prog. Biophys. Mol. Biol.* **74**, 63-91 (2000).

[119] Dammer, U. *et al.* Binding strength between cell adhesion proteoglycans measured by Atomic Force Microscopy. *Science* **267**, 1173-1175 (1995).

[120] Mizuguchi, S., *et al.* Chondroitin proteoglycans are involved in cell division of Caenorhabditis elegans. *Nature* **423**, 443-448 (2003).

[121] Properzi, F., Asher, R. A., Fawcett, J. W. Chondroitin sulphate proteoglycans in the central nervous system: changes and synthesis after injury. *Biochem. Soc. Trans.* **31**, 335-336 (2003).

[122] Truant, S., *et al.* Requirement of both mucins and proteoglycans in cell-cell dissociation and invasiveness of colon carcinoma HT-29 cells. *Int. J. Cancer* **104**, 683-694 (2003).

[123] Fannon, M., *et al.* Binding inhibition of angiogenic factors by heparan sulfate proteoglycans in aqueous humor: potential mechanism for maintenance of an avascular environment. *FASEB J.* **17**, 902-904 (2003).

[124] Suzuki, S., Perry, M., Thibault, P., Honda, S. Structures of carbohydrates found in animals and bacteria. *Methods. Mol. Biol.* **213**, 285-305 (2003).

[125] Esquenazi, D., de Souza, W., Alviano, C. S., Rozental, S. The role of surface carbohydrates on the interaction of microconidia of Trichophyton mentagrophytes with epithelial cells. *FEMS Immunol. Med. Microbiol.* **35**, 113-123 (2003).

[126] Janin, J., Wodak, S. J. Protein modules and protein-protein interaction. Introduction. *Adv. Protein Chem.* **61**, 1-8 (2002).

[127] Audette, G. F., Delbaere, L. T., Xiang, J. Mapping protein: carbohydrate interactions. *Curr. Protein Pept. Sci.* **4**, 11-20 (2003).

[128] Krishna, N. R., Agrawal, P. K. Molecular structure of the carbohydrate-protein linkage region fragments from connective-tissue proteoglycans. *Adv. Carbohydr. Chem. Biochem.* **56**, 201-234 (2000).

[129] Taga, A., Honda, S. Determination of association constant of carbohydrate-protein interaction. *Methods Mol. Biol.* **213**, 275-284 (2003).

[130] van Soest, R. W. M., van Kempen, Th. M. G., Braekman, J. C. Sponges in time and space. *A.A. Balkema* (1994).

[131] Bucior, I., Scheuring, S., Engel, A., Burger, M. M. Carbohydrate-carbohydrate interaction provides adhesion force and specificity for cellular recognition. *J. Cell Biol.* **165**, 529-537 (2004).

[132] Fritz, J., Katopodis, A. G., Kolbinger, F., Anselmetti, D. Force-mediated kinetics of single P-selectin/ligand complexes observed by atomic force microscopy. *Proc. Natl. Acad. Sci. USA* **95**: 12283-12288 (1998).

[133] Hanley, W., *et al.* Single molecule characterization of P-selectin/ligand binding. *J. Biol. Chem.* **278**, 10556-10561 (2003).

[134] Hinterdorfer, P., Baumgartner, W., Gruber, H. J., Schilcher, K., Schindler, H. Detection and localization of individual antibody-antigen recognition events by atomic force microscopy. *Proc. Natl. Acad. Sci. USA* **93**, 3477-3481 (1996).

[135] Saleh, O. A., Sohn, L. L. Direct detection of antibody-antigen binding using an on-chip artificial pore. *Proc. Natl. Acad. Sci. U S A* **100**, 820-824 (2003).

[136] Baumgartner, W., *et al.* Cadherin interaction probed by atomic force microscopy. *Proc. Natl. Acad. Sci. U S A* **97**, 4005-4010 (2000).

[137] Tromas, C., *et al.* Adhesion forces between Lewis^x determinant antigens as measured by atomic force microscopy. *Angew. Chem. Int. Ed.* **40**, 3052-3055 (2001).

[138] Guerardel, Y., Czeszak, X., Sumanovski, L., Karamanos, Y., Popescu, O., Strecker, G., Misevic, G. N. Molecular fingerprinting of carbohydrate structures phenotypes of three porifera proteoglycan-like glyconectins, *J. Biol. Chem.* **279**, 15591-15603 (2004).

[139] Braccini, I., Grasso, R. P., Perez, S. Conformational and configurational features of acidic polysaccharides and their interactions with calcium ions: a molecular modeling investigation. *Carbohydr. Res.* **317**, 119-130 (1999).

[140] Grandbois, M., Beyer, M., Rief, M., Clausen-Schaumann, H., Gaub, H. E. How strong is a covalent bond? *Science* **283**, 1727-1730 (1999).

[141] Bucior I, Burger MM. Carbohydrate-carbohydrate interactions in cell recognition. *Curr. Opin. Struct. Biol.* **14**, 631-637 (2004).

VIII. ACKNOWLEDGMENTS

I would like to express my gratitude and thank all those who supported and helped me in many ways to get this work done. Especially:

IX. LIST OF FIGURES

X. LIST OF TABLES

<u>XI. APPENDIX A</u>

Journal of Cell Biology, Volume 165, Number 4,

May 24, 2004

pages 529-537

Carbohydrate–carbohydrate interaction provides adhesion force and specificity for cellular recognition

Iwona Bucior,[1,2] Simon Scheuring,[3] Andreas Engel,[3] and Max M. Burger[1,2]

[1]Friedrich Miescher Institute, 4058 Basel, Switzerland
[2]Marine Biological Laboratories, Woods Hole, MA 02543
[3]M.E. Müller Institute for Microscopy, Biozentrum, University of Basel, 4056 Basel, Switzerland

The Journal of Cell Biology

The adhesion force and specificity in the first experimental evidence for cell–cell recognition in the animal kingdom were assigned to marine sponge cell surface proteoglycans. However, the question whether the specificity resided in a protein or carbohydrate moiety could not yet be resolved. Here, the strength and species specificity of cell–cell recognition could be assigned to a direct carbohydrate–carbohydrate interaction. Atomic force microscopy measurements revealed equally strong adhesion forces between glycan molecules (190–310 piconewtons) as between proteins in antibody–antigen interactions (244 piconewtons).

Quantitative measurements of adhesion forces between glycans from identical species versus glycans from different species confirmed the species specificity of the interaction. Glycan-coated beads aggregated according to their species of origin, i.e., the same way as live sponge cells did. Live cells also demonstrated species selective binding to glycans coated on surfaces. These findings confirm for the first time the existence of relatively strong and species-specific recognition between surface glycans, a process that may have significant implications in cellular recognition.

Introduction

One of the fundamental features of a living cell is a prompt and adequate behavior during formation, maintenance, and pathogenesis of tissues. Short-term adhesion events, e.g., leukocyte recruitment (Robinson et al., 1999), development of the nervous system (Stipp and Hemler, 2000), or microbial pathogenesis (Feizi and Loveless, 1996) require reversible, but still specific molecular surface interactions, rather than tight and stable adhesions between stationary cells (Spillmann and Burger, 1996). Carbohydrates, the most prominently exposed structures on the surface of living cells, with flexible chains and many potential binding sites are ideal to serve as important players in these events. Molecular interactions where carbohydrates are involved are usually considered as weak interactions (Varki, 1994; Spillmann and Burger, 1996), and therefore, biological relevance of carbohydrate–carbohydrate interactions is often questioned. Hakomori's group has been first to show glycosphingolipid self-interactions to occur by way of Lewis[x] determinant (Galβ1→4[Fucα1→3]

GlcNAcβ1→3Galβ1→4Glcβ) (Le[x]) to Le[x] carbohydrate-dependent cell adhesion in the compaction of mouse embryo (Eggens et al., 1989) and autoaggregation of human embryonal carcinoma cells (Song et al., 1998). Extended studies revealed specific cellular recognition between lymphoma and melanoma cells based on gangliotriaosylceramide (GalNAcβ1→4Galβ1→4Glcβ1→1Cer)–sialosyllactosylceramide (NeuAcα2→3Galβ1→4Glcβ1→1Cer) interaction, and sialosyllactosylceramide (NeuAcα2→3Galβ1→4Glcβ1→1Cer)-dependent adhesion of melanoma cells, which led to spreading and enhancement of cell motility (Kojima and Hakomori, 1989; Iwabuchi et al., 1998).

The very first experimental demonstration of cellular recognition and adhesion phenomena in the animal kingdom came from an invertebrate system, i.e., from marine sponges (Wilson, 1907), and was later assigned to cell surface proteoglycans (Humphreys, 1963). Dissociated sponge cells from two different species have the capacity to reaggregate through surface proteoglycans (Fernandez-Busquets and Burger, 2003) in a Ca^{2+}-rich environment (10 mM, i.e., physiologic for seawater) by sorting out according to their

Figure 1.   **Specific recognition between live cells, and between cells and glycan-coated beads.** (A) Homotypic aggregation between *Microciona prolifera* red cells during a 4-h rotation-mediated aggregation in seawater with physiological Ca^{2+}. (B) Species specific sorting out between cells from two different sponge species with red (*Microciona prolifera*) and yellow (*Suberites fuscus*) natural pigment. (C) Inhibition of the cell–cell aggregation in the absence of Ca^{2+}. (D) Inhibition of the homotypic aggregation between *Microciona* cells by the antibody directed

against the carbohydrate epitope of *Microciona* proteoglycan. (E) Homotypic aggregation between yellow cells (*Suberites*) and their own surface glycans coated on red beads during a 4-h rotation-mediated aggregation in seawater with physiological Ca^{2+}. (F) Species specific sorting out between yellow cells and red beads carrying glycans from cells from another sponge species. (G) Inhibition of the cell–glycan aggregation in the absence of Ca^{2+}. (H) Inhibition of the homotypic aggregation between red *Microciona* cells and their glycan coated on red beads by the antibody directed against the carbohydrate epitope of *Microciona* proteoglycan.
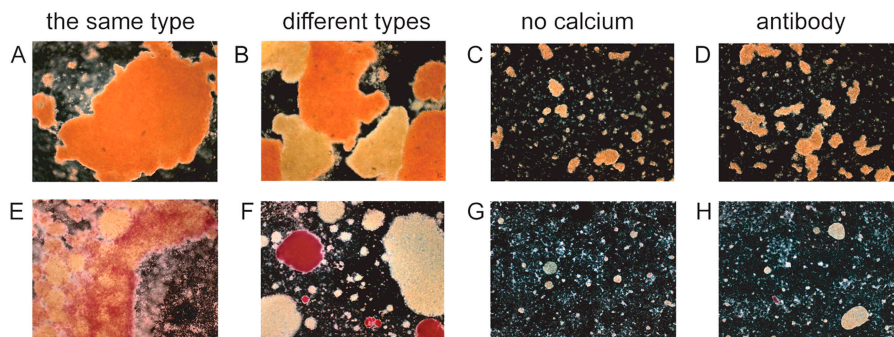
species of origin, in the same way as dissociated embryonic cells from two different vertebrate tissues sort out according to their tissue of origin. Consequently, this simple and highly specific cellular recognition phenomenon in sponges has been used for almost a century as a model system to study recognition and adhesion events in multicellular organisms. Sponge cell–cell aggregation involves Ca^{2+}-independent binding of proteoglycans to a cell surface and Ca^{2+}-dependent self-association of proteoglycans (Turner and Burger, 1973; Jumblatt et al., 1980). A monoclonal antibody raised against the purified proteoglycan from *Microciona prolifera* sponge inhibited the proteoglycan self-association and the epitopes were identified as short carbohydrate units of the 200-kD glycan (Misevic and Burger, 1993): a sulfated disaccharide (Spillmann et al., 1995) and a pyruvylated trisaccharide (Spillmann et al., 1993). Recently, Vliegenthart's group could demonstrate self-interactions of the sulfated disaccharide using surface plasmon resonance (Haseley et al., 2001). However, species-specific interactions between 200-kD glycans from different sponge species have not yet been demonstrated in order to prove the existence of species-specific carbohydrate–carbohydrate recognition system.

200-kD glycan moieties from adhesion proteoglycans from four different marine sponge species were purified here and the species specificity of a glycan–glycan interaction was investigated in aggregation and adhesion assays. Atomic force microscopy (AFM) measurements were performed to measure the binding strength between single interacting glycan molecules and to demonstrate quantitative differences in binding forces between different species of 200-kD glycans. Results confirm the concept of the relatively strong and species-specific carbohydrate–carbohydrate interaction as an important player in cellular recognition.

Results

Live cells specifically aggregate with glycan-coated beads

In the classical assay for specific cell–cell recognition, live sponge cells can recognize their own kind and form big homogeneous aggregates on a shaker at the right shear forces, i.e., rotor speed, as shown for red cells of *Microciona prolifera* (Fig. 1 A). At too high rotation speed no cell aggregates are

formed because shear forces are too high. At too low rotation speed unspecific, faulty initial contacts will remain because such cells do not get a second or third chance to form higher affinity adhesions with other cells. When cells from two different sponge species were shaken together in suspension (red cells, *Microciona prolifera*; yellow cells, *Suberites fuscus*), they sorted out into separate aggregates consisting of cells from the same species only (Fig. 1 B), and no heterotypic mixtures consisting of cells from different species would form. Specific cellular recognition could be inhibited by the absence of Ca^{2+} ions (Fig. 1 C). Recognition between *Microciona* (red) cells could be inhibited by the antibody directed against the carbohydrate epitope of the *Microciona* proteoglycan (Fig. 1 D), and much smaller cell aggregates could be seen as compared with aggregation in physiological Ca^{2+} (Fig. 1 A). There was no visible effect of the antibody on homotypic interactions between cells from other species (unpublished data).

In a cell–glycan recognition assay, live cells were allowed to aggregate with glycan-coated red beads (1-μm diam) similar in size to small sponge cells (2-μm diam), under the same shear forces, i.e., rotor speed as for cell–cell aggregation. Yellow cells (*Suberites*) specifically recognized red beads coated with their own glycans and formed large mixed aggregates (Fig. 1 E). Yellow cells, however, did not mix but separated from aggregates of red beads coated with glycans from a different species, namely *Microciona* (Fig. 1 F). As in cell–cell recognition, the absence of Ca^{2+} ions (Fig. 1 G) inhibited the cell–glycan recognition. The antibody directed against the carbohydrate epitope of *Microciona* proteoglycan could only inhibit the homotypic interaction between red *Microciona* cells and their glycans coated on red beads (Fig. 1 H). Aggregation between cells from other species and their glycans coated on red beads could not be inhibited by that antibody (unpublished data).

Aggregation of glycan-coated beads mimics species-specific cellular aggregation

An assay for glycan–glycan recognition was designed, which mimics the classical assay for specific aggregation of sponge cells. Glycan-coated red and green beads the size of small sponge cells were allowed to aggregate under identical shear
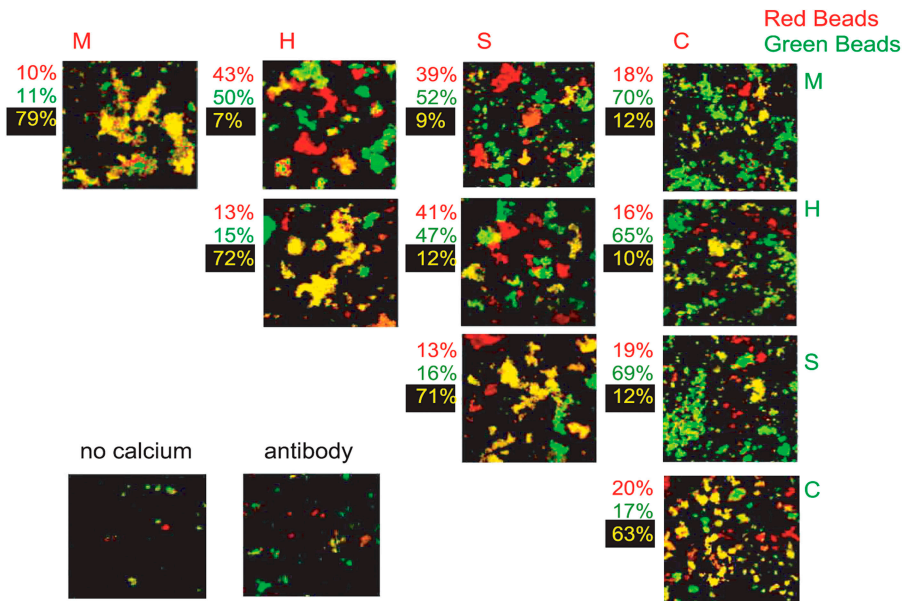
Figure 2. **Specific recognition between glycan-coated beads.** Red and green glycan-coated beads sorted out specifically during a 4-h rotation-mediated aggregation in seawater with physiological Ca^{2+}. Yellow areas depict clumps of mixed red and green beads coated with identical glycans. Red and green areas reflect clumps of separated beads coated with different glycans. The colored numbers on the left side of each picture represent the percentage of clumps of the respective color. The glycan–glycan recognition could be inhibited by the absence of Ca^{2+} ions. The antibody directed against the carbohydrate epitope of *Microciona* proteoglycan inhibited homotypic aggregation between *Microciona* glycans coated on red and green beads. M, *Microciona*; H, *Halichondria*; S, *Suberites*; C, *Cliona*.

forces, i.e., rotor speed as used for cell–cell recognition assays. Beads coated with glycans from identical proteoglycans formed 63–79% yellow aggregates, which are the result of intermingling of red and green beads (Fig. 2). In stark contrast, beads coated with glycans derived from proteoglycans from different species did separate into red and green aggregates. In this case yellow aggregates, i.e., heterotypic mixtures of glycans originating from different species, never formed >12% of aggregated patches.

There were two possible modes for the color distribution in the glycan-coated bead–bead aggregation: either it was random or species specific. Random distribution, which can be described by Pascal's triangle (Pickover, 2001), applies to the homotypic glycan-coated bead–bead aggregation, i.e., between glycans from the same species. In this case, red and green beads coated with identical glycans were mixing in a casual manner leading to a high number of yellow patches. However, based on Pascal's triangle analysis, the color distribution in the heterotypic glycan-coated bead–bead aggregation, i.e., between glycans from two different species, was not random but species specific. Red and green beads coated with glycans from two different species were specifically sorting out into separate red and green aggregates.

As in cell–cell and cell–glycan recognition, the absence of Ca^{2+} ions inhibited the glycan–glycan recognition. The antibody directed against the carbohydrate epitope of the *Microciona* proteoglycan inhibited the homotypic interaction between *Microciona* glycans coated on red and green beads. There was no visible effect of the antibody on homotypic interactions between other species glycans (unpublished data). Results obtained with glycan-coated beads (Fig. 2) reflect thus the same results obtained with live cells (Fig. 1, A–D).

It has been reported previously that 400 molecules of *Microciona* proteoglycan bound per cell cause live cells to aggregate (Jumblatt et al., 1980). The number of 200-kD glycan copies per proteoglycan molecule was determined from the mass of total carbohydrate recovered in 200-kD glycan fractions either after gel electrophoresis or gel filtration (Misevic

and Burger, 1993). Because 37% of the total carbohydrate content of the proteoglycan molecule occurred in the form of 200-kD glycan ($\sim$70% of the proteoglycan mass is carbohydrate; proteoglycan $M_r = 2 \times 10^7$), one proteoglycan carries $\sim$26 copies of this glycan. Therefore, $\sim$10,400 glycan molecules (400 proteoglycan molecules) per cell cause living cells to aggregate. In our experiments, binding measurements indicated that $\sim$2,500 molecules of 200-kD glycan per bead specifically aggregated glycan-coated beads. The number was calculated from the specific absorbance of stained glycans after reversing the binding to beads (which gave the number of moles: 0.192×10^{-11}) and Avogadro's number, and was divided by the number of beads (4.5×10^8). Surface areas of the cell and the bead were calculated from diameters, and they were 12.56 μm^2 and 3.14 μm^2 accordingly. This led to the final assessment that the glycan density per cell and per bead causing species-specific live cell and glycan-coated bead recognition and aggregation is similar: 828 molecules/μm^2 for cell–cell aggregation and 810 molecules/μm^2 for glycan-coated bead–bead aggregation.

Live cells and cell surface glycans adhere species specifically to glycans coated on a plastic surface

The binding of live cells to glycans from their surface proteoglycans coated onto a solid polystyrene phase was assessed (Fig. 3, A–D). The binding to glycans from proteoglycans from different species of origin was three to five times lower. Cell adhesion showed clear dependence on the quantity of the glycan coated, and could be abolished in the absence of Ca^{2+} ions. Pretreatment of *Microciona* cells with the antibody directed against the carbohydrate epitope of their surface proteoglycan inhibited 86% of these cells from adhesion to their own glycan (Fig. 3 E). In this assay, little cross-reactivity of the antibody (Misevic et al., 1987) could be detected because it blocked only 23% or less adhesion between other cells and their 200-kD glycans.

Similarly to cell–glycan adhesion, 200-kD glycans adhered strongly to surface-bound glycans from identical pro-
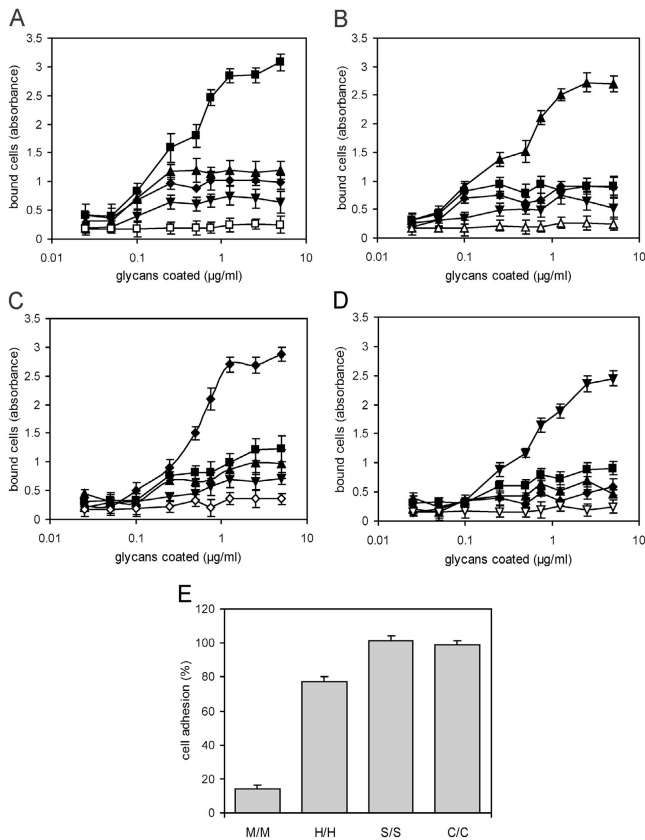
Figure 3. Adhesion of live cells to glycan-coated plates.
(A) *Microciona*, (B) *Halichondria*, (C) *Suberites*, and (D) *Cliona* live cells were incubated for 2 h in seawater with physiological Ca^{2+} in 96-well flat bottom polystyrene plastic plates coated with *Microciona* (■), *Halichondria* (▲), *Suberites* (◆), and *Cliona* (▼) glycans isolated from surface proteoglycans of mother sponges. (□, △, ◇, ▽) Binding of the respective cells to their glycans coated on plates without the presence of Ca^{2+}. (E) Effect of the carbohydrate directed *Microciona* proteoglycan antibody on cell adhesion to glycan-coated plates. Error bars represent SD of four to six independent experiments. M, *Microciona*; H, *Halichondria*; S, *Suberites*; C, *Cliona*.

Figure 4. Adhesion of surface glycans to glycan-coated plates.
(A) *Microciona*, (B) *Halichondria*, (C) *Suberites*, and (D) *Cliona* glycans were incubated for 2 h in seawater with physiological Ca^{2+} in 96-well flat bottom polystyrene plastic plates coated with various quantities of *Microciona* (■), *Halichondria* (▲), *Suberites* (◆), and *Cliona* (▼) glycans isolated from surface proteoglycans. (□, △, ◇, ▽) Binding of the respective glycans to their glycan-coated plates in the absence of Ca^{2+}. (E) Effect of the carbohydrate directed *Microciona* proteoglycan antibody on glycan adhesion to glycan-coated plates. Error bars represent SD of four to six independent experiments. M, *Microciona*; H, *Halichondria*; S, *Suberites*; C, *Cliona*.

teoglycans in a dose-dependent manner (Fig. 4, A–D). The adhesion to glycans from different species was 2.5–6 times lower. This specific glycan–glycan adhesion could only be observed in the presence of Ca^{2+} ions. The antibody against the carbohydrate epitope of *Microciona* proteoglycan blocked 93% of the adhesion between its 200-kD glycans and produced little cross-reactivity (Misevic et al., 1987) by blocking 12% or less of the adhesion between glycans from other proteoglycans (Fig. 4 E).

The glycan–glycan adhesion force is in the piconewton range

Intermolecular adhesive force measurements between 200-kD glycan molecules coated on a probe tip and a surface (Fig. 5 A) were performed using AFM (Rief et al., 1997; Alonso and Goldmann, 2003). Based on fluorescence imaging with labeled glycans, no clustering of glycans was observed either on the probe tip or the surface. During retraction of the tip the glycan structure was lifted, stretched and finally noncovalent bonds between two molecules were be-

ing broken one by one. The existence of multiple noncovalent bonds between carbohydrates of glycan molecules is suggested by the presence of multiple peaks on the force curves, as recorded in the presence of Ca^{2+} (Fig. 5 B, lines 3–8). There was no interaction recorded between gold–gold (Fig. 5 B, line 1) or in the absence of Ca^{2+} (Fig. 5 B, line 2). Force measurements taken directly at the surface (<10 nm) were due to nonspecific interactions between the cantilever tip and the surface (Carrion-Vazquez et al., 2000), e.g., the first rupture peak in Fig. 5 B (lines 3, 5, and 8) and the first two in Fig. 5 B (lines 4 and 7). Only those measured at distances >10 nm from the surface were considered as direct interactions between glycan molecules. Strong multiple interactions were observed between glycans from the same species and noncovalent bonds between two interacting glycan molecules of the same origin (one peak) were ruptured at the forces between 190 and 310 piconewtons (pN; Fig. 6 A). The strength of the attachment of 200-kD glycans through S to the Au surface of the probe tip and the substrate is much stronger: 1.4 nanonewtons (Grandbois et al., 1999).
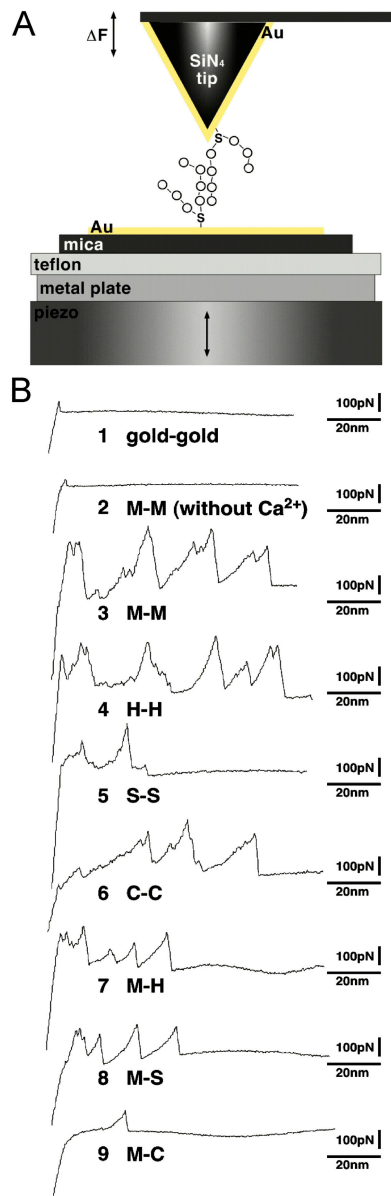
Figure 5. **AFM measurements of glycan–glycan binding forces.** (A) Scheme of AFM set up for the measurement of the intermolecular forces between glycan molecules in seawater with physiological Ca^{2+}. (B) Examples of AFM force curves. Lines 1 and 2 represent control curves: (1) gold–gold interaction and (2) glycan–glycan interaction in seawater without Ca^{2+}. Lines 3–6 represent curves of interactions between glycans from the same species in seawater with physiological Ca^{2+}, whereas lines 7–9 represent curves of interactions between different species of glycans. M, *Microciona*; H, *Halichondria*; S, *Suberites*; C, *Cliona*.

Single glycan–glycan adhesion force is species specific

In stark contrast to strong binding forces between glycans from the same species, clearly reduced forces were recorded between glycans from different species (Fig. 6 A). The single noncovalent bond between two interacting glycan molecules from two different species was ruptured at the forces between 110 and 210 pN. In a statistical analysis, the binding forces between glycans from the same species were always stronger than those between glycans from different species. P values for the difference in binding force between the two,

Table I. **Trace amino acid composition of 200-kD glycans**

	Microciona	*Halichondria*	*Suberites*	*Cliona*
	mol amino acid/mol glycan			
Asp	0.9	0.7	0.8	0.5
Glu	0.4	0	0	0
Ser	0	0.1	0.2	0
His	0	0	0	0
Gly	0.3	0.3	0.5	0.3
Thr	0.2	0.1	0	0
Ala	0.3	0.2	0.3	0.3
Arg	0	0	0	0
Tyr	0	0	0	0
Val	0	0	0	0
Met	0	0	0	0
Phe	0	0	0	0
Ile	0	0	0	0
Leu	0	0	0.1	0
Lys	0	0.1	0	0
Pro	0	0	0	0
Asn	0	0	0	0
Gln	0	0	0	0
Trp	0	0	0	0
Ca	0	0	0	0
Total	2.1	1.5	1.9	1.1

The values are the average from two determinations. Cys was ND.

calculated from Mann-Whitney test, were clearly below 0.01 and showed that the difference is statistically significant.

Specificity of the carbohydrate–carbohydrate interaction is also reflected in the polyvalence

The characteristic feature of the glycan–glycan interaction is the repetition of interactive sites along the glycan chain, which further increases the strength of the interaction and thus the specificity. The distance between the peak numbers 1 and 2 (2 and 3, etc.) on force curves was measured to produce a histogram of the peak periodicity (Fig. 6 B). 80% of force curves between glycans from the same species of cells showed more than one interaction peak, with a distance between binding motifs of ~20 nm. In contrast, <35% of force curves between glycans from different species of cells showed multiple interaction peaks, demonstrating the preference for one rather unspecific binding event during the interaction.

The glycan molecules used here have chain-like structures of an average folded length of ~40 nm as imaged by AFM (Jarchow et al., 2000), whereas the extended structure has a length of up to 180 nm (Dammer et al., 1995). 75% of the total lengths of the force curves for the same species glycans were 20–50 nm, and in some cases the curves showed extensions up to 130 nm (Fig. 6 C). This then indicates that the interaction sites are located along the carbohydrate chain and not only at its end. In contrast, 70% of the force curves for glycans from two different species showed total interaction lengths of 10–30 nm only.

Pronase digestion of glycans is essentially complete

Proteoglycan molecules were subjected to an extensive pronase digestion in order to obtain protein-free glycans.

Figure 6. **A quantitative evaluation of species specific versus nonspecific AFM measurements.** (A) Adhesion force values of the interactions between glycans from the same species or from different species attached to the AFM tip and the mica surface. On the ordinate number of rupture events are provided normalized to 1.0 for the category of the highest number of events. (B) Periodicity measurements showing distances between rupture peaks, which indicate the distances between binding motifs on the carbohydrate chain. The white bar reflects the number of probe lift events where only one rupture event could be registered. (C) The length of the force curves measured from the lift-off point to the last peak, indicating the total length of the interacting carbohydrate chain. M, *Microciona* glycan; H, *Halichondria* glycan; S, *Suberites* glycan; C, *Cliona* glycan.
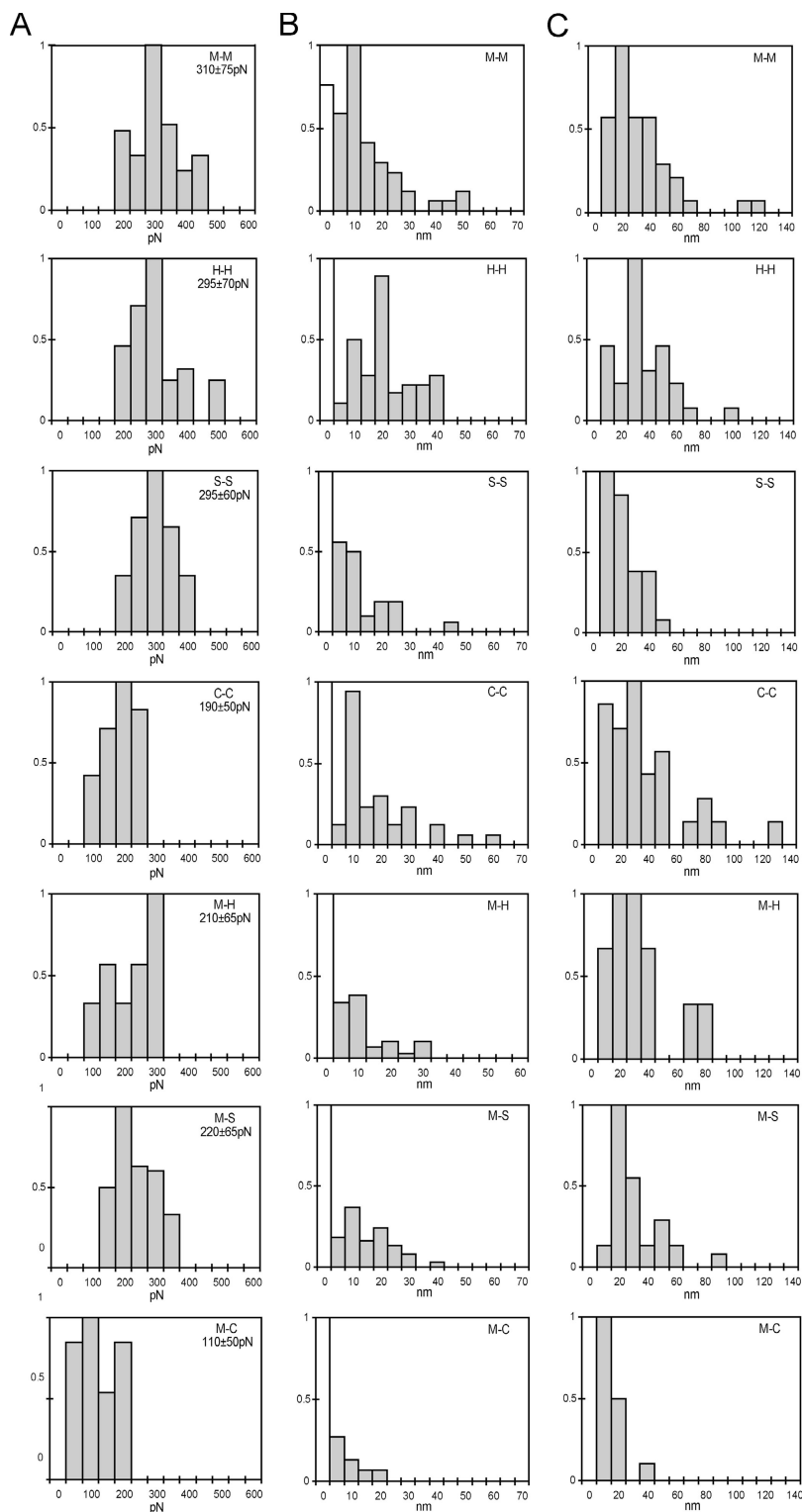
The total 200-kD glycans were separated from free amino acids and peptides by gel filtration and ion-exchange chromatography (Misevic et al., 1987). The 200-kD glycan has an apparent $M_r = 200 \times 10^3 \pm 40 \times 10^3$, and electrophoretic and chromatographic separation techniques indicated that the glycan is a single molecular species with possible charge and size microheterogeneities (Misevic et al., 1987). There have been essentially no losses of carbohydrates during the purification procedures because the carbohydrate yield of the glycan fractions was ~97%. Amino acid analysis of glycans from the four sponge species used showed that there was from 0.5 (*Cliona celata*) to 0.9 (*Microciona prolifera*) mole of linker aspartate/mol of glycan (Table I). Only trace amounts of a few other amino acids were detected. This indicates that the digestion was complete and that the purification pro-

cedure for the 200-kD glycans led to essentially pure gly-can fractions, free of any protein contaminations.

Discussion

Virtually all animal cells produce proteoglycans, which vary greatly in structure, expression, and functions (Kjellen and Lindahl, 1991). Nevertheless, they do have a general propensity to be ECM components and to mediate specific interactions related to different aspects of cell adhesion phenomena through their protein or carbohydrate portions (Truant et al., 2003). In contrast to the rapid progress in studies of cell recognition and adhesion through protein–protein or protein–carbohydrate interactions (Feizi, 2000; Hynes and Zhao, 2000), the number and progress of studies on the possible role of carbohydrate–carbohydrate interactions in these events is still very small. Cell recognition and adhesion processes controlling the remarkable ability of sponge cells to species specifically aggregate after mechanical dissociation to finally reconstitute a functional sponge with canals, mineral skeleton, and collagen fibrils and fibers (Wilson, 1907; Galtsoff, 1925) is mediated by proteoglycans and this function may reside in the glycan portion. Data presented here significantly broaden the current views on the role of carbohydrates in cellular recognition by a novel demonstration of the species-specific character of the glycan–glycan interaction based on relatively strong single binding forces in the range of several hundred pN, providing an adequate affinity and avidity to mediate specific cell–cell recognition.

The examination of carbohydrate–carbohydrate interactions at the atomic level is critical in understanding the nature of these interactions and their biological role. Measured adhesive forces between identical glycans (190–310 pN) compare well with the range of forces between the entire proteoglycan molecules, which vary from 50 to 400 pN, depending on the number of binding sites ruptured (Dammer et al., 1995; Popescu et al., 2003). Similar values are also reported for other biologically relevant forces, e.g., for single protein–glycan interactions (Fritz et al., 1998; Hanley et al., 2003), when interaction of P-selectin from leukocytes with its carbohydrate ligand from endothelial cells was measured (165 pN), or for single antibody–antigen recognition (Hinterdorfer et al., 1996; Saleh and Sohn, 2003) with rupture forces of 244 pN. The force spectra shown in Fig. 5 exhibit the general shape anticipated for simple entropic polymers that extend until the carbohydrate–carbohydrate interaction ruptures. Considering molecular compliance it should be noted that the rupture forces measured here are below those inducing the chair-boat transition, which could have interfered with the interpretation of the results.

The density of glycans on the AFM probe tip and the substrate was adjusted to meet the expectation that the surface layers are neither multilayered nor clustered, and therefore, direct glycan–glycan interactions were measured. The exact number of single rupture events between two interacting glycan molecules is difficult to define with certainty because it cannot be excluded that a so-called "single event" may be a composite of more than one bond rupture. Nevertheless, because the statistical analysis of pull-off distances show that the overall lengths of force curves (from 20 nm up to 130

nm) are less than the expected extended length of the glycan (160–180 nm), it can be assumed that single glycan molecule and not multiple glycan molecule interactions were measured here.

The specificity of glycan-mediated recognition is guaranteed both by the higher adhesion forces per binding site as well as by the higher amount of polyvalent interactions between glycans from the same species versus glycans from different species. The repetition of the binding motif along the carbohydrate chain ensures sufficient binding strength to function in vivo. Polyvalence can be controlled by various means: e.g., by surface density of presented structures, ionic strength modulating attractive versus repulsive forces, subtle changes in biosynthesis of the carbohydrate sequences, etc. These allow changing the affinity of the interactive molecules and therefore, creating a highly flexible and specific model of recognition system. The model assumes gradual adhesion during initial contact between two different cells or cell and matrix by allowing cells to test surrounding surfaces and first create weak random contacts before releasing or reinforcing adhesion (Burger, 1979). Therefore, interactions between two different species of glycans could still be recorded in AFM measurements, though of lower stability than these between glycans from the same species. Similarly, some amount of heterotypic aggregates consisting of different species of glycans was present in glycan-coated bead aggregation experiments.

Ca^{2+} ions or other divalent cations are crucial in carbohydrate–carbohydrate interactions. Here, the presence of Ca^{2+} ions was essential. No interaction between cells, cells and surface glycans, and between surface glycans could be observed in the absence of Ca^{2+}. Also no adhesion forces between single glycan molecules could be detected during AFM measurements. However, it has been reported that the presence of Ca^{2+} ions did not contribute significantly to the adhesion force in Le^x–Le^x interaction (Tromas et al., 2001). On the other hand, self-aggregation of Le^x molecules in aqueous solution, where the molecules move freely, occurred only in the presence of Ca^{2+} ions (de la Fuente et al., 2001). On the molecular level, Ca^{2+} ions probably provide coordinating forces (Haseley et al., 2001), though ionic forces cannot be excluded. These Ca^{2+} interactions are thought to stabilize conformations and can thereby lead to hydrogen bonds and hydrophobic interactions elsewhere in the glycan molecule (Spillmann and Burger, 1996). Further studies are required to resolve the exact role of Ca^{2+} and other divalent cations in carbohydrate–carbohydrate interactions.

Inhibition of sponge cell recognition and aggregation by species-specific carbohydrate epitope antibodies as shown earlier (Misevic et al., 1987; Misevic and Burger, 1993) do not prove glycan–glycan interactions to be relevant because they leave the option of glycan–protein interactions open. The same interpretation holds for two of the approaches presented here: species specificity for the glycan-coated bead interaction with live sponge cells (Fig. 1, E–H) and for the live cells binding to glycan-coated plastic surfaces (Fig. 3). The specificity found here for glycan–glycan interaction (Fig. 4), for glycan-coated bead sorting (Fig. 2), and the force and specificity shown in the AFM measurements (Fig. 6) make, however, a role for carbohydrate–carbohydrate in

sponge cell recognition and adhesion likely. The fact that the outermost cell surface is made up primarily of a dense layer of hydrophilic glycans supports the notion that upon first contact between cells such reversible and flexible glycan–glycan interactions may play a pivotal role in cell recognition processes.

Materials and methods

Sponges, live cells, cell surface proteoglycans, and glycans

Sponges, i.e., *Microciona prolifera*, *Halichondria panicea*, *Suberites fuscus*, and *Cliona celata* were collected by the Marine Biological Laboratory Marine Resources Dept. Live sponge cells were isolated as described previously (Misevic et al., 1987). Isolation of cell surface proteoglycans and pronase digestion of the core protein 200-kD glycans were performed as described previously (Misevic et al., 1987).

Analytical methods

For amino acid analyses, dry glycan samples were diluted in 1-ml of ultra pure water and the aliquots of 25 µl were lyophilized and hydrolyzed during 24 h. After hydrolysis, the black residues were suspended in 100 µl of 50 mM HCl containing 50 pmol/µl Sar and Nva each while ultrasonicated for 15 min. After a 15-min centrifugation, the transparent solutions were transferred into new reagent tubes and analyzed on a Hewlett-Packard AminoQuant II analyzer.

Aggregation assay

4.5×10^8 freshly sonified amine-modified beads (1-µm diam; Molecular Probes) were coupled with isolated glycans (1.5 mg/ml) by incubation in Ca^{2+}- and Mg^{2+}-free artificial seawater buffered with 20 mM Tris, pH 7.4, supplemented with 2 mM CaCl₂ (CSW), and 2 mg of 5,5′-dithiobis-(2-nitrobenzoic acid) (Molecular Probes) overnight at RT. Coupling efficiency was determined by measuring the glycan concentration (by staining with 1% Toluidine blue) on the beads after reversing the 5,5′-dithiobis-(2-nitrobenzoic acid) cross-linking with the disulfide-reducing agent DTT. The number of 200-kD glycan molecules bound per bead was calculated from the specific absorbance of stained glycans, which gave the number of moles (0.192×10^{-11}) multiplied by Avogadro's number (6.022×10^{23}), and was divided by the number of beads (4.5×10^8).

9×10^6 glycan-coated beads in 400 µl of CSW were allowed to aggregate with cells or other glycan-coated beads on a rotary shaker at 60 rpm for 4 h after the addition of 10 mM CaCl₂. Images of aggregates were acquired with a confocal laser-scanning microscope (Leica) equipped with an argon/krypton laser and a 10× objective (PL Fluotar, N.A. 0.3). Image processing was performed using Adobe Photoshop version 6.0. Quantifications were performed using UTHSCSA Image Tool version 2.00 Alpha.

Binding of cells and glycans to glycan-coated plates

Solutions of 200-kD glycans in CSW were placed in each well of a 96-well plastic plate (Falcon; 0.3 ml/well vol). After 2 h, each well was washed with CSW, 100 µl of glycans in 0.1 mg/ml CSW were added and incubated for 2 h at RT, after addition of 10 mM CaCl₂. Afterwards, nonbound glycans were washed off with CSW containing 10 mM CaCl₂. Bound glycans were stained with 1% Toluidine blue and absorbance was measured at 630 nm. The absorbance of glycans used as a coat was deducted from the total absorbance measured after the addition of glycans to coated wells to give the absorbance of bound glycans.

100 µl of live cells (5×10^3) in CSW were added to each glycan-coated well, supplemented with 200 µl of CSW containing 10 mM CaCl₂ and incubated for 2 h at RT. Afterwards, plates were immersed in CSW with 10 mM CaCl₂ in a large container, suspended upside down for 10 min with gentle shaking to allow nonadherent cells to sediment out of plates. Bound cells were lysed for 10 min in 2 M NaCl, 20 mM Tris-HCl, pH 7.5. 200 ng Hoechst stain in 20 mM Tris-HCl, pH 7.5, was added to cell lysates and the fluorescence was measured at $\lambda_{ex} = 360$ nm and $\lambda_{em} = 450$ nm.

AFM

Force measurements were performed with a commercial Nanoscope III AFM (Digital Instruments) equipped with a 162-µm scanner (J-scanner) and oxide-sharpened Si_3N_4 cantilevers with a thickness of 400 nm and a length of 100 µm. Cantilever spring constants k measured according to Chon et al. (2000) for a series of cantilevers from the same region of the wafer revealed on average k = 0.085 N/m and SD = 0.002 N/m. We observed a variation of <15% for k values from different cantilever batches. However, all measurements were done with cantilevers from the same batch.

AFM supports were built as described previously (Müller et al., 1999). The mica was cleaved using scotch tape, masked using a plastic ring mask with an inner diameter of 5 mm, and brought into the vacuum chamber of the gold sputter coater (Bal-Tec SCD 050). A vacuum of 10^{-2} mbar was generated and interspersed by rinsing the chamber with argon gas. At the pressure of 5×10^{-2} mbar a 20-nm gold layer was deposited on the mica surface and the tip controlled by a quartz thickness and deposition rate monitor (Bal-Tec QSG 050). Gold coated Si_3N_4 tips and micas allowed covalent chemisorptions of the naturally sulfated carbohydrates. Both the support and the tip were overlaid with CSW containing 10 mM CaCl₂ and the gold–gold interaction was measured. Afterwards, the support and the tip were incubated with isolated glycans (1 mg/ml) for 15 min at RT. Nonbound glycans were washed off with CSW, and glycan–glycan force measurements were performed in CSW containing 10 mM CaCl₂. For each measurement, a new tip was coated with 200-kD glycan and a new Au substrate was prepared. The AFM stylus approached and retracted from the surface ∼100 times with a speed of 200 nm/s. The tip was moved laterally by 50 nm after recording five force-distance curves.

Surface clustering of 200-kD glycans was determined by fluorescence imaging. Glycans were labeled through their amino groups of the amino acid portion with 5(6)-carboxyfluorescein-*N*-hydroxysuccinimidester (Boehringer). Labeled glycans were separated from free labeling substance via a P-6 sizing column (Amersham Biosciences) in 100 mM pyridine-acetate buffer, pH 5.0.

References

Alonso, J.L., and W.H. Goldmann. 2003. Feeling the forces: atomic force microscopy in cell biology. *Life Sci.* 72:2553–2560.

Burger, M.M. 1979. The role of intercellular signals: navigation, encounter, outcome. *In* Life Sciences Research Report 14. J.G. Nicholls, editor. Verlag Chemie GmbH, Weinheim, Germany. 119–134.

Carrion-Vazquez, M., A.F. Oberhauser, T.E. Fisher, P.E. Marszalek, H. Li, and J.M. Fernandez. 2000. Mechanical design of proteins studied by single-molecule force spectroscopy and protein engineering. *Prog. Biophys. Mol. Biol.* 74:63–91.

Chon, J.W.M., P. Mulvaney, and J.E. Sader. 2000. Experimental validation of theoretical models for the frequency response of atomic force microscope cantilever beams immersed in fluids. *J. Appl. Physics.* 87:3978–3988.

Dammer, U., O. Popescu, P. Wagner, D. Anselmetti, H.J. Guntherodt, and G.N. Misevic. 1995. Binding strength between cell adhesion proteoglycans measured by atomic force microscopy. *Science.* 267:1173–1175.

de la Fuente, J.M., A.G. Barrientos, T.C. Rojas, J. Rojo, J. Canada, A. Fernandez, and S. Penades. 2001. Gold glyconanoparticles as water-soluble polyvalent models to study carbohydrate interactions. *Angew. Chem. Int. Ed. Engl.* 40:2257–2261.

Eggens, I., B. Fenderson, T. Toyokuni, B. Dean, M. Stroud, and S. Hakomori. 1989. Specific interaction between Lex and Lex determinants. A possible basis for cell recognition in preimplantation embryos and in embryonal carcinoma cells. *J. Biol. Chem.* 264:9476–9484.

Feizi, T. 2000. Progress in deciphering the information content of the "glycome"– a crescendo in the closing years of the millennium. *Glycoconj. J.* 17:553–565.

Feizi, T., and R.W. Loveless. 1996. Carbohydrate recognition by Mycoplasma pneumoniae and pathologic consequences. *Am. J. Respir. Crit. Care Med.* 154(4 Pt 2):S133–S136.

Fernandez-Busquets, X., and M.M. Burger. 2003. Circular proteoglycans from sponges: first members of the spongican family. *Cell. Mol. Life Sci.* 60:88–112.

Fritz, J., A.G. Katopodis, F. Kolbinger, and D. Anselmetti. 1998. Force-mediated kinetics of single P-selectin/ligand complexes observed by atomic force microscopy. *Proc. Natl. Acad. Sci. USA.* 95:12283–12288.

Galtsoff, P.S. 1925. Regeneration after dissociation: an experimental study on

sponges. *J. Exp. Zool.* 42:223–251.

Grandbois, M., M. Beyer, M. Rief, H. Clausen-Schaumann, and H.E. Gaub. 1999. How strong is a covalent bond? *Science.* 283:1727–1730.

Hanley, W., O. Mc, S. Carty, Y. Jadhav, D. Tseng, K. Wirtz, and K. Konstantopoulos. 2003. Single molecule characterization of P-selectin/ligand binding. *J. Biol. Chem.* 278:10556–10561.

Haseley, S.R., H.J. Vermeer, J.P. Kamerling, and J.F.G. Vliegenthart. 2001. Carbohydrate self-recognition mediates marine sponge cellular adhesion. *Proc. Natl. Acad. Sci. USA.* 98:9419–9424.

Hinterdorfer, P., W. Baumgartner, H.J. Gruber, K. Schilcher, and H. Schindler. 1996. Detection and localization of individual antibody-antigen recognition events by atomic force microscopy. *Proc. Natl. Acad. Sci. USA.* 93:3477–3481.

Humphreys, T. 1963. Chemical dissolution and *in vitro* reconstruction of sponge cell adhesions. I. Isolation and functional demonstration of the components involved. *Dev. Biol.* 53:27–47.

Hynes, R.O., and Q. Zhao. 2000. The evolution of cell adhesion. *J. Cell Biol.* 150:89–95.

Iwabuchi, K., S. Yamamura, A. Prinetti, K. Handa, and S. Hakomori. 1998. GM3-enriched microdomain involved in cell adhesion and signal transduction through carbohydrate-carbohydrate interaction in mouse melanoma B16 cells. *J. Biol. Chem.* 273:9130–9138.

Jarchow, J., J. Fritz, D. Anselmetti, A. Calabro, V.C. Hascall, D. Gerosa, M.M. Burger, and X. Fernandez-Busquets. 2000. Supramolecular structure of a new family of circular proteoglycans mediating cell adhesion in sponges. *J. Struct. Biol.* 132:95–105.

Jumblatt, J.E., V. Schlup, and M.M. Burger. 1980. Involvement of a carbohydrate group in the active site for surface guided reassociation of animal cells. *Biochemistry.* 19:1038–1042.

Kjellen, L., and U. Lindahl. 1991. Proteoglycans: structures and interactions. *Annu. Rev. Biochem.* 60:443–475.

Kojima, N., and S. Hakomori. 1989. Specific interaction between gangliotriaosylceramide (Gg3) and sialosyllactosylceramide (GM3) as a basis for specific cellular recognition between lymphoma and melanoma cells. *J. Biol. Chem.* 264:20159–20162.

Misevic, G.N., and M.M. Burger. 1993. Carbohydrate-carbohydrate interactions of a novel acidic glycan can mediate sponge cell adhesion. *J. Biol. Chem.* 268:4922–4929.

Misevic, G.N., J. Finne, and M.M. Burger. 1987. Involvement of carbohydrates as multiple low affinity interaction sites in the self-association of the aggregation factor from the marine sponge Microciona prolifera. *J. Biol. Chem.* 262:5870–5877.

Müller, D.J., W. Baumeister, and A. Engel. 1999. Controlled unzipping of a bacterial surface layer with atomic force microscopy. *Proc. Natl. Acad. Sci. USA.* 96:13170–13174.

Pickover, C.A. 2001. Wonders of numbers. Oxford University Press, Oxford, UK.

Popescu, O., I. Checiu, P. Gherghel, Z. Simon, and G.N. Misevic. 2003. Quantitative and qualitative approach of glycan-glycan interactions in marine sponges. *Biochimie.* 85:181–188.

Rief, M., F. Oesterhelt, B. Heymann, and H.E. Gaub. 1997. Single molecule force spectroscopy on polysaccharides by atomic force microscopy. *Science.* 275:1295–1298.

Robinson, S.D., P.S. Frenette, H. Rayburn, M. Cummiskey, M. Ullman-Cullere, D.D. Wagner, and R.O. Hynes. 1999. Multiple, targeted deficiencies in selectins reveal a predominant role for P-selectin in leukocyte recruitment. *Proc. Natl. Acad. Sci. USA.* 96:11452–11457.

Saleh, O.A., and L.L. Sohn. 2003. Direct detection of antibody-antigen binding using an on-chip artificial pore. *Proc. Natl. Acad. Sci. USA.* 100:820–824.

Song, Y., D.A. Withers, and S. Hakomori. 1998. Globoside-dependent adhesion of human embryonal carcinoma cells, based on carbohydrate-carbohydrate interaction, initiates signal transduction and induces enhanced activity of transcription factors AP1 and CREB. *J. Biol. Chem.* 273:2517–2525.

Spillmann, D., and M.M. Burger. 1996. Carbohydrate-carbohydrate interactions in adhesion. *J. Cell. Biochem.* 61:562–568.

Spillmann, D., K. Hard, J.E. Thomas-Oates, J.F. Vliegenthart, G. Misevic, M.M. Burger, and J. Finne. 1993. Characterization of a novel pyruvylated carbohydrate unit implicated in the cell aggregation of the marine sponge Microciona prolifera. *J. Biol. Chem.* 268:13378–13387.

Spillmann, D., J.E. Thomas-Oates, J.A. van Kuik, J.F. Vliegenthart, G. Misevic, M.M. Burger, and J. Finne. 1995. Characterization of a novel sulfated carbohydrate unit implicated in the carbohydrate-carbohydrate-mediated cell aggregation of the marine sponge Microciona prolifera. *J. Biol. Chem.* 270:5089–5097.

Stipp, C.S., and M.E. Hemler. 2000. Transmembrane-4-superfamily proteins CD151 and CD81 associate with alpha 3 beta 1 integrin, and selectively contribute to alpha 3 beta 1-dependent neurite outgrowth. *J. Cell Sci.* 113:1871–1882.

Tromas, C., J. Rojo, J.M. De La Fuente, A.G. Barrientos, R. Garcia, and S. Penades. 2001. Adhesion forces between Lewis^x determinant antigens as measured by atomic force microscopy. *Angew. Chem. Int. Ed. Engl.* 40:3052–3055.

Truant, S., E. Bruyneel, V. Gouyer, O. de Wever, F.R. Pruvot, M. Mareel, and G. Huet. 2003. Requirement of both mucins and proteoglycans in cell-cell dissociation and invasiveness of colon carcinoma HT-29 cells. *Int. J. Cancer.* 104:683–694.

Turner, S.R., and M.M. Burger. 1973. Involvement of a carbohydrate group in the active site for surface guided reassociation of animal cells. *Nature.* 244:509–510.

Varki, A. 1994. Selectin ligands. *Proc. Natl. Acad. Sci. USA.* 91:7390–7397.

Wilson, H.V. 1907. On some phenomena of coalescence and regeneration in sponges. *J. Exp. Zool.* 5:245–258.

416 pp.

XII. APPENDIX B

Glycoconjugate Journal, in press, 2004,

pages 1-36

Carbohydrate-carbohydrate interaction as a major force initiating cell-cell recognition

Iwona Bucior[1,2], Max M. Burger[1,2]

[1]Friedrich Miescher Institute, Novartis Research Foundation, Maulbeerstrasse 66, 4058 Basel, Switzerland
[2]Marine Biological Laboratories, 7 MBL Street, Woods Hole, MA 02543, USA

Address correspondence to Max M. Burger, Novartis Science Board, Novartis International AG, WKL-125.13.02, 4002 Basel, Switzerland. Tel: +41-61 696 7690.
E-mail: max.burger@group.novartis.com

Abstract

Sponges were the earliest multicellular organisms to evolve through the development of cell recognition and adhesion processes mediated by cell surface proteoglycans. Information on sponges has an extra added value because, as a group, they are the oldest Metazoans alive and contribute more to our understanding of life on earth than knowledge of other animal groups. Although the proteoglycans are emerging as key players in various physiological and pathophysiological cellular events, little is known about the carbohydrate moiety of the proteoglycan molecule. Until recently there was no evidence provided for the existence of specific and biologically significant carbohydrate-carbohydrate interaction. We show here that the interaction between single oligosaccharides of surface proteoglycans is relatively strong (in the 200-300 piconewtons range) and in the same range as other relevant biological interactions, like those between antibodies and antigens. This carbohydrate-carbohydrate recognition is highly species-specific and perfectly mimics specific cell-cell recognition. Both the strength and the species-specificity of the carbohydrate-carbohydrate interaction are guaranteed by polyvalency, by compositional and architectural differences between carbohydrates, and by the arrangement of the carbohydrate chain in a three-dimensional context. Ca^{2+}-ions are essential and probably provide coordinating forces. Our findings confirm the existence and character of species-specific carbohydrate-carbohydrate recognition fundamental to cell recognition and adhesion events.

Introduction

Studies of the molecular recognition of carbohydrates are at a crossroads similar to that of the nucleic acids and peptides a few decades ago. Interest in carbohydrates has increased parallel to improvements in methods for their separation and analysis and the biological functions of these compounds are now being defined. It is well established that signaling and recognition involve protein-protein and/or carbohydrate-protein interactions. Direct carbohydrate-carbohydrate interactions are in general considered to be weak and not able to provide sufficient strength and specificity for cellular recognition. However, the definition of "weak interaction" is rather arbitrary and based upon the binding strength shown by carbohydrates during the extensive washing in such procedures as direct binding to cells, affinity chromatography, or detection by blotting [1,2]. More recent measurements of the forces between individual surface oligosaccharides of sponge proteoglycan molecules have shown that interaction can not only be as strong but also as specific as, for example, that between antibody and antigen [3].

Carbohydrates can operate at cell surfaces, where they often occur as components of glycoproteins [4], glycolipids [5], or proteoglycans [6] anchored in the cell membrane. The composition of glycolipids at the cell surface is strongly correlated with embryonic cell developmental stages and can serve as mediators of the crosstalk between tumor cells and host cells [7,8] Interaction of these glycolipids with receptors on other cell surfaces plays a signaling and regulatory role in cell development and adhesion [9,10]. These interactions involve carbohydrate-carbohydrate recognition and are dependent on divalent cations such as calcium (Ca^{2+}) and magnesium. For example, compaction of the mouse embryo at the morula stage [11,12] and the aggregation of mouse embryonic cells [12] occur as a result of recognition between Lewis^x trisaccharide structures in a Ca^{2+}-mediated association.

Proteoglycans are found in all connective tissues, in the extracellular matrix, and on the surfaces of virtually all animal cells. Despite their structural and functional diversity [13], proteoglycans have a general propensity to be extracellular matrix components, mediating specific matrix interactions and biological activities related to cell adhesion [14] via their carbohydrate chains or core proteins. However, it could not be resolved until recently

whether the specificity of proteoglycan-mediated cell adhesion events resigns in a protein-carbohydrate or in a carbohydrate-carbohydrate interaction.

The first experimental demonstration of cell recognition and adhesion phenomena in the animal kingdom involved cell surface proteoglycan [15] of invertebrates, i.e. from the marine sponge model system [16]. Sponges are the simplest and earliest multicellular organisms. Remarkably, dissociated sponge cells from two different species can reaggregate through surface proteoglycans by species-specific associations that approach the selectivity of the evolutionarily advanced Ig superfamily. Consequently, this simple and highly specific cellular recognition phenomenon has been used for almost a century as a model system to study specific cellular recognition and adhesion during tissue and organ formation in multicellular organisms.

Specific cell-cell adhesion in most multicellular animals is mediated by two distinct classes of molecules: a Ca^{2+}-independent activity typical of the glycoproteins from the Ig superfamily [17], and Ca^{2+}-dependent cell-cell adhesion, the best example being the cadherins [18]. Interestingly, sponge proteoglycans reunite both functions in the same molecule and mediate species-specific cell-cell recognition via two functionally distinct domains: 1) a Ca^{2+}-independent cell-binding domain and 2) a Ca^{2+}-dependent self-association domain, which provide the intercellular adhesion force.

Sponge proteoglycans [19], otherwise known as aggregation factors (AFs), are large molecules with approximate molecular weights ranging from 2×10^4 kDa [20] to 1.4×10^6 kDa [21]. Based on atomic force microscope (AFM) images [22], proteoglycan molecules show either a linear or a sunburst-like core structure with 20-25 radiating arms. The best analyzed proteoglycan of *Microciona prolifera* carries two N-linked glycan molecules: one with a mass of 6.3 kDa present in the arms of the proteoglycan molecule that binds to a cell surface receptor independently of Ca^{2+} ions [23], and one with a mass of ~200 kDa and present in the core structure that self associates in a Ca^{2+}-dependent manner [24]. Carbohydrate moiety participation in the adhesion process was anticipated after it was found that glycosidase treatment [25] and periodate oxidation [26] destroyed the aggregation activity of proteoglycan molecules. Glass aminopropyl beads coated with protein-free 200-

4

kDa glycan showed a Ca^{2+}-dependent aggregation equivalent to that of proteoglycan-coated beads [24]. The biological specificity and selectivity of the glycan-glycan interaction could then, however, not yet be proven. The monoclonal antibody raised against the purified surface proteoglycan of *Microciona prolifera* blocked cell aggregation, for which the epitopes were identified as short carbohydrate units of the 200-kDa glycan: a sulfated disaccharide [27] and a pyruvylated trisaccharide [28]. The concept of self-recognition of defined carbohydrate epitopes was confirmed using surface plasmon resonance to mimic the role of carbohydrates in cellular adhesion of *Microciona* [29]. The results showed self-recognition of the sulfated disaccharide and this event was proposed as a major force behind Ca^{2+}-dependent cell-cell recognition. Nevertheless, the biological relevance, i.e. the species-specific character of interactions between 200-kDa glycan molecules in sponges has been investigated only recently. It was shown for the first time that direct carbohydrate-carbohydrate interaction is highly species-specific and can play a major role in proteoglycan-mediated cellular recognition and adhesion events.

Here, we elaborate on recently published investigations on the strength and species-specific character of direct carbohydrate-carbohydrate interaction [3] and extend these studies. The 200-kDa glycans from core structures of four sponge species (*Microciona prolifera*, *Halichondria panicea*, *Suberites fuscus* and *Cliona celata*) were purified and their species-specific carbohydrate compositions revealed. In functional self-assembly cells, cells and glycan-coated beads, glycan-coated carboxylate-modified beads displayed species-specific recognition. Finally, atomic force microscopy (AFM) measurements of the forces between single 200-kDa glycan molecules from *Microciona* proteoglycan revealed that glycan-glycan interaction is Ca^{2+}-dependent and that increase in Ca^{2+} concentration leads to the enhancement in adhesive forces. We propose that these outermost cell surface structures serve as important players initiating the first contacts between cells through flexible but nevertheless specific carbohydrate-carbohydrate chain interactions.

Materials and Methods

Sponges, live cells, cell surface proteoglycans and glycans

Microciona prolifera, *Halichondria panicea*, *Suberites fuscus* and *Cliona celata* were collected at the Marine Biological Laboratory Marine Resources Department in Woods Hole, Mass. Live sponge cells were isolated as described previously [26]. Isolation of cell surface proteoglycans and pronase digestion of 200-kDa glycans from core structures were carried out as described [24,30]. Only freshly prepared cells and glycans were used for all experiments and analyses.

Analytical methods

For carbohydrate composition, proteoglycans were hydrolyzed in 4 M TFA at 100ºC for 4 h and the remaining TFA removed by methanol-aided evaporation. Carbohydrates were analyzed by high performance anion exchange chromatography using a Dionex BioLC system and a CarboPac PA1 column. The column was equilibrated with 16 mM NaOH and eluted with linear gradients of 16 mM NaOH to 0.1 M NaOH/50mM Na-acetate or to 0.1 M NaOH/180 mM Na-acetate. Pulsed amperometric detection was carried out using PAD 2 cells with E1 = +0.05 V, 480 ms, E2 = +0.75 V, 180 ms, and E3 = -0.20 V, 360 ms. Relative amounts were calculated using relative response factors from standard samples containing 2 nM of the respective monosaccharides treated in the same way as the polysaccharide samples.

Amino acid analyses were performed as described [3]. Briefly, dry glycan samples were hydrolyzed for 24 h and the black residues were suspended in 100 µl of 50 mM HCl containing 50 pM/µl Sar and Nva. After centrifugation, the transparent solutions were transferred into new reagent tubes and analyzed with a Hewlett-Packard AminoQuant II analyzer.

Long term EDTA-treatment of sponge proteoglycans

2 ml of 0.7 mM EDTA, pH 7.0 was added to lyophilized proteoglycans, and left at 4ºC for a 4-week period. Following this treatment, separation of the core structures and the arms was achieved on A-15m BioRad column (1.5 x 90 cm), eluted with 0.5 M NaCl, 10 mM Tris, pH 7.4. Collected fractions were lyophilized.

Aggregation assays

Freshly sonicated fluorescent carboxylate-modified beads (3.6×10^8) (Molecular Probes, 1 µm diameter) were incubated overnight at room temperature, pH 6.0, with 200-kDa glycans (1.5 mg/ml) in Ca^{2+}- and Mg^{2+}-free artificial seawater buffered with 20 mM Tris pH 7.4 supplemented with 2 mM $CaCl_2$ (CSW), 3 mg water-soluble 1-ethyl-3-(3 dimethylaminopropyl) carbodiimide (EDAC, Molecular Probes), and 1 mg N-hydroxysulfosuccinimide (Molecular Probes). Coupling efficiency was determined by dotting a bead aliquot on a Zeta probe membrane and Alcian Blue staining. The density of 200-kDa glycan molecules on the bead surface was calculated from the specific absorbance of stained glycans, which gave the number of moles (0.15×10^{-11}), Avogadro's number (6.022×10^{23}) and the number of beads (3.6×10^8).

Glycan-coated red amine-modified beads (9×10^6) [3] in 400 µl of CSW were allowed to aggregate with cells, and glycan-coated carboxylate-modified beads (3.6×10^8) in 400 µl of CSW were allowed to aggregate with other glycan-coated carboxylate-modified beads on a rotary shaker at 50 rpm for 4 h after the addition of 10 mM $CaCl_2$. Images of aggregates were acquired with a confocal laser-scanning microscope (Leica Lasertechnik, Heidelberg, Germany) equipped with an argon/krypton laser and a x10 objective (PL Fluotar, N.A. 0.3). Image processing was performed using Adobe Photoshop version 6.0. Data were quantified using UTHSCSA Image Tool version 2.00 Alpha.

Binding of cells and glycans to glycan-coated plates

Solid phase polystyrene plastic surfaces coated with 200-kDa glycans were prepared as described [3]. Binding of cells to glycan-coated plates was done as before [3]. Briefly, 100 µl of live cells (5×10^3) in CSW were added to each glycan-coated well and incubated for 2 h at room temperature after addition of 200 µl of CSW containing 10 mM $CaCl_2$. Afterwards, non-adherent cells were washed off with CSW containing 10 mM $CaCl_2$. Bound cells were lysed for 10 min in 2 M NaCl, 20 mM Tris-HCl, pH 7.5. Hoechst stain (200 ng) in 20 mM Tris-HCl, pH 7.5 was added to cell lysates and the fluorescence measured at λ_{ex}=360 nm and λ_{em}=450 nm. Glycans (100 µl) in CSW (0.1 mg/ml) were added to glycan-coated plates and

incubated for 2 h at room temperature after addition of 10 mM $CaCl_2$. Afterwards, non-bound glycans were washed off with CSW containing 10 mM $CaCl_2$. Bound glycans were stained with 1% Toluidine Blue and absorbance measured at 630 nm. The absorbance of glycans used as a coat was deducted from the total absorbance of glycans coated on wells and glycans bound to glycan-coated plates to give the final absorbance of bound glycans.

Atomic force microscopy

Force measurements were performed as before [3] with a commercial Nanoscope III AFM (from Digital Instruments, Santa Barbara, Calif., USA) equipped with a 162-μm scanner (J-scanner) and oxide-sharpened Si_3N_4 cantilevers with a thickness of 400 nm and a length of 100 μm. Measurements of cantilever spring constants for a series of cantilevers from the same region of the wafer gave an average of k=0.085 N/m and a standard deviation of 0.002 [31]. All measurements were done with cantilevers from the same batch. AFM supports were built as described [32]. Gold (20 nm) was deposited on the mica surface and the tip using a pressure of 5 x 10^{-2} mbar controlled by a quartz thickness and deposition rate monitor (Bal-Tec QSG 050).

Gold coated Si_3N_4 tips and micas allowed covalent chemisorptions of the naturally sulfated carbohydrates. The support and the tip were incubated with 200-kDa glycans (1 mg/ml) in CSW for 15 min at room temperature. Non-bound glycans were washed off with CSW and glycan-glycan force measurements performed in CSW containing 10 mM or 100 mM $CaCl_2$. For each measurement, a new tip was coated with 200-kDa glycan and a new Au substrate was prepared. The AFM stylus approached and retracted from the surface approximately 100 times with a speed of 200 nm/s. The tip was moved laterally 50 nm after recording five force-distance curves.

Surface clustering of 200-kDa glycans on the support and on the tip was determined by fluorescence imaging of bound glycans labeled at the amino groups of the amino acid portion with 5(6)-carboxyfluorescein-N-hydroxysuccinimidester (Boehringer Mannheim).

Results

Species-specific aggregation between live cells and between cells and cell surface glycan coated on beads

Mechanically dissociated sponge cells sort out and reaggregate species-specifically in artificial seawater at physiological Ca^{2+} concentrations (10 mM) under carefully controlled shear forces, i.e. rotor speed. Too high rotation causes cell aggregates to come apart and too low rotation leads to formation of unspecific, faulty aggregates between cells that do not get a second or third chance to form higher affinity adhesions with other cells. When live cells from the same species were shaken in suspension at the right shear forces, they formed large homogenous aggregates (Fig. 1A). However, cells from two different species sorted out into separate aggregates consisting only of cells from the same species (Fig. 1B). This specific cell-cell recognition was drastically reduced in the absence of Ca^{2+} in the artificial seawater (Fig. 1C). A monoclonal antibody directed against the carbohydrate epitope of *Microciona* cell surface proteoglycan reduced the aggregation of *Microciona* cells only (Fig. 1D).

Red beads similar in size to small sponge cells were coated with 200-kDa glycans isolated from the core structures of different proteoglycans. Glycan-coated beads were allowed to aggregate with live cells under the conditions used for cell-cell aggregation. Cells specifically recognized beads coated with their own surface glycans (Fig. 1E). However, they did not mix but formed separate aggregates with beads coated with glycans from different species (Fig. 1F). The absence of Ca^{2+} reduced this species-specific cell-glycan recognition (Fig. 1G). The monoclonal antibody against the carbohydrate epitope of *Microciona* proteoglycan reduced only the recognition between *Microciona* cells and beads coated with their glycan (Fig. 1H).

Species-specific aggregation between glycan-coated beads mimicking species-specific cell-cell aggregation

It has been shown recently that amine-modified beads coated with 200-kDa glycans from different species can aggregate species-specifically in the same way as live cells [3]. A further type of bead, carboxylate-modified beads that require different method for coupling of glycans, was coated with different 200-kDa glycans and examined for aggregation under the conditions used previously for cell-cell and cell-glycan recognition. Beads coated with glycans from identical proteoglycans formed 80% to 74% yellow aggregates, which are the result of the intermingling of red and green beads (Fig. 2). In stark contrast, beads coated with glycans derived from proteoglycans of different species separated into red and green aggregates. In this case, yellow aggregates, i.e. heterotypic mixtures of glycans originating from different species, formed only 4% to 13% of patches. As shown previously for cell-cell and cell-glycan recognition, the absence of Ca^{2+}-ions inhibited glycan-glycan recognition (Fig. 2). The monoclonal antibody against the carbohydrate epitope of the *Microciona* proteoglycan inhibited only the homotypic interaction between *Microciona* glycans coated on red and green beads (Fig. 2).

It has been reported previously that 400 molecules of *Microciona* proteoglycan bound per cell caused live cells to aggregate [26]. As one proteoglycan carries ~26 copies of 200-kDa glycan, ~10'400 glycan molecules per cell cause living cells to aggregate. In our studies, binding measurements indicated that ~2500 molecules of 200-kDa glycan per bead specifically aggregated glycan-coated carboxylate-modified beads. This was calculated from the number of moles and Avogadro's number, divided by the number of beads (see Materials and Methods). Surface areas of cells and beads were calculated from their diameters. Thus, the glycan densities causing species-specific live cell and glycan-coated bead recognition and aggregation are similar: 828 molecules/μm^2 for cell-cell aggregation and 800 molecules/μm^2 for glycan-coated bead-bead aggregation.

Species-specific adhesion of live cells and cell surface glycans to glycans coated on plastic surfaces

Plastic surfaces were coated with 200-kDa glycans from four different species of surface proteoglycans. Mechanically dissociated cells were added to wells and the ability and specificity of live sponge cells to adhere to different glycans coated onto a solid phase were studied. Live cells strongly adhered to glycans from their own surface proteoglycans in the presence of physiological 10 mM Ca^{2+}-ions in artificial seawater. The binding of cells to glycans from different species of proteoglycans was 4- to 4.5-fold lower (Fig. 3A). This species-specific cell-glycan adhesion was clearly dependent on the amount of the glycan coated and was almost completely abolished in the absence of Ca^{2+}. Pretreatment of cells with a monoclonal antibody directed against the carbohydrate epitope of *Microciona* proteoglycan inhibited homotypic interactions between *Microciona* cells and their own glycan coated on the surface (Fig. 3B). Only little cross-reactivity of the antibody was detected and it blocked 12% of the homotypic interactions between cells from three other studied species and their glycans.

Similarly, the ability of glycans isolated from the core structures of different sponge proteoglycans to adhere to glycan-coated surfaces was studied. Glycans mimicked live cells and only adhered strongly to surface-bound glycans from the same species proteoglycan (Fig. 3C). They adhered 3.5- to 4-fold less to glycans from different species proteoglycans. As in the adhesion of live cells to glycan-coated surfaces, the glycan-glycan adhesion was also dependent on the amount of the glycan coated and was abolished in the absence of Ca^{2+}. Pretreatment of glycans with a monoclonal antibody directed against the carbohydrate epitope of *Microciona* proteoglycan inhibited only homotypic *Microciona* glycan-glycan adhesion (Fig. 3D). The antibody blocked only 6% of the homotypic glycan-glycan adhesion between other sponge species.

AFM measurements of the carbohydrate-carbohydrate interaction

AFM has the precision and sensitivity necessary for studying molecular recognition under native conditions at the level of single events at forces in the pN range. An AFM tip and a surface were coated with 200-kDa glycan molecules from different sponge species (Fig. 4A) [3]. There were no multilayers or clusters of glycans on the tip or the surface. Intermolecular adhesion force measurements between single glycan molecules were performed in artificial seawater with physiological 10 mM Ca^{2+}. During retraction of the tip, the glycan structure was lifted and stretched and non-covalent bonds between two molecules were eventually broken one by one. The existence of multiple non-covalent bonds between carbohydrates of glycan molecules was suggested by the presence of multiple peaks on force curves, as recorded in the presence of Ca^{2+} (Fig. 4B, line 3).

Monitored cantilever deflection is a direct measure of the forces between interacting glycan molecules. No interaction was recorded between gold-gold (Fig. 4B, line 1), in the absence of Ca^{2+} (line 2) or during the surface approach. On retraction, the sensor tip detected strong multiple interactions between 200-kDa glycans from the same species (Fig. 4B, line 3). Clearly reduced interactions were detected between glycans from two different species (Fig. 4B, line 4). Binding forces between glycans from the same species were on average 275 pN (Fig. 4C), compared with binding forces between glycans from different species of 180 pN (Fig. 4D). A statistical analysis using the Mann-Whitney test (P values clearly below 0.01) showed the difference to be significant.

The interactions between single 200-kDa glycans were polyvalent, i.e. interactive sites were repeated along the carbohydrate chain; this is suggested by the presence of multiple peaks on force curves. The distance between peak numbers 1 and 2 (2 and 3, etc) was measured to produce a histogram of the peak periodicity (Fig. 4E, F). Force curves representing interactions between two single glycan molecules from the same species showed convincing multiple interaction peaks. Over 80 % of force curves representing interactions between glycans from the same species showed more than one interaction peak, with a distance between binding motifs of 10-20 nm. In contrast, only ~25% of force curves

between glycans from different species showed multiple interaction peaks, demonstrating a preference for one rather unspecific binding event during the interaction.

Interaction sites for glycans from the same species were located along the carbohydrate chain and not only at its end. The total lengths of most force curves did not exceed 50 nm (~75%), though in some cases the curves extended up to 130 nm (Fig. 4G). In contrast, force curves for the glycans from different species showed less extensions and almost 80% of the total lengths were only 10-40 nm (Fig. 4H).

Enhancement of the strength of the carbohydrate-carbohydrate interaction by increasing Ca^{2+}

The role of Ca^{2+}-ions in carbohydrate-carbohydrate interactions was studied by increasing the Ca^{2+} concentration in artificial seawater from physiological 10 mM to 100 mM during AFM measurements of the adhesion forces between single *Microciona prolifera* 200-kDa glycans. A single non-covalent bond between two interacting *Microciona* glycan molecules was ruptured at 310 pN in 10 mM Ca^{2+} (Fig. 5B). This adhesion force increased to 375 pN when the Ca^{2+} concentration was increased to 100 mM (Fig. 5F). A statistical analysis revealed P values clearly below 0.01 and, therefore, showed the difference between these two interactions to be significant.

The occurrence of polyvalent interactions between single glycan molecules was higher in 100 than in 10 mM Ca^{2+}. In 100 mM Ca^{2+}, up to 85% of force curves showed the presence of multiple interaction sites with a distance between binding motifs of 10-20 nm (Fig. 5G). In 10 mM Ca^{2+}, ~70% of force curves also showed multiple peaks, indicating repetition of binding sites along the interacting carbohydrate chain of the glycan molecule (Fig. 5C).

The total lengths of interacting carbohydrate chains did not change with the change in Ca^{2+} concentration. In both cases, the greatest extensions of the interacting carbohydrate chain were up to 120 nm (Fig. 5D, H). The total lengths of force curves were mainly 20-50

nm in 10 and in 100 mM Ca^{2+}. However, longer force curves, i.e. longer interacting carbohydrate chains, were more frequent for glycan-glycan interaction in 100 than in 10 mM Ca^{2+}. Up to 13% of force curves were more than 80 nm long in 100 mM Ca^{2+} (Fig. 5H) compared with only ~3% in 10 mM Ca^{2+} (Fig. 5D).

Species-specific carbohydrate composition of proteoglycan molecules from different species

Proteoglycan molecules from four different sponge species were subjected to EDTA-treatment to separate the core structures from the arms (Fig. 6A). Extensive pronase digestion of purified core structures led to essentially pure 200-kDa glycan fractions, which mediate cell-cell recognition through self-interactions, and pronase digestion of purified arms gave pure 6-kDa glycan fractions, which mediate binding of the proteoglycan to the cell surface (Fig. 6B). 200-kDa glycans were free of protein contamination (Table 1). There was essentially no loss of carbohydrates during the purification procedures (carbohydrate yield ~97%). Amino acid analysis of purified glycans showed 0.7 (*Cliona celata*) to 1.1 (*Microciona prolifera*) mol of linker aspartate per mol glycan. Only trace amounts of a few other amino acids were detected. We are aware that aspartate is not a classical linker amino acid in proteoglycans, but the EM morphology and size of these sponge glycoconjugate molecules are similar to the mammalian proteoglycans. Its sulfate and glucoronate content and cellular location led to the term sponge proteoglycans 30 years ago and we prefer, until a detailed structure is known, to stay with this terminology.

The carbohydrate compositions of purified proteoglycans from four different sponge species were analyzed by high performance anion exchange chromatography. All proteoglycans contained galactose (Gal), fucose (Fuc), mannose (Man), N-acetylglucosamine (GlcNAc), N-acetylgalactosamine (GalNAc), and glucuronic acid (GlcUA). The carbohydrate makeup of proteoglycans from different individuals of the same species was very similar, while proteoglycans from different species showed large differences (Table 2). *Microciona* proteoglycan was characterized by high fucose, while *Halichondria* proteoglycan had 3-fold less. *Microciona* and *Halichondria* proteoglycans showed high galactose, while

Cliona proteoglycans had 3- to 4-fold less. The latter was the only species with significant amounts of GalNAc. On the other hand, only *Microciona* proteoglycan contained significant amounts of GlcUA.

Discussion

Until recently, specific proteoglycan-mediated cell adhesion and recognition processes could not be assigned to glycan-glycan recognition. This report presents comparative data on species-specificity and strength of self-interactions between glycans derived from cell surface proteoglycans. The glycan-glycan interaction is characterized by binding forces in the range of 200-300 pN, by species-specificity, polyvalency, and is stabilized by Ca^{2+}-ions.

Adhesive forces measured between glycans from the same species (275 pN) are the strongest forces reported to date for direct carbohydrate-carbohydrate interactions [3]. They are as strong as forces measured for the proteoglycan-proteoglycan interaction (50-400 pN) [33] as well as those for single antibody-antigen recognition (244 pN) [34,35]. These observations support the notion that direct carbohydrate-carbohydrate interaction is strong enough to manifest itself in biologically relevant cellular recognition. However, even lower values of adhesion forces, e.g. the adhesion force for glycosphingolipid self-interactions in the interactions between Lewis[x] structures (20 pN) [36], cannot exclude biological relevance. Carbohydrate molecules offer the multivalent presence of oligosaccharide chains on cell surfaces that could easily enhance weak binding forces and affinities to the levels found in biologically relevant interactions [37].

The species-specificity of glycan-mediated recognition is guaranteed not only by the greater adhesion forces but also by higher frequency of polyvalency in interactions between identical glycans versus different glycans, by differences in carbohydrate composition, and probably by the arrangement of glycan chains in a three-dimensional context. Polyvalency, i.e. the repetition of interactive sites along the carbohydrate chain, can generate sufficient affinity and/or avidity for carbohydrates to function in biologically relevant recognition events. A suitable mechanism for keeping two interacting carbohydrate chains arranged in a polyvalent array would be a zipper. This model provides both the simplicity and driving force by which nature may create specificity between two compositionally rather similar structures interacting with one another [38]. Polyvalent glycans on cell surfaces, therefore, represent a highly flexible and specific model for a recognition system that allows cells to test

surrounding surfaces and first create weak, random contacts before releasing or reinforcing the adhesion.

Differences in carbohydrate composition and the arrangement of a glycan chain in a three-dimensional context can also define the specificity of the carbohydrate-carbohydrate interaction. The carbohydrate composition (Fuc, Gal, Man, GalNAc, GlcNAc, and GlcUA) is highly conserved between individuals of the same species, whereas large differences are seen between different species. Detailed structural analyses of different proteoglycans have revealed species-specific sequences [39]. Diversity of polysaccharide primary structure affords diversity in higher order structure, and the specificity of the carbohydrate-carbohydrate interaction may be provided also by the three dimensional spatial relationships of the sugars.

Ca^{2+}-ions or other divalent cations are crucial in carbohydrate-carbohydrate interaction. In marine sponges they are essential. At the molecular level, Ca^{2+} probably reinforces the contact between the interacting oligosaccharides of glycan molecules, since an increase in Ca^{2+}in the buffer led to an increase in adhesion forces and in polyvalent interactions. In measurements of adhesion forces between sulfated disaccharides, it was also reported that Ca^{2+} probably provides coordinating forces [29]. However, the presence of Ca^{2+}-ions did not contribute significantly to the adhesion force in Le^x-Le^x interactions measured by AFM [36]. There is also no Ca^{2+} in the Le^x crystal [40]. Therefore, it was implied that calcium is only responsible for the approach and organization of the carbohydrates in the cell membrane. In contrast, corneal epithelial cell-cell adhesion through the Le^x determinant turned out to be highly dependent on the presence of Ca^{2+}-ions [41]. Similarly, self-aggregation of Le^x molecules in aqueous solution, where the molecules move freely, occurs only in the presence of Ca^{2+}-ions [42].

Rare ionic interactions cannot be excluded as most carbohydrates are neutral or negatively charged due to carboxy- and sulfate- groups, and even positively charged glycans also occur. However, the Ca^{2+} effect is not merely a charge effect. It has been shown that acidic sponge glycans do not all interact in the presence of Ca^{2+} [43]. Although single hydroxyl groups are too weak to coordinate cations, the combination of just two well-

positioned hydroxyl groups on one sugar residue or over two neighboring residues can lead to coordinate bonds between two interacting carbohydrate chains in the presence of water molecules. These Ca^{2+} interactions together with hydrogen bonds may lead to a sort of super-structure which then could bring about and allow even internal lipophilic interactions [1].

The role of Ca^{2+} in carbohydrate-carbohydrate interactions is still not well understood. Ca^{2+}-ions could be responsible for the approach and organization of the sugar moieties providing the surfaces for interaction, or they could enhance directly the adhesion force between complementary surfaces, acting as a bridge between specific hydroxy groups. Further experimental contributions to these potential models are now required before any of these proposals could be considered as relevant, in particular biologically relevant.

Better methods for the synthesis and characterization of carbohydrates are creating numerous opportunities for elucidation of the biological roles of these outermost cell surface structures. Carbohydrate-carbohydrate recognition is only one of the many possible oligosaccharide interactions for which a molecular level understanding is deficient or lacking completely. If carbohydrate-carbohydrate interactions may ensure adequate cell behavior during the formation, maintenance, and pathogenesis of tissues, a thorough understanding of the chemical and molecular nature of specific carbohydrate-carbohydrate recognition will be a prerequisite for the development of strategies to modify it and to progress thereby in an understanding of its biological relevance.

Acknowledgements

Abbreviations

AFM, atomic force microscopy

pN, piconewtons

CSW, calcium- and magnesium-free Tris-buffered seawater; artificial seawater

Le^x, Lewis^x determinant (Galβ1→4[Fucα1→3]GlcNAcβ1→3Galβ1→4Glcβ)

TFA, trifluoroacetic acid

References

1. Spillmann D, Burger MM, Carbohydrate-carbohydrate interactions in adhesion, *J Cell Biochem* **61**, 562-568 (1996).

2. Varki A, Selectin ligands, *Proc Natl Acad Sci* USA **91**, 7390-7397 (1994).

3. Bucior I, Scheuring S, Engel A, Burger MM, Carbohydrate-carbohydrate interaction provides adhesion force and specificity for cellular recognition, *J Cell Biol* **165**, 529-537 (2004).

4. Nakano M, Kakehi K, Tsai MH, Lee YC, Detailed structural features of glycan chains derived from {alpha}1-acid glycoproteins of several different animals-The presence of hypersialylated, O-acetylated sialic acids but not disialy residues, *Glycobiology* **14**, 431-444 (2004).

5. Bush CA, Martin-Pastor M, Imberty A, Structure and conformation of complex carbohydrates of glycoproteins, glycolipids, and bacterial polysaccharides, *Annu Rev Biophys Biomol Struct* **28**, 269-293 (1999).

6. Berninsone PM, Hirschberg CB, The nematode Caenorhabditis elegans as a model to study the roles of proteoglycans, *Glycoconj J* **19**, 325-330 (2002).

7. Hakomori S, Structure, organization, and function of glycosphingolipids in membrane, *Curr Opin Hematol* **10**, 16-24 (2003).

8. Hakomori S, Handa K, Glycosphingolipid-dependent cross-talk between glycosynapses interfacing tumor cells with their host cells: essential basis to define tumor malignancy, *FEBS Letters* **531**, 88-92 (2002).

9. Kasahara K, Sanai Y, Functional roles of glycosphingolipids in signal transduction via lipid rafts, *Glycoconj J* **17**, 153-162 (2000).

10. Hakomori S, Cell adhesion/recognition and signal transduction through glycosphingolipid microdomain, *Glycocon J* **17**, 143-151 (2000).

11. Fenderson BA, Zehavi U, Hakomori S, A multivalent lacto-N-fucopentaose III-lysyllysine conjugate decompacts preimplantation mouse embryos, while the free oligosaccharide is ineffective, *J Exp Med* **160**, 1591-1596 (1984).

12. Eggens I, Fenderson B, Toyokuni T, Dean B, Stroud M, Hakomori S, Specific Interaction between Le[x] and Le[x] determinants. A possible basis for cell recognition in

preimplantation embryos and in embryonal carcinoma cells, *J Biol Chem* **264**, 9476-9484 (1989).

13. Iozzo RV, Matrix proteoglycans: From molecular design to cellular function, *Annu Rev Biochem* **67**, 609-652 (1998).

14. Truant S, Bruyneel E, Gouyer V, De Wever O, Pruvot FR, Mareel M, Huet G, Requirement of both mucins and proteoglycans in cell-cell dissociation and invasiveness of colon carcinoma HT-29 cells, *Int J Cancer* **104**, 683-694 (2003).

15. Humphreys T, Chemical dissolution and *in vitro* reconstruction of sponge cell adhesions. Isolation and functional demonstration of the components involved, *Dev Biol* **8**, 27-47 (1963).

16. Wilson HV, On some phenomena of coalescence and regeneration in sponges. *J. Exp. Zool.* **5**, 245-258 (1907).

17. Crossin KL, Cell adhesion molecules activate signaling networks that influence proliferation, gene expression, and differentiation, *Ann N Y Acad Sci* 2002 **961**, 159-60 (2002).

18. Cavallaro U, Christofori G, Cell adhesion and signalling by cadherins and Ig-CAMs in cancer, *Nat Rev Cancer* **4**, 118-32 (2004).

19. Férnandez-Busquets X, Burger MM, Circular proteoglycans from sponges: first members of the spongican family, *Cell Mol Life Sci* **60**, 88-112 (2003).

20. Henkart P, Humphreys S, Humphreys T, Characterization of sponge aggregation factor. A unique proteoglycan complex, *Biochemistry* **12**, 3045-3050 (1973).

21. Müller WE, Beyer R, Pondeljak V, Müller I, Zahn RK, Species-specific aggregation factor in sponges. XIII. Entire and core structure of the large circular proteid particle from *Geodia cydonium*, *Tissue Cell* **10**, 191-199 (1978).

22. Jarchow J, Fritz J, Anselmetti D, Calabro A, Hascall VC, Gerosa D, Burger MM, Fernandez-Busquets X, Supramolecular structure of a new family of circular proteoglycans mediating cell adhesion in sponges, *J Struct Biol* **132**, 95-105 (2000).

23. Misevic GN, Burger MM, The species-specific cell-binding site of the aggregation factor from the sponge *Microciona prolifera* is a highly repetitive novel glycan containing glucuronic acid, fucose and mannose, *J Biol Chem* **265**, 20577-20584 (1990).

24. Misevic GN, Burger MM, Carbohydrate-carbohydrate interactions of a novel acidic glycan can mediate sponge cell adhesion, *J Biol Chem* **268**, 4922-4929 (1993).

25. Turner SR, Burger MM, Involvement of carbohydrate group in the active site for surface guided reassociation of animal cells, *Nature* **244**, 509-510 (1973).

26. Jumblatt JE, Schlup V, Burger MM, Cell-cell recognition: Specific binding of Microciona sponge aggregation factor to homotypic cells and the role of calcium ions, *Biochem* **19**, 1038-1042 (1980).

27. Spillmann D, Thomas-Oates JE, van Kuik JA, Vliegenthart JF, Misevic G, Burger MM, Finne J, Characterization of a novel sulfated carbohydrate unit implicated in the carbohydrate-carbohydrate-mediated cell aggregation of the marine sponge *Microciona prolifera*, *J Biol Chem* **270**, 5089-5097 (1995).

28. Spillmann D, Hard K, Thomas-Oates J, Vliegenthart JF, Misevic G, Burger MM, Finne J, Characterization of a novel pyruvylated carbohydrate unit implicated in the cell aggregation of the marine sponge *Microciona prolifera*, *J Biol Chem* **268**, 13378-13387 (1993).

29. Haseley SR, Vermeer HJ, Kamerling JP, Vliegenthart JFG, Carbohydrate self-recognition mediates marine sponge cellular adhesion, *PNAS* **98**, 9419-9424 (2001).

30. Beeley JG, Structural analysis. In *Glycoprotein and proteoglycan techniques*, (Elsevier Science Publishers, Amsterdam, 1989), pp. 153-296.

31. Chon JWM, Mulvaney P, Sader JE, Experimental validation of theoretical models for the frequency response of atomic force microscope cantilever beams immersed in fluids, *J Appl Phys* **87**, 3978-3988 (2000).

32. Müller DJ, Baumeister W, Engel A, Controlled unzipping of a bacterial surface layer with atomic force microscopy, *Proc Natl Acad Sci* USA **96**, 13170-13174 (1999).

33. Dammer U, Popescu O, Wagner P, Anselmetti D, Guntherodt HJ, Misevic GN, Binding strength between cell adhesion proteoglycans measured by Atomic Force Microscopy, *Science* **267**, 1173-1175 (1995).

34. Hinterdorfer P, Baumgartner W, Gruber HJ, Schilcher K, Schindler H, Detection and localization of individual antibody-antigen recognition events by atomic force microscopy, *Proc Natl Acad Sci* USA **93**, 3477-3481 (1996).

35. Saleh OA, Sohn LL, Direct detection of antibody-antigen binding using an on-chip artificial pore, *Proc Natl Acad Sci* USA **100**, 820-824 (2003).

36. Tromas C, Rojo J, de la Fuente JM, Barrientos AG, Garcia R, Penades S, Adhesion forces between Lewis[x] determinant antigens as measured by atomic force microscopy, *Angew Chem Int Ed* **40**, 3052-3055 (2001).

37. Misevic GN, Finne J, Burger M, Involvement of carbohydrates as multiple low affinity interaction sites in the self-association of the aggregation factor from the marine sponge Microciona prolifera, *J Biol Chem* **262**, 5870-5877 (1987).

38. Spillmann D, Carbohydrates in cellular recognition: from leucine-zipper to sugar-zipper?, *Glycoconj J* **11**, 169-171 (1994).

39. Guerardel Y, Czeszak X, Sumanovski L, Karamanos Y, Popescu O, Strecker G, Misevic GN, Molecular fingerprinting of carbohydrate structures phenotypes of three porifera proteoglycan-like glyconectins, *J Biol Chem* **279**, 15591-15603 (2004).

40. Perez S, Mouhous-Riou N, Nifant'ev NE, Tsvetkov YE, Bachet B, Imberty A, Crystal and molecular structure of a histo-blood group antigen involved in cell adhesion: the Lewis x trisaccharide, *Glycobiology* **6**, 537-542 (1996).

41. Cao Z, Zhao Z, Mohan R, Alroy J, Stanley P, Panjwani N, Role of the Lewis[x] glycan determinant in corneal epithelial cell adhesion and differentiation, *J Biol Chem* **276**, 21714-21723 (2001).

42. de La Fuente JM, Barrientos AG, Rojas TC, Rojo J, Canada J, Fernandez A, Penades S, Gold glyconanoparticles as water-soluble polyvalent models to study carbohydrate interactions, *Angew Chem Int Ed Engl* **40**, 2257-2261 (2001).

43. Spillmann D, Burger MM, Carbohydrate/carbohydrate interactions. In *Oligosaccharides in Chemistry and Biology*, *A Comprehensive Handbook* (Wiley-VCH Verlag GmbH, Weinheim, 2000), pp. 1061-1091.

Table 1. **Trace amino acid composition of 200 kDa glycans from four sponge species.** The values are the average of four determinations. Cys was not determined.

	Microciona	*Halichondria*	*Suberites*	*Cliona*
	mol amino acid/mol glycan			
Asp	1.1	0.9	0.9	0.7
Glu	0.4	0.3	0.4	0.2
Ser	0.2	0.1	0.2	0
His	0	0	0	0
Gly	0.3	0.3	0.2	0.3
Thr	0.4	0.1	0	0.1
Ala	0.2	0.1	0.1	0
Arg	0	0	0	0
Tyr	0	0	0	0
Val	0	0	0	0
Met	0	0	0	0
Phe	0	0.1	0	0
Ile	0	0	0	0
Leu	0	0.1	0.1	0
Lys	0	0	0	0
Pro	0	0	0	0
Asn	0	0	0	0
Gln	0	0	0	0
Trp	0	0	0	0
Ca	0	0	0	0
Total	2.6	2.0	1.9	1.3

Table 2. **Comparison of the carbohydrate composition of proteoglycans from four sponge species.** The average values were obtained from four sponge individuals of each species.

	Microciona	*Halichondria*	*Suberites*	*Cliona*
	carbohydrates (mol %)			
Fuc	30.2	8.2	15.0	22.1
Gal	33.5	40.9	25.0	10.8
Man	9.7	15.2	12.4	14.0
GalNAc	3.7	1.2	2.0	10.1
GlcNAc	18.3	14.1	34.2	27.5
GlcUA	9.1	3.0	1.9	4.5

Figure legends

Figure 1 **Specific recognition between live cells (A-D), and between cells and glycans (E-H). A,** Yellow cells from the same species (*Suberites fuscus*) formed large homogenous aggregate during a 4-h rotation-mediated aggregation in artificial seawater with physiological 10 mM $CaCl_2$. **B,** Cells from two different species, with red (*Microciona prolifera*) and grey (*Halichondria panicea*) natural pigments, form separated bright red and grey aggregates. **C,** Absence of Ca^{2+} inhibited cell-cell aggregation (aggregation between *Halichondria* and *Suberites* cells as an example). **D,** The monoclonal antibody directed against the carbohydrate epitope of *Microciona* proteoglycan reduced aggregation between *Microciona* cells (40 μg of the antibody with 5 x 10^3 cells). **E,** Grey cells (*Halichondria*) formed one big aggregate with their own surface glycans coated on red beads. **F,** Grey cells (*Halichondria*) formed their own aggregates separated from red aggregates of beads carrying glycans from another species. **G,** The absence of Ca^{2+} reduced cell-glycan aggregation (aggregation between *Halichondria* cells and *Microciona*-coated beads as an example). **H,** The monoclonal antibody directed against the carbohydrate epitope of *Microciona* proteoglycan reduced aggregation between *Microciona* cells and their glycan coated on beads (40 μg of the antibody with 4.5 x 10^8 glycan-coated beads).

Figure 2 **Specific recognition between glycan-coated beads.** Glycan-coated carboxylate-modified beads sorted out specifically during a 4-h rotation-mediated aggregation in artificial seawater with physiological 10 mM $CaCl_2$. The numbers on the left side of each picture represent the percentage clumps of the respective color. Yellow areas depict aggregates of mixed red and green beads coated with identical glycans. Red and green areas reflect aggregates of separated beads coated with different glycans. The absence of Ca^{2+} in artificial seawater inhibited glycan-coated bead-bead aggregation. The monoclonal antibody directed against the carbohydrate epitope of *Microciona* proteoglycan inhibited aggregation between *Microciona* glycans coated on beads (40 μg of the antibody with 9 x 10^6 glycan-coated beads). M, *Microciona*; H, *Halichondria*; S, *Suberites*; C, *Cliona*.

Figure 3 **Specific adhesion of live cells and glycans to glycan-coated plates. A,** Cells adhered species-specifically to 200-kDa glycans from core structures of different sponge

27

proteoglycans coated on plastic plates. (■), Homotypic adhesion of live cells to their own glycans coated on plates (average from experiments where live cells from 4 different sponge species: *Microciona prolifera*, *Halichondria panicea*, *Suberites fuscus*, and *Cliona celata* were tested for binding to their own glycans coated on plates); (▲), Heterotypic adhesion of live cells to different glycans coated on plates (average of experiments where live cells from 4 different sponge species were tested for binding to glycans from species different from their own) ; (□), Adhesion of live cells from 4 different species to their own glycans without the presence of Ca^{2+}. **B,** Effect of the monoclonal antibody directed against the carbohydrate epitope of *Microciona* proteoglycan on homotypic adhesion between *Microciona* cells and *Microciona* glycan coated on plates (40 µg of the antibody with 5 x 10^3 cells). **C,** Glycans adhered species-specifically to glycan-coated plastic plates. (■), Homotypic adhesion of 200-kDa glycans to the same glycans coated on plates (average from experiments where glycans from 4 different sponge species: *Microciona*, *Halichondria*, *Suberites*, and *Cliona* were tested for binding to the same glycans coated on plates); (▲), Heterotypic adhesion of 200-kDa glycans to different glycans coated on plates (average of experiments where glycans from 4 different sponge species were tested for binding to glycans from species different from their own); (□), Adhesion of glycans from 4 different species to the same glycans coated on plates without the presence of Ca^{2+}. **D,** Effect of the monoclonal antibody directed against the carbohydrate epitope of *Microciona* proteoglycan on homotypic adhesion between *Microciona* glycans (40 µg of the antibody with 10 µg of glycans). M/M, *Microciona-Microciona* adhesion; H/H, *Halichondria-Halichondria* adhesion; S/S, *Suberites-Suberites* adhesion; C/C, *Cliona-Cliona* adhesion. ± SD from 16 independent experiments.

Figure 4 **Atomic Force Microscopy (AFM) measurements of glycan-glycan binding forces. A,** Scheme of AFM set-up for the measurement of the intermolecular forces between single glycan molecules. **B,** Examples of AFM force curves. Line 1 and 2 represent control curves: gold-gold interaction (1) and homotypic glycan-glycan interaction in artificial seawater without Ca^{2+} (2). Line 3 represents a curve of the homotypic interaction between glycans from the same species, and line 4 the heterotypic interaction between glycans from two different species in the presence of physiological 10 mM Ca^{2+}. **C,** Adhesion force values of the homotypic interactions between glycans from the same species attached to the tip and the mica surface (average from homotypic binding experiments between glycans from 4

sponge species: *Microciona prolifera*, *Halichondria panicea*, *Suberites fuscus*, and *Cliona celata*). **D,** Adhesion force values of the heterotypic interactions between glycans from different species (average from heterotypic binding experiments between glycans from 4 different sponge species). **E,** Periodicity measurements showing distances between individual rupture peaks, which indicate the distances between binding motifs on the carbohydrate chain for homotypic interactions between the same species glycans and **F,** for heterotypic interactions between glycans from different species. The white bar reflects the number of probe lift events where only one rupture event was registered. **G,** The length of the force curves measured from the lift-off point to the last peak, indicating the total length of the interacting carbohydrate chain between the same species glycans and **H,** between different species glycans. On the ordinate, the number of rupture events is provided normalized to 1.0 for the category of the highest number of events.

Figure 5 **Quantitative evaluation of interactions between single glycan molecules in physiological 10 mM Ca^{2+} (A-D) versus interactions in 100 mM Ca^{2+} (E-H).** Interactions between *Microciona prolifera* glycans were measured in artificial seawater with 10 and 100 mM Ca^{2+}. **A,** An example of AFM force curve of the glycan-glycan interaction in 10 mM Ca^{2+}. **B,** Adhesion force values for glycan-glycan interactions in 10 mM Ca^{2+}. **C.** Periodicity measurements of distances between rupture peaks, which indicate the distances between binding motifs on the carbohydrate chain, in 10 mM Ca^{2+}. **D,** The total length of the interacting carbohydrate chain in glycan-glycan interactions in 10 mM Ca^{2+}. **E,** An example of AFM force curve of the glycan-glycan interaction in 100 mM Ca^{2+}. **F,** Adhesion force values for glycan-glycan interactions in 100 mM Ca^{2+}.and H, 100 mM Ca^{2+}. **G,** Periodicity measurements of distances between rupture peaks in 100 mM Ca^{2+}. **H**, The total length of the interacting carbohydrate chain in glycan-glycan interactions in 100 mM Ca^{2+}.

Figure 6 **Separation of glycans obtained by pronase digestion of core structures and arms of different sponge proteoglycans. A**, Separation of two proteoglycan subunits on A-15m sizing column after prolonged EDTA-treatment of proteoglycan molecules (an example of separation of *Microciona prolifera* proteoglycan subunits; peak nr 1: core structures of the proteoglycan, peak nr 2: arm fragments of the proteoglycan). **B**, PAGE electrophoresis of

glycans obtained by pronase digestion of two subunits. **a-d,** 200-kDa glycans from 4 different sponge species obtained from the peak nr 1; **e-h**, 6-kDa glycans from 4 different species obtained from the peak nr 2. **a** and **e**, *Microciona prolifera* glycans; **b** and **f**, *Halichondria panicea* glycans; **c** and **g**, *Suberites fuscus* glycans; **d** and **h**, *Cliona celata* glycans. Molecular weight standards: HA, hyaluronic acid; CS, chondroitin sulfate.
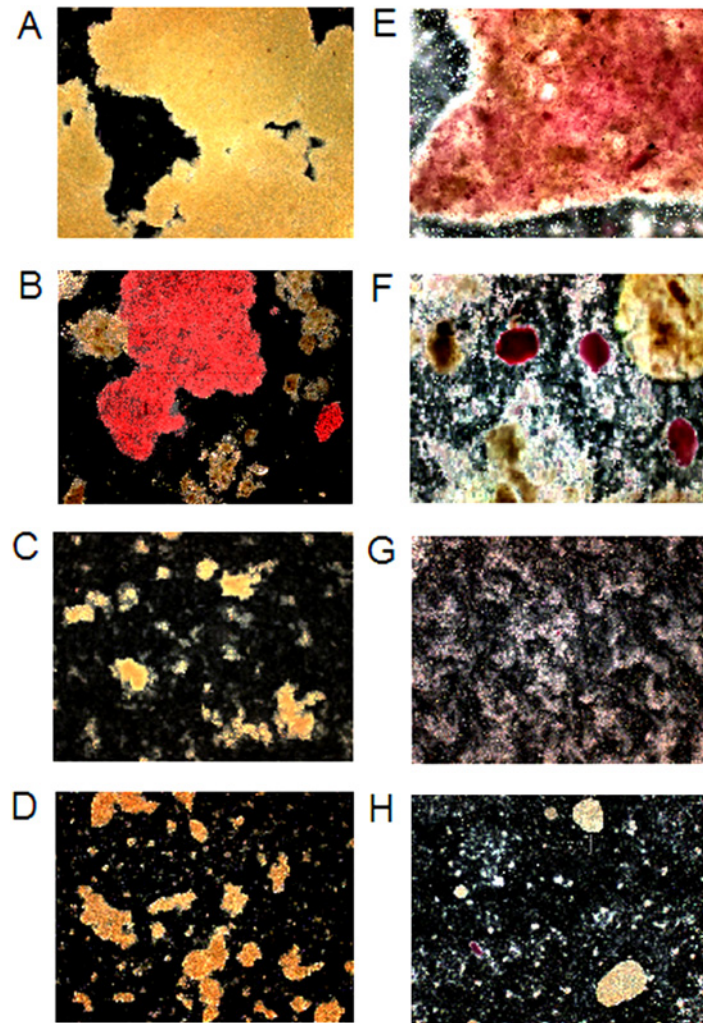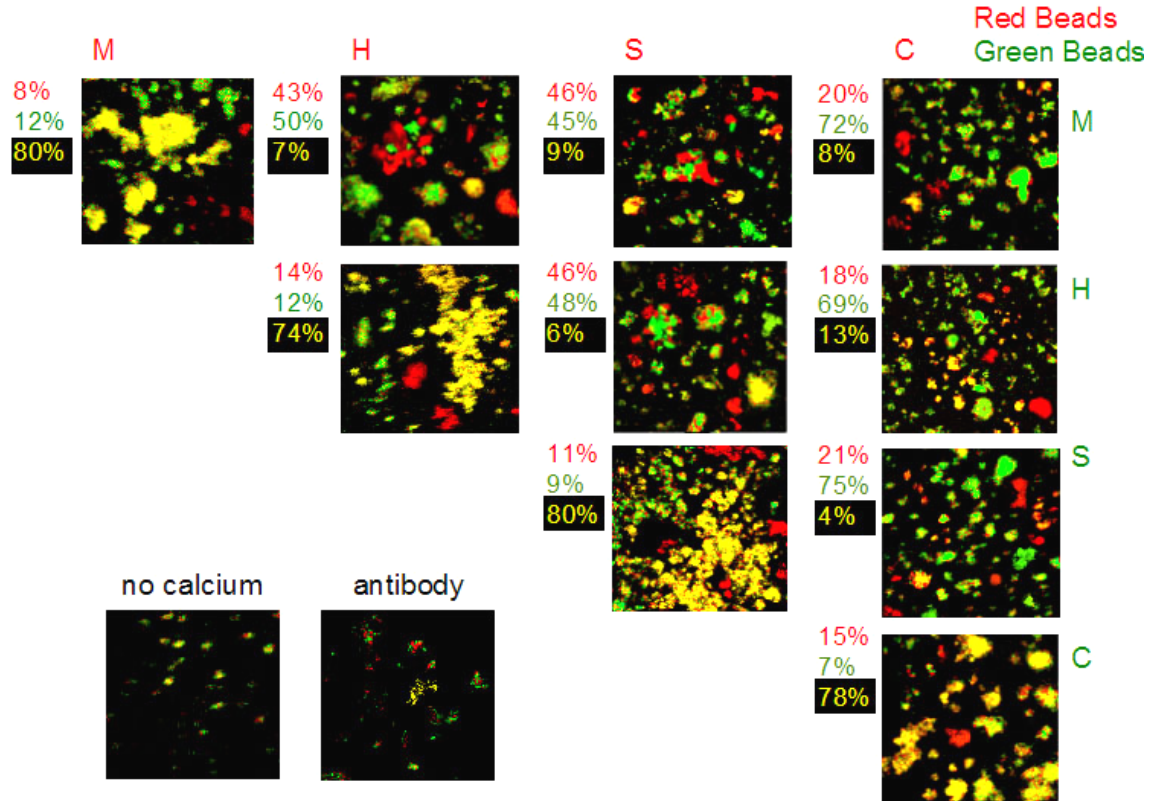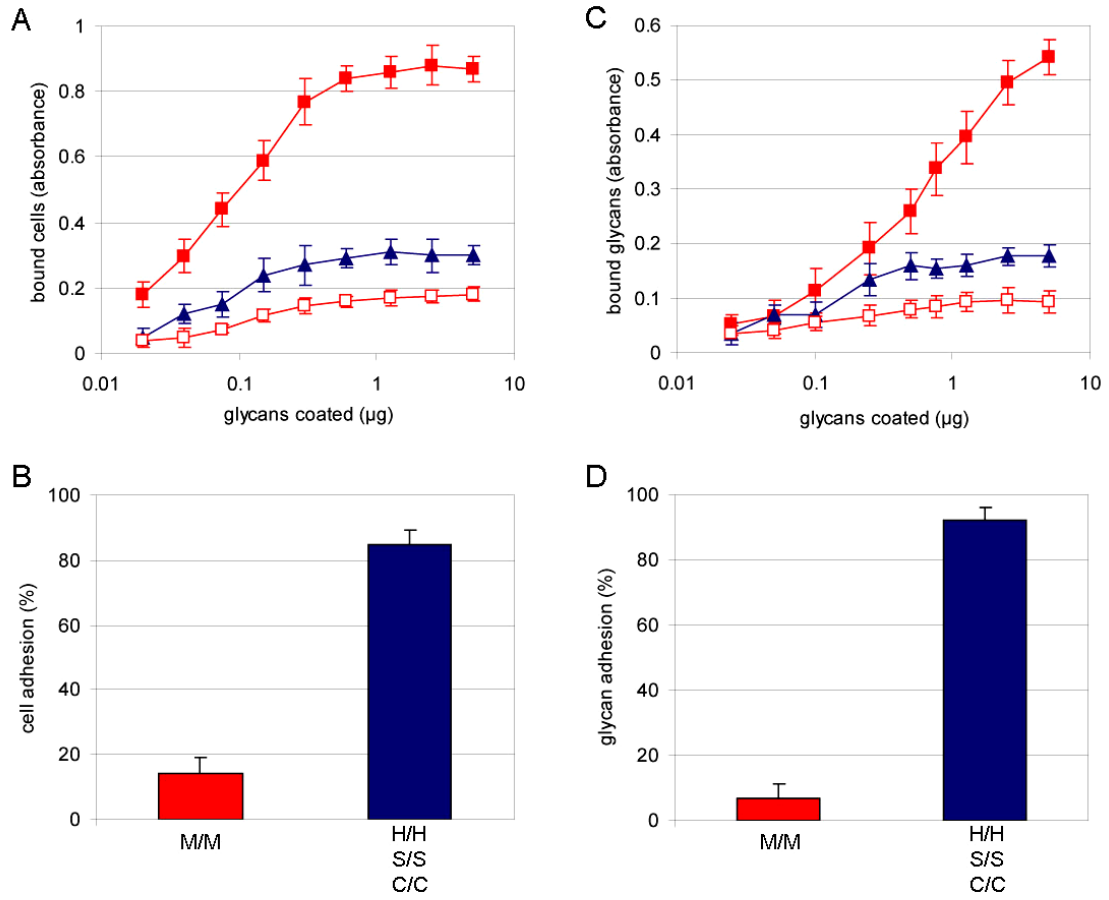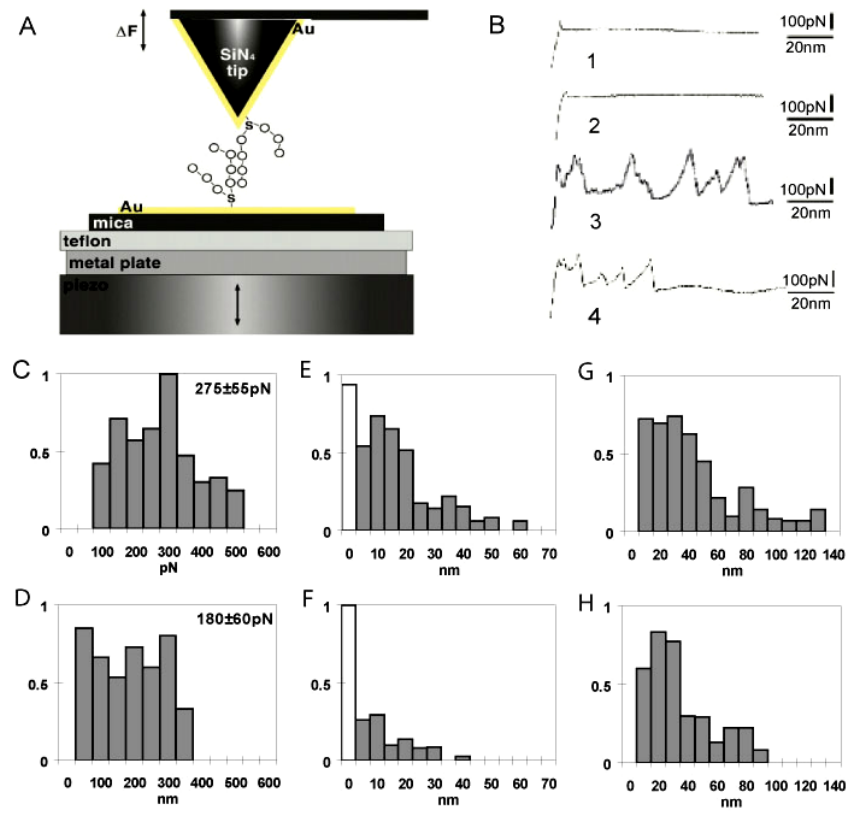
Figure 1

Figure 2

Figure 3

Figure 4

Figure 5

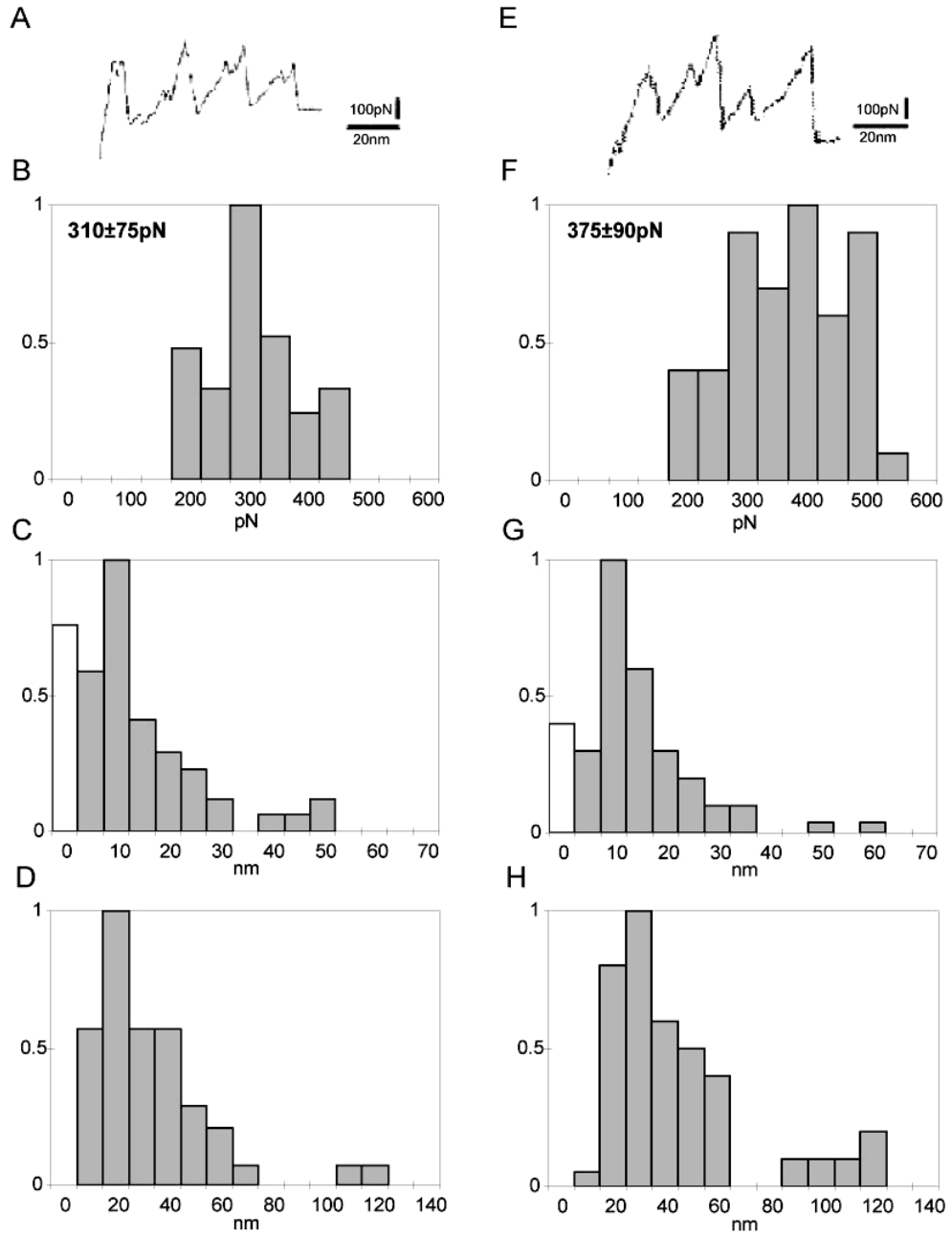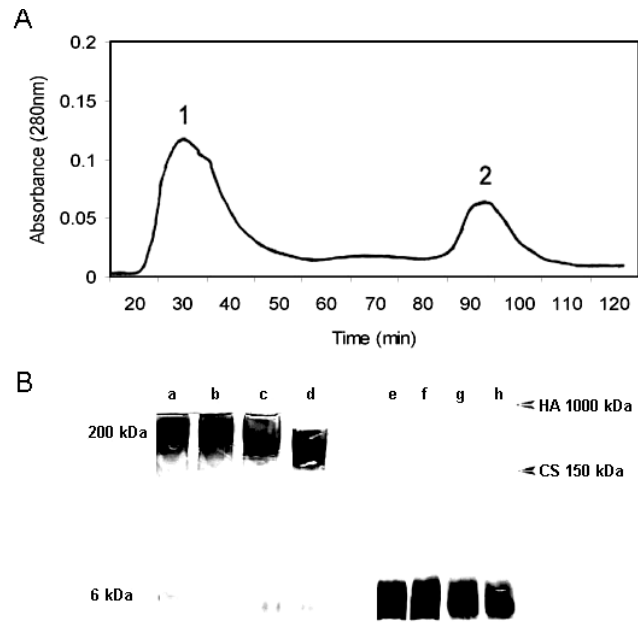Figure 6

CURRICULUM VITAE

Last Name: **Bucior**

First Name: **Iwona**

Nationality: **Polish**

Date of Birth: **24/06/1973**

EDUCATION

09/1988- 05/1992	Secondary School nr3 in Gdynia, Poland	biol-chem profile with an extended course of English	GCSE with honors
10/1994- 09/1998	Intercollegiate Faculty of Biotechnology, Medical Academy of Gdansk, and Department of Pharmaceutical Technology, University of Gdansk, Poland	diploma thesis: mechanisms of antitumor action of anthracyclines in leukemia cells and in AML patients	MSc with honors
03/1999- 10/2004	Friedrich Miescher Institute, Basel, Switzerland and Marine Biological Laboratory, Woods Hole, MA, USA	PhD thesis: carbohydrate- carbohydrate interactions in cellular recognition and adhesion events	PhD

TRAINING/INTERNSHIP

01/1989- 11/1992	Garrison Housing Administration, Gdynia, Poland	Personnal Assistant to Director General	professional experience
05-09 1991	Mayfair School of English, London, UK	English language course, class level: advanced	certificate
01-07 1993	Faculty of Hydrotechnique, Technical University, Gdansk, Poland	training in geodesy	passed with honors
09/1994- 07/1995	University College London Hospitals, London, UK	MSc studies; stem cell transplantation (culture and sensitivity tests of the bone marrow samples)	apprenticeship
08-12 1995	Intercollegiate Faculty of Biotechnology Medical Academy and University of Gdansk, Poland	training in zoology and parasitology	passed with honors
01-08 1996	Medical Academy of Gdansk, Poland	training in medical informatics	passed with honors
11/1996- 05/1998	Frauenklinik, Ludwig-Maximilians Universität, München, Germany	training in Forensic Medicine; identification and validation of diagnostic fertility markers	apprenticeship
02-06 1997	Medical Academy of Gdansk, Poland	training in informatics in molecular biology	passed
04-05 2000	Laboratory of Sen-itiroh Hakomori, Pacific Northwest Research Institute, Seattle, WA, USA	studying functions of sphingoglycolipids in transmembrane signalling and cellular interactions	apprenticeship
09/2000	Universite des Sciences & Technologies de Lille, Laboratoire de Chimie Biologique, Lille, France	FEBS-Advanced Course on Glycoconjugates	certificate

CONFERENCES/PUBLICATIONS

2003   Annual Conference of the Society for Glycobiology, San Diego, CA, USA;
            abstract and poster: "May the force and specificity be with carbohydrate-carbohydrate
            interactions."

2003   2nd International Symposium on Signal Transduction Modulators in Cancer
            Therapy (STM-2003), Amsterdam, the Netherlands;
            abstract and poster: **"**Atomic force microscopy study of proteoglycan adhesion:
            relationship between function and structure by single molecule force spectroscopy."

2002   XXIst International Carbohydrate Symposium, Cairns, Australia;
            abstract and poster: "Carbohydrate-carbohydrate interaction provides specificity and
            adhesion strength for cellular recognition."

2001   Annual Conference of the Society for Glycobiology, San Francisco, CA, USA;
            abstract and poster: "Carbohydrate-carbohydrate interaction = cell-cell recognition?"

2000   Proceedings of 91st Meeting of American Association for Cancer Research,
            San   Francisco, CA, USA;
            abstract and poster: "Interstrand DNA crosslinking induced by anthracyclines in AML
            cells as the possible antitumor mechanism of action."

1999   Annual Conference of Polish Biochemistry Society, Muszyna, Poland;
            abstract: "Interstrand DNA crosslinking is induced by anthracyclines in leukemia cells
            in vitro and in AML patients undergoing therapy with these drugs."

1998   Invited speaker, 6th International Students' Scientific Conference, Gdansk, Poland;
            abstract: "Interstrand DNA crosslinking induced by anthracyclines in leukemia cells *in
            vitro* and in AML patients treated with these drugs."

Bucior, I., Burger, M. M. Carbohydrate-carbohydrate interactions in cell recognition. Review. *Curr. Opin. Struct. Biol.* 14: 631-637 (2004).

Bucior, I., Scheuring, S., Engel, A., Burger, M. M. Carbohydrate-carbohydrate interaction provides adhesion force and specificity for cellular recognition. *J. Cell Biol.* 165: 529-537 (2004).

Bucior, I., Burger, M. M. Carbohydrate-carbohydrate interaction as the major force initiating cell-cell recognition. *Glycocon. J.* in press (2004).

Bucior, I. Antitumor effects of the anthracycline antibiotics. Review. *Proceed. Polish Biochem. Soc.* 7: 22-26 (1999).

Bucior, I. Interstrand DNA crosslinking induced by anthracyclines in murine and human leukemia cells in vitro, and in AML patients undergoing therapy with these drugs. Diploma thesis (1998).

Bucior, I., Hellman, A., Konopa, J. Anthracyclines induce apoptosis through interstrand DNA crosslinking in leukemia cells in vitro and in AML patients undergoing therapy with these drugs. *Proceed. Polish Biochem. Soc.* 2: 12-14 (1998).

AWARDS and HONORS

2004   Front cover of the *EMBO Journal*, Volume 23

2003   Winner of the Eurosport Best Picture Competition

2002   Recipient of the Young Scientist's Award at the XXIst International Carbohydrate Symposium in Cairns, Australia

1995-   Fellowship of the Polish National Scholarship Foundation, Warsaw, Poland
1998

1994   Honorable Diploma for Outstanding Results at the Faculty of Hydrotechnique, Technical University of Gdansk, Poland

1992   Outstanding student of the year, Secondary School, Gdynia, Poland

1980-   6x National Junior Swimming Champion, 3x European Junior Swimming Champion
1987   and 3x World Junior Swimming Champion

TECHNICAL SKILLS

Experience in the fields of:
- cell biology: general tissue culture, peripheral blood cells culture, cell transfection, immunohistochemistry, DNA binding and DNA crosslinking assays, assays for DNA-topoisomerase II complexes, reporter gene assay, cell cycle analysis, cytotoxicity assay, proliferation and apoptosis assays.
- molecular biology: siRNA technology, quantitative radioactive RT-PCR, Taqman RT-PCR, cloning, SDS-PAGE, Western blotting.
- biochemistry: HPLC, FPLC, gel chromatography, protein purification, amino-acid analysis.
- glycobiology: glycan purification, carbohydrate composition analysis, glycan binding assays, neoglycolipid technology, preparation of liposomes.
- biotechnology: fertility markers, paternity tests, cell culture for bone marrow transplantations.

Microscopy techniques

- Optical and fluorescence imaging
- Time-lapse imaging
- Confocal microscopy
- Atomic force microscopy

Computer

Macintosh and PC
- MS Office Software
- Adobe Photoshop, Illustrator and Premiere
- Micrografix Picture Publisher and Designer
- Metamorph
- Databanks
- Statistics and databases
- Molecular design

Languages

- Polish: native
- English: fluent
- German: good
- Russian: good
- Spanish: basic
- Czechs: basic